

NATIONAL TRANSPORTATION SAFETY BOARD

Office of Research and Engineering
Materials Laboratory Division
Washington, D.C. 20594



May 21, 2012

MATERIALS LABORATORY FACTUAL REPORT

Report No. 11-055

A. INVESTIGATION INFORMATION

Place : Marshall, Michigan
Date : July 25, 2010
Vehicle : 30-inch diameter crude oil pipeline
NTSB No. : DCA10MP007
Investigator : Matt Nicholson, RPH-20

B. COMPONENTS EXAMINED

50-foot length of 30-inch diameter pipe from Enbridge Line 6B.

C. ACCIDENT SUMMARY

On the evening of Sunday, July 25, 2010, at approximately 5:58 p.m.¹ the Enbridge Energy (Enbridge) control center in Edmonton, Alberta, Canada, was in the final stages of executing a scheduled shutdown of their 30-inch diameter crude oil pipeline (Line 6B). As the last pump was stopped, a segment, located approximately $\frac{3}{4}$ mile downstream of the Marshall, Michigan pump station, ruptured. The initial and subsequent alarms associated with the event were not recognized as a line-break through two attempts at start-up and over multiple control center shifts. Residents near the rupture site began calling the Marshall City 911 dispatch center to report odors at 9:25 p.m. on Sunday; however, no calls were placed to the Enbridge control center until 11:17 a.m. the following day. Once the Enbridge control center was notified, nearly 17 hours after the initial rupture, remote controlled valves were closed, bracketing the ruptured segment within a three-mile section.

The accident resulted in an Enbridge-reported release estimate of 20,082 barrels (843,444 gallons) of crude oil with no injuries or fatalities. The rupture location is in a high consequence area² within a mostly rural, wet, and low-lying region. The released oil pooled into a marshy area over the rupture site before flowing 700 feet south into Talmadge Creek, which ultimately carried it into the Kalamazoo River.

Line 6B was constructed in 1969 as a 293-mile long extension of the Lakehead pipeline system, stretching from Griffith, Indiana to Sarnia, Ontario. The failed segment was a cathodically-protected, tape-coated pipe manufactured by Italsider s.p.a.³ per the

¹ All times are expressed in local accident time, Eastern Daylight Time.

² As defined by PHMSA under 49 CFR §195.450.

³ Societa Per Azioni (Italian). The Italsider pipe was purchased from Siderius Inc. of New York.

1968 API⁴ Standard 5LX, *Specification for High-Test Line Pipe*, X52 specification with 0.25-inch thick wall and a double submerged arc welded (DSAW) longitudinal seam. The maximum operating pressure (MOP) for Line 6B was 624 psig; however, at the time of the accident, this segment was under a 523 psig Enbridge imposed pressure restriction. The maximum-recorded discharge pressure at Marshall, before the rupture, was 486 psig.

D. DETAILS OF THE EXAMINATION

The ruptured pipe was examined initially on-scene by the On-scene Materials Working Group, which was comprised of participants representing the NTSB Materials Laboratory, Enbridge, and the Department of Transportation Pipeline and Hazardous Materials Safety Administration (PHMSA). After the on-scene work was completed, a separate Materials Group was formed with participants representing Enbridge and PHMSA. A consultant for the Environmental Protection Agency (EPA) also observed Materials Group activities. Group examinations were held by the Materials Group on August 23 through August 27, 2010, at the NTSB Training Center in Ashburn, Virginia; September 20 through September 24, 2010, at the NTSB Materials Laboratory in Washington, DC; and November 16 through 18, 2010, at the NTSB Materials Laboratory in Washington, DC.

In Enbridge line 6B, joints are typically lengths of approximately 40 feet each. Girth welds at either end of the joints are typically numbered increasing by 10 for each weld, and joint numbers correspond to the number of the girth weld at the upstream end of the joint. The rupture was located within joint number 217720. For the ruptured joint, the upstream girth weld was GWD217720 and the downstream girth weld was GWD217730. A 2-inch diameter fitting was located approximately 126 feet upstream from the rupture location, and this fitting was used as a reference point on the pipe on scene. GWD217720 was located 96.791 feet downstream of the 2-inch diameter fitting, and GWD217730 was located 137.034 feet downstream of the 2-inch diameter fitting. The chainage for GWD217720 and GWD217730 was 753268.681 feet and 753308.924 feet, respectively, from 2009 ultrasonic wall measurement tool in-line inspection (ILI) data. The depth of cover at the rupture site was approximately 5 feet.

A trench was dug at the accident scene to expose the ruptured pipe joint and an additional 50 feet upstream and downstream of the ruptured joint. The pipe was supported by cradles as it was excavated. An overall view of the exposed pipeline in the trench is shown in figure 1. Views of the rupture as it was observed in the trench at the accident site are shown in figure 2. The rupture measured 6 feet 8.25 inches long. The upstream end of the rupture was located 24 feet 5.75 inches downstream of GWD217720. The longitudinal seam in joint 217720 was located 99.5 degrees clockwise⁵ from top dead center. The rupture was located 0.5 to 1.5 inches clockwise from the center of the longitudinal seam. The crack opening displacement between

⁴ American Petroleum Institute, New York, New York.

⁵ Unless stated otherwise, clock positions are as viewed looking along the axis of the pipeline in the flow direction.

mating fracture surfaces was 5.32 inches at the widest point, which was located 4 feet from the upstream end of the rupture.

A review of ILI data from 2005 and 2009 was conducted on-scene. ILI data showed lengths of pipe within joint 217720 that had indications of crack-like features and/or metal loss generally located near the longitudinal seam. The lengths of pipe where ILI features were noted are shown as shaded areas in figure 3.

The pipe was cut at 2 locations: approximately 5 feet upstream of GWD217720 and approximately 5 feet downstream of GWD217730. After the first cut was completed, the relative displacement between the cut ends was measured, and the total displacement was less than 3 inches in the lateral and vertical directions. After the second cut was completed, the approximately 50-foot piece was hoisted out of the trench. In order to facilitate shipping and handling of the pipe, the joint was cut on-scene at a location 18.5 feet downstream from GWD217720 within an area where ILI data did not show indications of crack-like features or metal loss.

Overall views of the two pipeline pieces received by the NTSB Materials Laboratory are shown in figure 4 and in the schematic drawing shown in figure 3. The pieces were adjacent pieces, with the upstream piece labeled A and the downstream piece labeled B. The pieces were from Enbridge line 6B manufactured in 1969 by Siderius. The pipe was specified as American Petroleum Institute (API) X52 with a 30-inch diameter and 0.25-inch nominal wall thickness. The pieces were comprised of all of joint 217720 and 5 feet of the adjacent joints 217710 and 217730 at the upstream and downstream ends of joint 217720. Girth weld numbers GWD217720 and GWD217730 were included in the pieces as shown in figure 3. Piece A measured 23 feet 4 inches in length, and piece B measured 26 feet 10.25 inches in length. The length of joint 217720 as measured on scene was 39 feet 10.75 inches. The longitudinal seams were located at 295 degrees, 99.5 degrees, and 137 degrees clockwise from top dead center in joints 217710, 217720, and 217730, respectively.

D.1. Microbiological Sampling

On August 6, 2010, during the on-scene portion of the examination, an EPA agent (chemist) extracted microbiological test samples by syringe from three areas of the pipe. All samples were taken from areas near the longitudinal seam where the coating was bulged outward. The areas where samples were taken or were attempted to be taken were labeled M1 to M4. Areas M1 to M4 were approximately 12 feet, 21 feet, 38 feet, and 24.5 feet from GWD217720, respectively. Area M2 was dry, so no samples were collected from that location. Samples from the remaining areas M1, M3, and M4 were used in MICKit[®] 5 test kits from BTI Products, LP, Bayfield, Colorado. The test kits contain bottles with liquid media that, when inoculated, are used to enumerate viable bacteria belonging to five types of bacterial groups. The samples M1, M3, M4, and a negative control were used to inoculate the kits in a series of four serial dilutions by volume, i.e., 0.1, 0.1, 0.01, then 0.01. Results from observations of the MICKit[®] 5 test kits at 3, 5, and 17 days from inoculation are combined and summarized in table 1. The control sample showed negative reactions in all bottles.

During the laboratory examination at the NTSB Training Center, an NTSB pipeline investigator extracted two additional microbiological test samples from areas of pipe piece A on August 27, 2010. The first sample (M5) consisted of material collected at two locations along the longitudinal seam: one location between 4 and 5 feet from GWD217720 and another location between 7 and 8 feet from GWD217720. The total area of collection was approximately 2 inches by 3 inches. The second sample (M6) was collected from an approximately 2-inch by 3-inch nodular area on the pipe surface located approximately at the 9 o'clock position. This location was about one foot downstream of GWD217720. Each sample of collected material was added to a preservative liquid in separate anaerobic diluting solution (ADS) bottles, and the solution from these ADS bottles was used for microbiological testing.

Test kits (Number 4) from Dixie Testing and Products, Inc., Houston, Texas, were used for the NTSB microbiological tests. The test kit bottles were inoculated to test for viable bacteria belonging to four types of bacterial groups. Samples M5, M6, and a negative control were used to inoculate the kits with a 5-decade serial dilution by volume. Inoculations were completed within 90 minutes of sample collection. A control test was also conducted. Results from observations on September 8 and 22, 2010, are combined and summarized in table 2. The control sample showed negative reactions in all bottles.

Table 1. Microbiological Test Results from EPA Tests

Bacteria Type	Area M1 Results (viable bacteria/ml)	Area M3 Results (viable bacteria/ml)	Area M4 Results (viable bacteria/ml)
Sulfate Reducing	Negative	Negative	Negative
Anaerobic or Facultatively Anaerobic	1,000 to 10,000	≥100,000	≥100,000
Organic Acid Producing	Negative	≥100,000	≥100,000
Low Nutrient	Negative	≥100,000	≥100,000
Iron-Related	Negative	1,000-10,000	≥100,000

Table 2. Microbiological Test Results from NTSB Tests

Bacteria Type	Sample M5 Results (viable bacteria/ml)	Sample M6 Results (viable bacteria/ml)
Sulfate Reducing	Negative	Negative
General Anaerobic	1 to 10	10 to 100
Anaerobic - Acid Producing	Negative	Negative
Aerobic – Acid Producing	10 to 100	Negative

D.2. Coating

The coating on the pipe pieces was specified as a Polyken 960-13 tape. The tape was spiral-wrapped, with the upstream wrap overlapping the downstream wrap. The tape had a nominal 18-inch width, and the overlap width measured at approximately top dead center ranged from 1.25 inches to 1.75 inches.

According to available data provided by the pipeline operator after an extensive records search, the tape coating for line 6B was applied in the field by a machine. The specified minimum and maximum overlap was 0.5 inch and 1.0 inch, respectively. The tape application specification included a Polyken 919 primer that was applied to a clean pipe surface in a thin, rapid-drying film.

Views of typical coating features are shown in figures 5 to 8. Longitudinally-oriented wrinkles were observed in the coating mostly near the 3 o'clock and 9 o'clock positions. Wrinkling was most severe at the 3 o'clock side near the longitudinal seam for joint 217720 at positions starting approximately 9 feet from girth weld GWD217720 up to girth weld GWD217730. A view of wrinkles at the 3 o'clock position on piece B is shown in figure 5. Wrinkled areas generally had a soft feel when pressed inward. In many areas, the coating also showed bulging at the upstream edge of the tape overlap generally near the 3 o'clock to 5 o'clock positions such as shown in figure 6.

Isolated round bulges in the coating were also observed primarily from the 3 o'clock position clockwise to the 10 o'clock position. These areas were generally firm to the touch when pressed inward. The nodules were generally larger with more space between nodules at the lower quadrant of the pipe with typical diameters ranging from approximately 0.25 inch to 0.5 inch, as shown in figure 7. At the side and upper quadrants, the nodules were spaced closer together and were approximately 0.25 inches or less in diameter. The nodules were generally smaller and less prominent from 8:30 o'clock to 12 o'clock and were minimal from 12 o'clock to 3 o'clock, as shown in figure 8.

Coating adhesion was tested using ASTM Standard D6677-01, *Standard Test Method for Evaluating Adhesion by Knife*.⁶ In the test, a utility knife was used to cut an X shape into the coating, with each leg of the X at least 1.5 inches long at an included angle of 45°. A utility knife was then used to lift the tape at the apexes of the 45° angles between the legs of the X back approximately 0.25 inch. The tape was then pulled back by nitrile-gloved fingers until the tape slipped out from the grip. The tape pulled back approximately 0.5 to 0.75 inch, corresponding to a rating of 2 according to table I in ASTM D6677-01. Adhesive from the tape remained largely adhered to the pipe. In two locations, the adhesion test was conducted on the tape overlap, and adhesion between layers of tape was tested. In these cases, the tape pulled back approximately 1.2 to 1.6 inches, and the adhesive layer remained attached to the tape layer that was peeled back.

The width of the coating tape was measured with a tape measure, and results are listed in table 3. At locations 2.8 and 6 feet from GWD217720, the tape was intact around at least 180 degrees in either circumferential direction from the location of the measurement. At locations 11.5 and 40.5 feet from GWD217720, the tape had been removed in the vicinity of the girth weld before the measurement. According to the tape manufacturer, a coating with an 18-inch nominal width would have a variation in width of $\pm 1/16$ inch, and when applied with the recommended tension, the width of the tape should decrease by 1 to 2 percent.

Table 3. Coating Tape Width Measurements

Position Lengthwise from GWD217720 (feet)	Circumferential Position	Coating Width (inches)
2.8	1 o'clock	18.0
6	5 o'clock	18.0
11.5	1 o'clock	18.0
40.5	11 o'clock	18.1

D.3. Coating Removal and Cleaning

The coating was removed from most of the surfaces on piece B, including the entire length of the longitudinal seams and most of girth weld GWD217730. The coating was also removed from most of the length of the longitudinal seams on piece A and part of girth weld GWD217720. Coating material was generally removed by cutting a longitudinal line away from areas of interest, then peeling the wrap back by hand or with a pair of pliers. In areas of wrinkles near the rupture area, a thick pasty white material was observed as the coating was removed. Views of this material are shown in

⁶ Annual Book of ASTM Standards, ASTM International (2004).

figure 9. In areas where nodules were observed, a powdery white material was observed. A view of the coating partially removed is shown in figure 10 with nodule material adhered to the pipe surface and to the removed coating material. When the nodule material was cleaned from the surface of the pipe, shallow areas of metal loss were observed.

Portions of the pipe pieces were cleaned using grit blasting. The outer surfaces were initially cleaned using 70 grit Olivine at 80 psi output pressure. The 80 psi output pressure setting did not acceptably remove adhesive that remained attached to the pipe surfaces, and the pressure was increased to 90 psi, which provided acceptable results. During cleaning, the fracture surfaces were protected with rubber hoses, and an area within 12 inches of the fracture surfaces was covered with carpet with the edges sealed with heavy-duty tape. Areas of the pipe, including markings such as the location of top dead center, were also covered with tape during the cleaning. Cleaned areas included all longitudinal seams and adjacent surfaces on piece B, most of the length of the longitudinal seam in piece A, portions of girth welds GWD217720 and GWD217730, and an area of the side wall on piece B where mechanical test specimens were fabricated.

Areas of metal loss due to corrosion were observed near the longitudinal seam in cleaned areas on piece B, both along the longitudinal seam for joint 217720 and joint 217730 and in the girth weld between the two longitudinal seams. Areas of corrosion generally appeared larger to the clockwise side of the seam.

D.4. Nondestructive Inspection

Nondestructive examination of the cleaned pipe external surfaces was completed by Eastern NDT, Hopewell, Virginia. Areas of the pipe surfaces that had been grit-blasted were examined using magnetic particle inspection (MPI). Clusters of longitudinally-aligned parallel crack indications were observed in areas of corrosion adjacent to the longitudinal seam in joint 217720, features associated with stress-corrosion cracking (SCC). Cracks were detected both clockwise and counterclockwise from the longitudinal seam in 17 areas downstream of the rupture to the girth weld as shown in figure 11. Areas where cracks were detected were denoted using parenthesis marks that were drawn on the surface of the pipe at either end of the clusters. The crack clusters did not necessarily have a continuous crack within the regions indicated. Clusters of crack indications were also detected in areas of corrosion at the clockwise side of the longitudinal seam upstream of the rupture at locations from 21 feet to 23.5 feet from the upstream girth weld. In piece A, clusters of crack indications were detected in three areas from 10.5 feet to 13.5 feet from the upstream girth weld also in areas of corrosion on the clockwise side of the longitudinal seam. Close views of several areas where clusters of crack indications were observed are shown in figures 12 and 13. Longitudinally-oriented faint crack indications were also detected within the weld bead in girth weld GWD217730 in areas shown circled in figure 11.

No crack indications were detected using MPI near the longitudinal seam in joints 2177210 or 217730, and no crack indications were detected in areas of the pipe wall inspected away from the longitudinal seam. However, crack-like features and corrosion were visible at the weld toes for the longitudinal seam in joint 217730. According to the ASNT Level III-certified inspector conducting the MPI, these features at the weld toes are not typically detected or noted as indications during MPI. Figure 14 shows an oblique view of the longitudinal seam where corrosion and crack-like features are visible at the toe of the weld on the clockwise side of the weld.

Several locations with stronger crack indications from the MPI were selected for inspection using an NDT Systems, Inc. (Huntington Beach, California) Avenger ultrasonic flaw detector to estimate crack depths. Results of this inspection for the area shown in figure 13 are shown in figure 15. Crack depths measured to the nearest 0.001 inch were marked with permanent marker on the surface of the pipe as shown in figure 15. The deepest crack penetration was estimated to be 0.187 inch in the area shown in figure 15, which was located clockwise from the longitudinal seam between approximately 11 feet 0 inches and 11 feet 11 inches from GWD217720. Areas shown in figure 12 (shown as viewed before testing) had maximum detected crack penetration values of 0.184 inch in the area of the upper photo and 0.183 inch in the area of the lower photo. The area shown in the upper photo in figure 12 was located counterclockwise from the longitudinal seam between approximately 36 feet 11 inches and 37 feet 4 inches from GWD217720. The area shown in the lower photo in figure 12 was located clockwise from the longitudinal seam between approximately 38 feet 4 inches to 39 feet 1 inch from GWD217720.

D.5. Sectioning and Cleaning

Using a plasma torch, four areas from piece B and one area from piece A were cut from the remainder of the pipe pieces for further examination and handling at the NTSB Materials Laboratory. Pieces were labeled A1 and B1 to B4. Piece A1 contained a length of the longitudinal seam from piece A where crack indications were detected. Piece B1 was a section of the longitudinal seam from joint 217730. Piece B2 was a length of the longitudinal seam downstream of the rupture and a portion of girth weld GWD217730 where crack indications were detected. Piece B3 was a section of the wall selected for baseline mechanical testing. Piece B4 contained the rupture. All cleaned surfaces were sprayed with WD-40 once cutting was complete to preserve the surfaces until further work was to be completed.

Piece B4 was cleaned using a combination of acetone, trichloroethylene, soft-bristle brushes, paper towels, and lint-free wipes. In areas away from corrosion, cracks, and fracture features, a wood wedge was used to scrape adhesive from the surface before cleaning. Overall views of the exterior and interior of piece B4 after cleaning are shown in figure 16.

D.6. Fractography of Rupture

Circumferential cuts were made from the counterclockwise edge of piece B4 intersecting the fracture surface near the ends of the rupture, thereby separating the counterclockwise fracture face from the mating face. One cut intersected the fracture face approximately 4.4 inches from the upstream end of the rupture and the other cut intersected the fracture face approximately 2.7 inches from the downstream end of the rupture. The 6-foot-1.25-inch-long separated piece was labeled B4-1. Fracture features on the counterclockwise fracture surface were cleaned using trichloroethylene, acetone, a soft-bristle brush, and lint-free wipes. Oil on the mating fracture surface was left in place.

The fracture surface was examined visually and photographed. Flat fracture regions with curving boundaries on slightly offset planes were observed, consistent with preexisting cracks emanating from multiple origins at the exterior surfaces. Evidence of preexisting cracks at various penetration depths was observed across nearly the entire length of the fracture surface on piece B4-1. An approximately 2-inch wide area of slant fracture across the thickness was the longest region observed without preexisting crack features. The area of deepest preexisting crack penetration relative to the local wall thickness was located 50.25 inches from the upstream end of the fracture. This area also closely corresponded to the location of the widest crack opening displacement measured at 4 feet from the upstream end of the fracture. At this location, the fracture face was located 1.38 inches clockwise away from the centerline of the longitudinal seam.

A continuous series of preexisting cracks were present at the outer edge of the fracture surface up to 10.8 inches upstream and 7.9 inches downstream of the area of deepest penetration. At the upstream end of the continuous series of preexisting cracks, the fracture surface intersected the outer surface at a slant angle over a distance of 0.2 inch before intersecting the next preexisting crack. At the downstream end of the continuous series of preexisting cracks, the fracture surface intersected the outer surface at a slant angle over a distance of 1 inch before intersecting the next preexisting crack.

Next, piece B4-1 was cut into 4 pieces labeled B4-1a to B4-1d to facilitate examination of the continuous series of preexisting cracks in the region of deepest penetration. Two circumferential cuts were made at either end of the continuous series of preexisting cracks, and then a longitudinal cut was made approximately 2 inches counterclockwise from the longitudinal seam. An overall view of the pieces as cut is shown in figure 17. The piece with fracture features examined further was labeled B4-1c.

Fracture features were cleaned progressively using trichloroethylene, acetone, and a solution of Alconox detergent in hot water and gentle scrubbing with a soft-bristle brush. A close view of the fracture surface after this cleaning procedure is shown in figure 18. Black oxide was observed on the flat fracture features consistent with oxidation in an oxygen-poor environment such as a preexisting crack.

Piece B4-1c was cut circumferentially at two locations using an abrasive cut-off saw to facilitate further cleaning and examination using scanning electron microscopy (SEM). The 3 pieces were labeled B4-1c-i, B4-1c-ii, and B4-1c-iii, as shown in figure 19.

Pieces were cleaned using different methods to remove oxides to facilitate further examination of fracture surfaces and adjacent pipe surfaces. Piece B4-1c-iii was first submerged in Evapo-Rust⁷ for 1 hour and 15 minutes then examined. To further facilitate oxide removal, piece B4-1c-iii was submerged in inhibited acid⁸ and lightly scrubbed with a soft-bristle brush for 5 minutes and then resubmerged in Evapo-Rust for 5 minutes. Pieces B4-1c-i and B4-1c-ii were submerged in inhibited acid and lightly scrubbed with a soft-bristle brush for approximately 5 minutes, rinsed in water, and then submerged in Evapo-Rust for 5 minutes, removed, and dried.

D.6.a. Cleaned Fracture Features

Close views of the fracture surface and the adjacent outer surface on piece B4-1c-ii in the area of deepest crack penetration after oxide removal are shown in figures 20 and 21. A closer view of the area of deepest penetration is shown in figure 22. Flat fracture features with curving arrest lines and boundaries were observed extending across up to approximately 81 percent of the wall thickness across the fracture face. The total wall thickness at this location as measured across the fracture face was 0.217 inch. Transgranular fracture features in planes perpendicular to the wall surfaces emanated inward from corrosion pits at the exterior surface consistent with preexisting cracks such as near-neutral-pH SCC or corrosion-fatigue.^{9,10,11} The extent of preexisting crack propagation in the area of deepest penetration is indicated with a dashed line in figure 22. The remainder of the fracture surface across the remaining 19 percent of the fracture face had matte gray rough fracture features on a slant plane consistent with overstress fracture.

The fracture surfaces of piece B4-1c-ii were examined using SEM, and views of the fracture surface near the area of deepest preexisting crack penetration are shown in figures 23 through 26. Fine crack arrest features such as those shown in figures 24 and 25 were typically observed within approximately 0.015 inch of the crack origins. Further from the origins, broad crack arrest features were observed such as those shown in figure 26. Crack arrest features are indications of preexisting cracks and can be associated with SCC or corrosion-fatigue. Microstructural features were also observed on the fracture surface and were oriented in planes generally parallel to the pipe inner and outer surfaces. Areas where the fracture intersected pearlite in the microstructure appeared brighter and rougher than areas corresponding to ferrite. These features

⁷ Evapo-Rust is manufactured by Harris International Laboratories, Springdale, Arkansas.

⁸ A solution of 500 ml hydrochloric acid, 500 ml water, and 3.5 g hexamethylenetetramine.

⁹ National Energy Board Report of the Inquiry MH-2-95, *Public Inquiry Concerning Stress Corrosion Cracking on Canadian Oil and Gas Pipelines*, National Energy Board Canada (1996).

¹⁰ *Fractography*, Metals Handbook, Ninth Edition, Vol. 12, ASM International (1987).

¹¹ J. I. Dickson and J. P. Bailon, *The Fractography of Environmentally Assisted Cracking*, Time Dependent Fracture: Proceedings of the Eleventh Canadian Fracture Conference, Ottawa, Canada (1984).

appeared on the fracture surfaces as alternating bands of brighter and darker areas that were oriented with the long direction of the bands parallel to the axis of the pipe.

D.6.b. Crack Depth Profile

A crack profile was created for the length of the rupture between the cuts made to remove piece B4-1. The fracture surface was examined at 0.25-inch increments, and within each increment, the maximum depth of preexisting crack propagation, corrosion depth, and local wall thickness was measured. Measurements were conducted on a Keyence model VHX-1000 microscope with a 20x setting on the objective zoom lens. With that setting on the lens, approximately a 0.6-inch length of the fracture surface was viewed on the 14.5-inch wide screen, allowing measurement of 2 increments. Whenever possible, a reference line was set for each pair of increments corresponding to the highest points on the exterior wall surface, and measurements for the 2 increments were made from that reference line. For some increment pairs, a separate reference line was required for each increment if the plane of fracture showed large step changes within the field of view. The pipe inner wall surface adjacent to the fracture showed reduction in area deformation consistent with ductile fracture, and measurements of local wall thickness were made from the reference line on the outer surface to the inner surface of the wall where the wall was thickest slightly below the plane of fracture as viewed under the microscope. Local wall thickness measurements were consistent with spot checks of thickness measured using a Vernier caliper at the fracture face. The maximum depth of preexisting crack penetration was measured within each 0.25-inch increment as measured from the same reference line used to measure local wall thickness. Corrosion depth was measured at the location of maximum crack penetration and did not necessarily represent the maximum depth of corrosion within the particular increment. A ball-flat micrometer was used to measure the wall thickness in areas where no metal loss was apparent adjacent to the areas of metal loss and cracking, and the average thickness was 0.254 inch. The difference between the micrometer measurement value and the local wall thickness measurement at the fracture plane value was added to the measured corrosion depth and the measured crack depth to obtain a total crack depth and metal loss depth relative to the estimated original external surface.

Results of the crack depth and external metal loss measurements are shown in the graph in figure 27. As shown in the graph, the maximum depth of penetration of the crack relative to the approximate original exterior wall surface was 0.213 inch at a location approximately 344 inches away from GWD217720. Figure 27 also shows results from the 2004 ultrasound wall measurement (USWM) and 2005 ultrasound crack detection (USCD) in-line inspection (ILI) tools. For more details regarding the ILI data, see section D.15 of this report.

D.6.c. Metallographic Examination

Two areas on piece B4-1c-iii were selected for metallographic preparation of circumferential cross-sections intersecting the fracture surface and secondary cracks adjacent to the fracture surface. The locations of the two metallographic mounts are

indicated by MM1 and MM2 in figure 19. Polished cross-sections were etched using 2 percent Nital etchant. Views of typical crack features in the mounted cross-sections are shown in figures 28 and 29. Multiple closely-spaced cracks with transgranular propagation paths and limited crack branching were observed, features consistent with near-neutral-pH SCC or corrosion-fatigue. The deepest of the secondary cracks shown in figure 28 extended through approximately 43 percent of the wall thickness.

D.7. Lab Fractures

Lab fractures were conducted to open cracks detected by NDI in 3 selected locations on the pipe. Samples were cut from pieces A1 (joint 217720 upstream of the rupture) and B2 (joint 217720 downstream of the rupture). Areas were selected that showed relatively stronger crack indications in the NDI results and also included the area where the 2005 ILI data showed the deepest crack-like feature within the ruptured joint. Views of the selected samples are shown in figures 30 to 32. Sample A1d2 shown in figure 30 was approximately 12.4 inches long with the upstream end located 10 feet 11.4 inches downstream from girth weld GWD217720. Sample B2b2 shown in figure 31 was approximately 11.3 inches long with the upstream end located 36 feet 5.5 inches from girth weld GWD217720. Sample B2d2 shown in figure 32 was approximately 9.8 inches long with the upstream end located 38 feet 3.5 inches downstream from girth weld GWD217720.

Transverse cuts were made in each of the lab fractures to divide the samples to be opened into approximately 2 to 3 inch lengths. Sample A1d2 was cut into 5 pieces numbered i to v, and samples B2b2 and B2d2 were each cut into 4 pieces numbered i to iv. Each sample was then soaked in liquid nitrogen for several minutes until temperature equilibrated. Samples were then placed with one end in a vice, and the opposite end was struck with a hammer.

Overall views of the lab-fractured specimens are shown in figure 33. Sample B2d2iv was the first sample to be fractured. In the case of sample B2d2iv, the specimen was placed in the vice with the vice clamped on the seam. The fracture appeared to initiate at the toe of the weld at the edge of the sample rather than at a crack. The remaining samples were all clamped on the pipe wall adjacent to the area of cracking with the seam located outside of the clamp. Sample B2b2i was not fractured.

D.7.a. Fractography

Overall views of the fracture surfaces are shown in figures 34 to 36. Each fracture surface showed dark areas with curving boundaries consistent with preexisting cracking such as SCC or corrosion-fatigue. Cracks emanated from multiple origins at the outer surface. The maximum depth of crack penetration was 69 percent, 50 percent, and 45 percent of the wall thickness in lab fractures from samples A1d2, B2b2, and B2d2, respectively.

Piece A1d2iii was selected for additional cleaning to reveal fracture features obscured by corrosion. Piece A1d2iii was submerged in inhibited acid and lightly

scrubbed with a soft-bristle brush for approximately 5 minutes, rinsed in water, and then submerged in Evapo-Rust for 5 minutes. An SEM view of the cleaned fracture surface in the area of deepest penetration is shown in figure 37, and closer views of features near one of the origin areas are shown in figures 38 and 39. Features observed on crack surfaces from this lab fracture were similar to those observed by SEM on the rupture surface. Relatively fine crack arrest features such as those shown in figure 39 were observed within approximately 0.032 inches of the origins. Further from the origin, broad crack arrest features were observed similar to those shown in figure 26 for the rupture fracture surfaces. Fracture features were consistent with near-neutral-pH SCC or corrosion-fatigue. Microstructural features were also observed on the fracture surface and were oriented in planes generally parallel to the pipe inner and outer surfaces.

D.7.b. Crack Profile

A crack depth profile along the length of sample A1d2 was created from lab fractures of pieces from sample A1d2. Methods used to create the crack profile for the rupture as described in section D.6.b were also used to create the crack profile for sample A1d2, but the average wall thickness measured using a ball-flat micrometer in adjacent areas appearing free of metal loss was 0.268 inch. Results of the crack depth and external metal loss measurements are shown in the graph in figure 40.

As shown in figure 40, the maximum depth of crack penetration relative to the estimated original wall surface was 0.194 inch at a location 137 inches from GWD217720. Results from the 2004 USWM and 2005 USCD ILI tools are shown also in figure 40. For more details regarding the ILI data, see section D.15 of this report.

D.8. Metallographic Examination of Joint 217730

Piece B1 was cut, as shown in figure 41, with longitudinal cuts above and below the longitudinal seam followed by transverse cuts near the middle of the piece to prepare sample MM3 for metallographic examination of crack-like features at the weld toe of the longitudinal seam of joint 217730. The sample was mounted, polished, and etched with 2 percent Nital. The resulting microstructure at the weld toes are shown in figure 42. As indicated in figure 42, the crack-like features observed visually at the weld toe showed blunt-tipped notch-shaped cross-sections consistent with corrosion at the toe of the weld. No cracks were detected in the cross-sections.

D.9. Thickness and Metal Loss Measurements

Thickness was measured at 5 locations around the circumference of the pipe at each of 3 positions along the length of the pipe joint using a Krautkramer Branson DME DL ultrasonic thickness gauge. Thickness was also measured at the same locations using a ball/flat micrometer in cases where the measurement location was adjacent to a cut surface. All measurements were taken in areas with coating removed and appearing free of corrosion. Thickness varied from 0.283 inch measured at 8 feet from

GWD217720 to 0.255 inch measured at 34.5 feet from GWD217720. Results of these measurements are listed in Table 4.

Table 4. Pipe Wall Thickness Measurements

Distance from GWD217720 (feet)	Circumferential Location (clock)*	Thickness: Ultrasound Measurement (inch)	Thickness: Micrometer Measurement (inch)
8	12	0.282	0.281
8	AW – CCW	0.279	0.277
8	AW – CW	0.279	0.276
8	6	0.281	0.279
8	9	0.283	0.282
23	12	0.264	
23	AW – CCW	0.260	0.258
23	AW – CW	0.261	0.257
23	6	0.261	
23	9	0.263	
34.5	12	0.260	0.261
34.5	AW – CCW	0.260	
34.5	AW – CW	0.255	
34.5	6	0.257	
34.5	9	0.262	

*"AW - CCW" indicates adjacent to the longitudinal seam weld to the counterclockwise side, and "AW – CW" indicates adjacent to the longitudinal seam weld to the clockwise side.

Additionally, thickness was measured using a ball/flat micrometer in areas that appeared to be free of corrosion on pipe pieces sectioned for lab fractures, metallurgical examination, or fractography. In pieces B4-1a, B4-1c, and B4-1d, the average thickness was 0.2577 inch and 0.2537 inch counterclockwise and clockwise from the longitudinal seam, respectively. In pieces B2b2 and B2d2, average thickness was 0.2563 inch and 0.2580 inch counterclockwise and clockwise from the longitudinal seam, respectively. In piece A1d2i, the average thickness was 0.2659 inch counterclockwise from the longitudinal seam, and the measured thickness was 0.2680 inch clockwise from the longitudinal seam. In piece B1b3 (joint 217730), the measured thickness was 0.2635 inch and 0.2637 inch counterclockwise and clockwise from the longitudinal seam.

Wall thickness was measured in corroded areas adjacent to the rupture and the lab fractures on several of the sectioned pieces and on intact pieces cut from joint 217730. Measurements were conducted with a point micrometer in areas within reach of the micrometer (approximately 1 inch or less from the fracture or the edge of the piece). Within each piece, measurements were conducted at the base of crater features that visually appeared deepest.

On piece B4-1c-ii, thickness was measured in the corroded area between the fracture and the longitudinal seam. The minimum thickness measured was 0.2161 inch, and the average thickness of 6 measurements was 0.2277 inch. Four measurements were also taken on the relatively smooth area directly adjacent to the longitudinal seam, and the average thickness in this area was 0.2517 inch.

On piece B2b2ii, the minimum thickness measured was 0.2136 inch, and the average of 4 measurements was 0.2180 inch. On piece B2b2iii, the minimum thickness within 1 inch of the fracture was 0.2156 inch and the average of 4 measurements was 0.2193. In one area further from the fracture on piece B2b2iii, the wall thickness at the base of one pit measured 0.1961 inch. On piece B2b2iv, the minimum thickness within 1 inch of the fracture was 0.2135 inch, and the average of 4 measurements was 0.2203 inch. Further from the fracture on piece B2b2iv, the wall thickness at the base of one pit measured 0.1814 inch.

On piece B2d2ii, the minimum thickness was 0.1852 inch, and the average of 11 measurements was 0.2144 inch. On piece B2d2iii, the minimum thickness was 0.1965 inch, and the average of 7 measurements was 0.2196 inch.

On piece A1d2iii, the minimum thickness within 1 inch of the fracture was 0.2299 inch, and the average of 7 measurements was 0.2366 inch. Further from the fracture, the minimum thickness measured in several areas of corrosion was 0.2212 inch.

In two areas on piece B4-1d, pit depths were measured with a pit depth gage in areas that could not be reached with the point micrometer. The pit depths for these two pits were 0.078 inch and 0.067 inch.

On piece B1b1 (joint 217730), the minimum thickness was 0.2073 inch, and the average of 9 measurements was 0.2159 inch. On piece B1b3, the minimum thickness was 0.2164 inch, and the average of 17 measurements was 0.2210 inch.

D.10. Coating Chemical Analysis

A sample of coating material, labeled Sample A2, was removed from pipe piece A and was sent for chemical analysis at Jordi Labs, an independent laboratory located in Bellingham, Massachusetts. Tests were conducted to determine the composition of the adhesive and the backing material. The tape backing component of the coating was analyzed using temperature rising elution fractionation (TREF), thermogravimetric analysis (TGA), and liquid chromatography mass spectroscopy (LCMS). The adhesive component of the coating was analyzed using Fourier transform Infrared spectroscopy (FTIR), pyrolysis gas chromatography mass spectroscopy (PYMS), nuclear magnetic resonance spectroscopy (NMR), and LCMS (the method also used to analyze the backing).

Results of the analysis of the tape backing showed that the backing was a blend of low density polyethylene (LDPE) and high density polyethylene (HDPE) containing

38 percent HDPE as determined using TREF. The TGA results showed the tape backing contained 0.99 percent carbon black. The LCMS results showed that the tape backing contained several common polymer additives including oleamide, stearic acid, Irgafos 38, and Ethyl Antioxidant 720.

The analysis of the adhesive showed the adhesive was composed of polyisoprene and polyisobutylene as determined from the FTIR, PYMS, and NMR results. The PYMS results showed the presence of limonene, which is a pyrolysis product and strong indicator of polyisoprene. The FTIR results showed a spectrum consistent with polyisoprene with an additional strong peak near 1000 cm^{-1} , which is generally attributed to C-O-C stretching in ethers or Si-O stretching in silicates. The presence of polyisobutylene was not easily detected by PYMS or FTIR, but NMR results showed the adhesive contained a polyisobutylene to polyisoprene ratio of 5.25 to 1. LCMS results showed that extractable components specific to the adhesive generally could only be identified by mass alone.

D.11. Mechanical Testing and Chemical Analysis

A piece from the pipe wall from joint 217720 labeled B3a was cut from piece B3 and sent to Lehigh Testing Laboratories, an independent laboratory in New Castle, Delaware, for tensile tests, Charpy impact tests, and chemical analysis. In addition, a piece labeled A1a was cut from piece A1 in an 8-inch long area, including the longitudinal seam where no corrosion was observed and no cracks were detected by NDI, and that piece (piece A1a) was sent to Lehigh Testing Laboratories for tensile testing of the longitudinal seam. A piece of the pipe wall from joint 217730 (piece B1a) was also sent to Lehigh Testing Laboratories for chemical analysis. Tensile tests and Charpy impact tests were conducted in accordance with ASTM Standard A370-07, *Standard Test Methods and Definitions for Mechanical Testing of Steel Products*.¹² Tensile specimens were full size, and Charpy impact test specimens were sub-standard size with dimensions of 5 mm by 10 mm by 55 mm in accordance with the standard. Chemical analysis was conducted in accordance with the applicable requirements of ASTM Standard A20/A20M-07, *Standard Specification for General Requirements for Steel Plates for Pressure Vessels*. Results of all tests are included in appendix B at the end of this report.

Results of tensile tests of three transverse tensile specimens from piece B3a showed an average yield strength (0.5 percent extension under load method) of 61,400 pounds per square inch and an average tensile strength of 82,400 pounds per square inch. Average total elongation in 2 inches was 26 percent. Tensile properties of all three test specimens conformed to the requirements for yield strength, tensile strength, and elongation of X52 pipe as specified in the 1968 API Standard 5LX, *Specification for High-Test Line Pipe*.

¹² Annual Book of ASTM Standards, ASTM International, 2007.

Tensile tests of 3 tensile specimens across the longitudinal seam from piece A1a showed an average tensile strength of 82,400 pounds per square inch. All 3 tensile tests across the longitudinal seam resulted in fracture in the base metal.

Charpy impact tests were completed on 18 specimens fabricated from piece B3a tested at 9 temperatures ranging from -20 °F to 120 °F with 2 specimens tested at each temperature. Results of Charpy impact tests are shown plotted in figure 43. Average impact energy ranged from 6.5 foot pounds at -20 °F to 20 foot pounds at 120 °F.

Chemical analysis was completed on pieces from joint 217720 and 217730, and results are listed in appendix B. Chemistry of each sample conformed to the requirements for carbon, sulfur, phosphorus, and manganese content of X52 pipe as specified in the 1968 API Standard 5LX, *Specification for High-Test Line Pipe*. The chemistry of each sample also conformed to a requirement for a maximum allowable combination of carbon and manganese content that was specified on the purchase order for the pipe.

D.12. Residual Stress Measurements

Two ring sections of pipe were torch-cut from the pipe pieces at the NTSB Materials Laboratory for residual stress testing. One piece labeled A3 was cut from piece A at a location 8 feet 4 inches to 9 feet 6 inches from GWD217720. The other piece labeled B5 was cut from piece B at a location 40 feet 11 inches to 42 feet 2 inches from GWD217720. Pieces A3 and B5 were from separate joints with A3 within the ruptured joint 217720, and B5 from joint 217730, located just downstream of the ruptured joint. The two ring sections were sent to Lambda Research, Inc., an independent laboratory in Cincinnati, Ohio, for measurement of residual stresses. The full lab report from Lambda Research is included in appendix C at the end of this report.

Sites at five locations on pipe pieces A3 and B5 were selected for residual stress measurement using the ring core method. Selected sites were located at least 4 inches away from the nearest circumferential cut and were within areas that were free of visible wall metal loss. In the ring core method, a strain gage was attached to the surface, and a 0.3-inch-diameter core was drilled around the gage. Changes in strain were measured as the core was incrementally drilled to a depth of 0.10 inch.

On piece A3, three sites were selected and labeled RS1 to RS3. Site RS1 was located 8 feet 9 inches from GWD217720 at a location 2 feet 11 inches circumferentially counterclockwise away from the longitudinal seam (near the top of the pipe). Sites RS2 and RS3 were located 8 feet 10 inches and 9 feet 1 inch from GWD217720, respectively, and were both located approximately 1 inch above the longitudinal seam centerline. Sites RS1 and RS2 were located within areas of the pipe where coating material was chemically removed, but pipe surfaces remained as-received. Site RS3 was located in an area that had been cleaned by grit blasting.

On piece B5, 2 sites were selected and labeled RS4 and RS5. Sites RS4 and RS5 were located 41 feet 6 inches and 41 feet 4 inches from GWD217720, respectively.

Site RS4 was located 3 feet 1 inch circumferentially counterclockwise away from the longitudinal seam (near the top of the pipe). Site RS5 was located approximately 0.5 inch above the seam centerline. Site RS4 was located within an area of the pipe where the coating material was chemically removed, but the pipe surface remained as-received. Site RS5 was located within an area that had been cleaned by grit blasting.

Results of the residual stress measurements are contained in the Lambda Research report included in Appendix C at the end of this report. In comparing results for sites RS2 and RS3, the effect of the grit blast cleaning on the residual stress is evident. At site RS2 with a chemically-cleaned surface, the residual stress profile in the hoop direction was a tensile stress of approximately 7.2 ksi to 10.3 ksi. However, at site RS3 with a grit-blast-cleaned surface, the residual stress profile in the hoop direction was compressive at -42.4 ksi near the surface, near neutral at a depth of 0.06 inch, and then increased up to a tensile stress of 1.1 ksi at depths greater than 0.06 inch.

In comparing results for sites RS1 and RS2, differences in location relative to the weld are apparent for chemically-cleaned surfaces. At site RS1 near the top of the pipe, the residual stress profile in the hoop direction varied from near neutral near the surface to a maximum tensile stress of 4.7 ksi, whereas at site RS2 near the weld, the residual stress profile in the hoop direction was a tensile stress of 7.2 ksi to 10.3 ksi.

Differences between the hoop stresses in piece A3 (from the ruptured joint) and piece B5 (from the adjacent joint downstream) are highlighted in comparing results between sites RS1 and RS4. Both sites RS1 and RS4 were located in chemically-cleaned areas located near the top of the pipe. The residual stress profile in the hoop direction at site RS4 was compressive at -7.0 ksi near the surface, neutral at a depth of 0.01 inch, and showed a maximum tensile stress of 1.5 ksi. At site RS1, the residual stress profile in the hoop direction was near neutral at 0.005 inch from the surface and increased to a maximum tensile stress of 4.7 ksi. In the grit-blast cleaned sites near the weld, site RS3 on the ruptured joint showed a compressive residual stress near the surface, near neutral stress at a depth of 0.06 inch, and a maximum tensile stress of 1.1 ksi at greater depths. Site RS5 in the downstream joint showed more compression at the surface and showed compressive residual stresses in the hoop direction throughout the profiled depth.

D.13. Hardness Measurements

Hardness measurements were conducted on mounted samples used for metallographic examination of the rupture site and of the longitudinal seam of joint 217730. Hardness was measured using a Rockwell indenter in the base metal away from the heat affected zone of the welds within each sample. Five hardness tests were conducted on each sample, and the reported hardness for each sample was the average of the five hardness measurements. For the two mounted samples from joint 217720, the hardness was 79.6 HRB and 81.7 HRB for mounts MM1 and MM2, respectively. For the mounted sample from joint 217730, the hardness was 81.8 HRB.

D.14. Corrosion Samples

Samples of corrosion product were collected from the pipe surfaces as coating was removed during the group examination as described in Section D.3. Four samples were collected from pipe piece B and were labeled B1 to B4. Sample B1 was collected from nodule features near the 5 o'clock position near the rupture area. Sample B2 was collected from an area located at the upstream end of the rupture. Sample B3 was collected from corrosion at a tape overlap near the longitudinal seam approximately 36.5 feet from girth weld GWD217720. Sample B4 was removed from adjacent to the longitudinal seam in the downstream joint 217730 approximately 1.5 feet from GWD217730.

All four samples had a white to yellow-white appearance when initially exposed and then began to turn more reddish-brown with longer exposure to the lab environment. The samples were collected into sealed plastic bags, and when analyzed several months later, the samples all had a reddish-brown appearance. Samples B1 to B3 had a powdery consistency and were easily crushed to a finer powder with tweezers. Sample B4 had a more solid consistency and was not easily crushed. However, when scraped with a scalpel, sample B4 crumpled easily into a powdery consistency.

Portions of the collected samples were analyzed using energy dispersive x-ray spectroscopy (EDS), and typical spectra observed are shown in figure 44. Each of the samples showed spectra (see the upper spectrum in figure 44) that typically showed high peaks of iron and oxygen with smaller peaks of carbon and manganese across most of the surfaces analyzed. In sample B2, some areas also showed a small peak of sulfur such as shown in the middle spectrum in figure 44. In one area of sample B2, small peaks of silicon and aluminum were also detected, and in this area, the peak for iron was relatively higher and the peak for oxygen was relatively lower than in other areas. In some areas of sample B4, a peak of aluminum was observed and was usually associated with relatively higher peaks of iron and carbon such as shown in the lower spectrum in figure 44. One area on sample B4 also showed peaks of silicon and sulfur.

D.15. In-Line Inspection (ILI) History

Line 6B was inspected in years before the rupture with several different ILI tools including the following.

- 2004: GE Oil & Gas UltraScan™ WM (USWM) ultrasonic wall measurement tool
- 2005: GE Oil & Gas UltraScan™ CD (USCD) ultrasonic crack detection tool
- 2007: GE Oil & Gas MagnaScan™ magnetic flux leakage (MFL) tool
- 2009: GE Oil & Gas USWM ultrasonic wall measurement tool
- 2009: BJ Pipeline Inspection Services Vectra™ MFL tool

Four different geometry tools were also run during that time period. At the time of the rupture, an inspection using a GE Oil & Gas UltraScan™ CD+ tool was in progress, but the tool had not yet passed the location of the rupture.

For reference in this section and as described in earlier sections of this report, the upstream end of the 6-foot-8.25-inch-long rupture was located 24 feet 5.75 inches downstream of GWD217720. The location of deepest preexisting crack penetration relative to the local wall thickness as measured on the fracture surface was 28 feet 7.25 inches downstream of GWD217720.

The PII Pipeline Solutions (PII)¹³ inspection report for the 2004 USWM tool listed 16 external metal loss features within joint 217720. Twelve of the 16 metal loss features were noted on the seam weld and the remaining 4 features were noted near the seam weld. All but 2 of the features were located at distances greater than 20 feet from GWD217720. One feature had a maximum depth of 34 percent of the local wall thickness, and the remaining features ranged in maximum depth from 18 percent of the local wall thickness to 25 percent of the local wall thickness.

At the location corresponding to the deepest preexisting crack penetration within the rupture, the 2004 USWM inspection report listed a metal loss feature measuring 18.5 inches long and 2.1 inches wide with a maximum depth of 0.087 inch (34 percent of the remaining wall thickness) with the upstream end of the feature located 27.92 feet from GWD217720. The local wall thickness at this location was reported as 0.252 inch. An adjacent upstream feature also located on the clockwise side of the longitudinal seam was 18.4 inches long and 0.7 inches wide with a maximum depth of 0.055 inch, with an upstream end located 24.5 inch from GWD217720, and with a local wall thickness of 0.252 inch. An adjacent downstream feature also located on the clockwise side of the longitudinal seam was 5.8 inches long and 0.3 inch wide with a maximum depth of 0.047 inch, with an upstream end located 29.70 feet from GWD217720, and with a local wall thickness of 0.252 inch. A graphical representation of these features relative to the post-accident measured crack profile is shown in figure 27.

At the location corresponding to the downstream end of the lab fractures from sample A1d2, the 2004 USWM inspection report listed a metal loss feature measuring 11.6 inches long and 0.3 inch wide with a maximum depth of 0.047 inch with the upstream end located 11.73 feet from GWD217720. The local wall thickness at this location was reported as 0.260 inch. A graphical representation of the upstream end of this feature relative to the post-accident measured crack profile is shown in figure 40. An adjacent feature measured 7 inches long and 0.2 inches wide with a maximum depth of 0.047 inch, with an upstream end located 10.22 feet from GWD217720, and with a local wall thickness of 0.268 inch.

Features were analyzed in the PII 2004 USWM inspection report using a modified B31G approach and a RSTRENG approach,¹⁴ and values were reported in terms of a rupture pressure ratio (RPR). The RPR is a calculation of the remaining strength of the pipe at a feature as compared to the specified minimum yield strength of

¹³ PII Pipeline Solutions, Houston, Texas, is a GE Oil & Gas and Al Shaheen joint venture.

¹⁴ J. F. Kiefner and P. H. Vieth, *Project PR3-805: A Modified Criterion for Evaluating the Remaining Strength of Corroded Pipe*, AGA Catalog No. L51609 (1989).

the pipe. Using the modified B31G approach, 2 features had RPR values less than 1.0, i.e., 0.899 and 0.971. Among all 16 external metal loss features within joint 217720, the feature with the lowest RPR (modified B31G) value of 0.899 was the 0.087-inch deep feature located at the area of deepest crack penetration. Using the RSTRENG approach, all features had RPR values greater than 1.0. The lowest RPR (RSTRENG) value was 1.077 for a 16.5-inch long, 0.7-inch wide feature with a maximum depth of 0.055 inch and an upstream end located 33.82 feet from GWD217720. The 0.087-inch deep feature located at the area of deepest crack penetration had an RPR (RSTRENG) value of 1.110.

Results of the 2005 USCD inspection, the 2007 MFL inspection, and the 2009 USWM inspection of joint 217720 are shown in figures 45 and 46. The areas where features were detected are shown plotted in the charts with the horizontal axis representing the longitudinal distance downstream from girth weld GWD217720 and the vertical axis representing the circumferential position in degrees clockwise from top dead center. ILI data placed the longitudinal seam for joint 217720 at 96 to 100 degrees, and the position of the longitudinal seam is represented by a dashed blue line in the plots. Vertical red lines indicate the location of girth welds at either end of joint 217720.

Data from the 2005 USCD ILI tool was first analyzed by PII. Six indications of crack-like features¹⁵ within joint 217720 were reported. The locations and extents of the features are shown in both figure 45 and 46 for reference. The deepest of the six features was located 11 feet 0.5 inch from GWD217720. The feature was 9.3 inches long, and depth was categorized within a range of 25 percent to 40 percent of the wall thickness.¹⁶ Among the remaining crack-like features on joint 217720, two of the features were categorized within a depth range of 12 to 25 percent of the wall thickness. These features were 25.5 inches and 51.6 inches long, located 23 feet 11 inches and 26 feet 8 inches from GWD217720, respectively. The maximum depth and location of the 25.5-inch and 51.6-inch long features relative to the post-accident measured crack profile are shown graphically in figure 27. The remaining three crack-like features had depths that were categorized as less than 12 percent of the wall thickness. These features were 14.1 inches, 40.1 inches, and 27.8 inches long, located 20 feet 10 inches, 31 feet 2 inches, and 36 feet 10 inches from GWD217720, respectively.

According to a PII representative, the reported depth for crack-like or crack field features¹⁷ detected by the USCD ILI tool is the depth measured from the adjacent surface. If the detected crack intersects the surface within an area of metal loss, the depth of the feature as reported by PII is the depth within the remaining wall, not the depth from the original wall surface. Additionally, if the surface near the crack is not

¹⁵ Typical anomalies associated with crack-like features include fatigue cracks; weld defects such as shrinkage cracks, hook cracks, or lack of fusion; relief cracks; and laminations with contact to the surface.

¹⁶ At PII, crack depths are initially determined in units of millimeters calculated from tool signal volume data. Per Enbridge reporting requirements at the time of the 2005 USCD report, PII reported crack depths to Enbridge as a percent of the measured wall thickness for the joint. Under current reporting requirements, PII now reports crack depths to Enbridge in terms of millimeters.

¹⁷ Crack field features are typically associated with stress corrosion cracking.

smooth such as the surface of a typical corrosion pit, the adjacent surface could scatter some of the signal, which could lead to underestimating the depth of the feature.

Wall thickness for joint 217720 was measured during the 2005 USCD ILI using wall thickness sensors on board the USCD tool. The thickness for joint 217720 reported by the 2005 USCD ILI tool was 0.285 inch. This wall thickness was used to calculate the depths of all crack-like features within joint 217720 that were reported as a percent of wall thickness. This wall thickness value was also used by Enbridge during the analysis of the 2005 USCD data for remaining strength calculations and for fatigue analysis before the accident.

After the 2005 USCD ILI run, pipe remaining strength calculations had been conducted by Enbridge at the crack-like features using CorLAS software by Det Norske Veritas (DNV), Houston, Texas. For the pipe remaining strength calculations, the features were analyzed individually as cracks having a depth equal to the maximum depth within the each category (12 percent, 25 percent, or 40 percent of the wall thickness) and a length equal to the reported length of the feature. The thickness of the wall used for the calculations was the joint thickness of 0.285 inch reported by the USCD tool. Results of the remaining strength analysis showed the pipe with a crack at 40 percent depth and 9.3-inch length had a strength that was less than the hydrostatic test pressure for the pipe at this location. Per Enbridge procedures at the time, Enbridge requested PII conduct a more precise depth determination of the crack depth, called a crack profile analysis, on the 9.3-inch long indication. Results of the crack profile analysis showed the maximum depth for the crack was 0.083 inch (29 percent of the reported wall thickness). The results of the crack profile analysis are represented graphically in figure 40. When pipe remaining strength was recalculated using the crack profile depth, the remaining strength was greater than the hydrostatic test pressure at this location. Pipe remaining strength for all other features in joint 217720 showed remaining strengths greater than the hydrostatic test pressure when analyzed at the category maximum depths of 12 percent or 25 percent of the wall thickness.

Also after the 2005 USCD ILI run, fatigue analysis had been conducted by Enbridge on the crack-like features. FlawCheck software by BMT Fleet Technology, Kanata, Ontario, Canada, was reported as the software most frequently used for the fatigue analysis. Spectrum loading based on historical pressure data was used in the crack growth model. Fatigue analysis of the crack-like features showed the remaining fatigue life for the deepest crack feature was 21 years. The two cracks in the 12 percent to 25 percent category had fatigue lives of 35 years.

During the 2005 USCD ILI data analysis, PII reported the features in joint 217720 as crack-like features and not crack field features.¹⁸ Results of the examination of joint 217720 after the accident revealed the presence of crack colonies in the areas that had

¹⁸ The features in joint 217720 were initially characterized as crack field features by the PII analyst that initially reviewed the data. During the quality control check of the report by a more experienced PII analyst, the characterization of features in joint 217720 were changed to crack-like features as listed in the final report to Enbridge.

been identified as crack-like features from the 2005 USCD ILI. Changes to PII's analysis processes made since the 2005 USCD ILI but before the accident include improvements in the feature identification process and changes to the algorithm for calculating the estimated depth of a crack field feature. The change to the sizing algorithm for crack field features was introduced in 2008 in response to feedback from more than 600 field excavations.¹⁹ In general, the 2008 sizing algorithm for a crack field feature will size the feature deeper than the sizing algorithm in place in 2005. Using the 2008 crack field sizing algorithm on the 51.6-inch feature from the 2005 USCD report, the maximum crack field feature depth was 2.3 mm (0.091 inch). In comparison using the crack field sizing algorithm in effect in 2005, the 51.6-inch long feature showed a maximum depth of 1.6 mm (0.063 inch). For a crack-like feature, the depth is determined as it was in 2005.

After the accident, PII manually reanalyzed the 51.6-inch long feature in joint 217720 using data from the 2005 USCD ILI with current analysis techniques. Using current rules and analysis techniques, including the crack field sizing algorithms developed in 2008, a PII analyst would likely analyze the signal response as three separate features consisting of a crack-like feature on the longitudinal seam with a depth of 1 mm, a crack field feature 6 degrees clockwise from the longitudinal seam with a maximum depth of 2 mm (0.079 inch), and a crack field feature 3 degrees counterclockwise from the longitudinal seam with a maximum depth of 2.3 mm (0.091 inch). The length of the longest individual crack in the crack field features would be equal to 3.5 inches. The location of the deepest crack penetration in the rupture corresponded to the location of the crack field feature that had a maximum depth of 2 mm (0.079 inch) located counterclockwise from the longitudinal seam.

Results of the 2007 MFL ILI for joint 217720 are shown in figure 45. The inspection report for the 2007 MFL ILI included calculations of the RPR for each MFL feature shown in figure 45. The remaining strength was calculated using the Modified B31G method. The feature with the lowest RPR in joint 217720 was feature 393122 at 34.14 feet from GWD217720 measuring 6.9 inches long, 5.5 inches wide, and up to 19 percent of the wall thickness deep with an RPR of 1.079. The deepest feature was feature 393131 at 37.03 feet from GWD217720, which had a maximum depth of 30 percent of the wall thickness and was 3.3 inches long and 5.4 inches wide with an RPR of 1.091. Both features were analyzed using the length adaptive pressure method developed by PII,²⁰ and by that method the RPR values were 1.110 and 1.116 for features 393122 and 393131, respectively.

Results of the 2009 USWM inspection of joint 217720 are shown in figure 46. The inspection report for the 2009 USWM ILI included calculations of the RPR for each

¹⁹ After availability of the new sizing algorithm and until 2011, Enbridge requested that PII provide reports from USCD tools using the previous algorithm to size crack fields. The PII inspection reports from all GE Oil and Gas UltraScan™ Duo and UltraScan™ CD Plus crack tools received by Enbridge used the current sizing algorithm starting with the first run of one of these tools in July 2009.

²⁰ T. Wheeler and K. Grimes, *Length Adaptive Pressure Assessment (L.A.P.A.) of Metal Loss Data*, Corrosion 99, San Antonio, TX, NACE International (1999).

USWM feature shown in figure 46. The feature with the lowest RPR in joint 217720 was feature 62278 located 28.2 feet from GWD217720. Feature 62278 measured 68.03 inches long and 17.05 inches wide with a peak depth of 27 percent of the local wall thickness and had an RPR of 0.925. One other feature (number 62279 located 34.24 feet from GWD217720) also had an RPR of less than 1.0 at 0.935. Both features were also analyzed using an effective area method, and in that calculation, the effective area RPR's were 1.056 and 1.049 for features 62278 and 62279, respectively. The deepest feature was feature 62279, located 34.03 feet from GWD217720, with a depth of 30 percent of the local wall thickness.

Matthew R. Fox
Senior Materials Engineer



Figure 1. Overall view of the pipeline within the trench dug at the accident scene as viewed facing east.



Figure 2. Views of the pipe in the trench showing the rupture location.

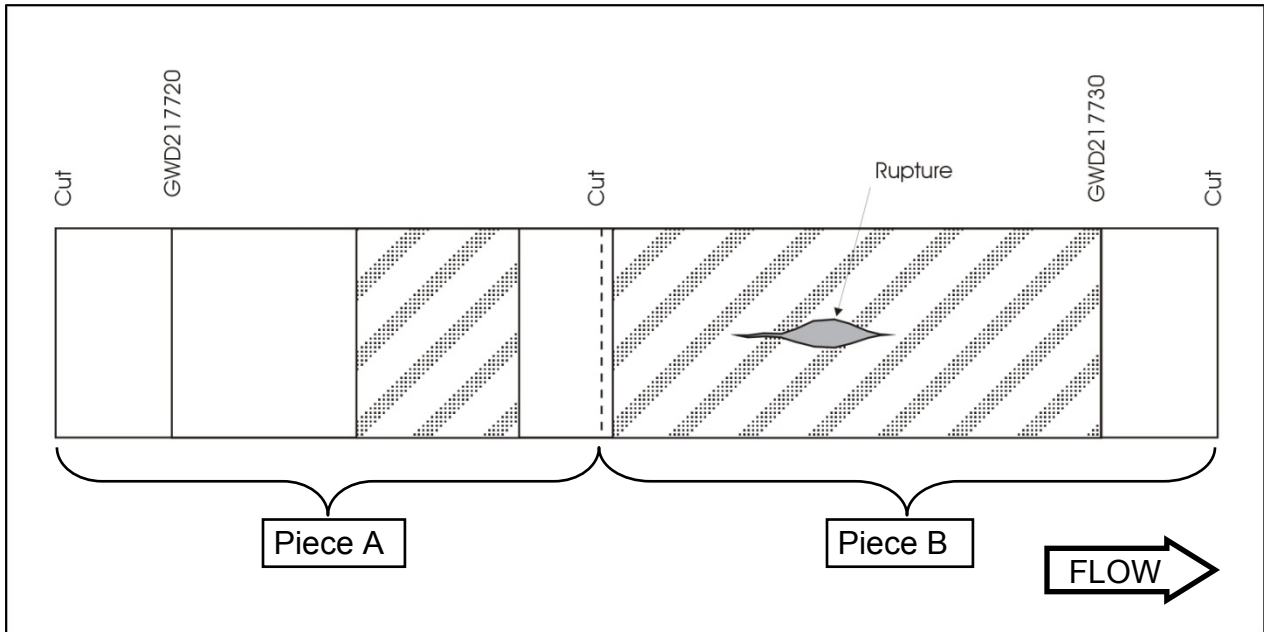


Figure 3. Schematic view of pieces A and B showing locations of girth welds, cuts, ILI features (diagonal shaded areas), and the rupture.



Figure 4. Overall views of Pieces A and B submitted to the NTSB Materials Laboratory as viewed during removal of the pipe pieces on scene.



Figure 5. 3 o'clock position on the pipe piece B showing wrinkles in the coating.

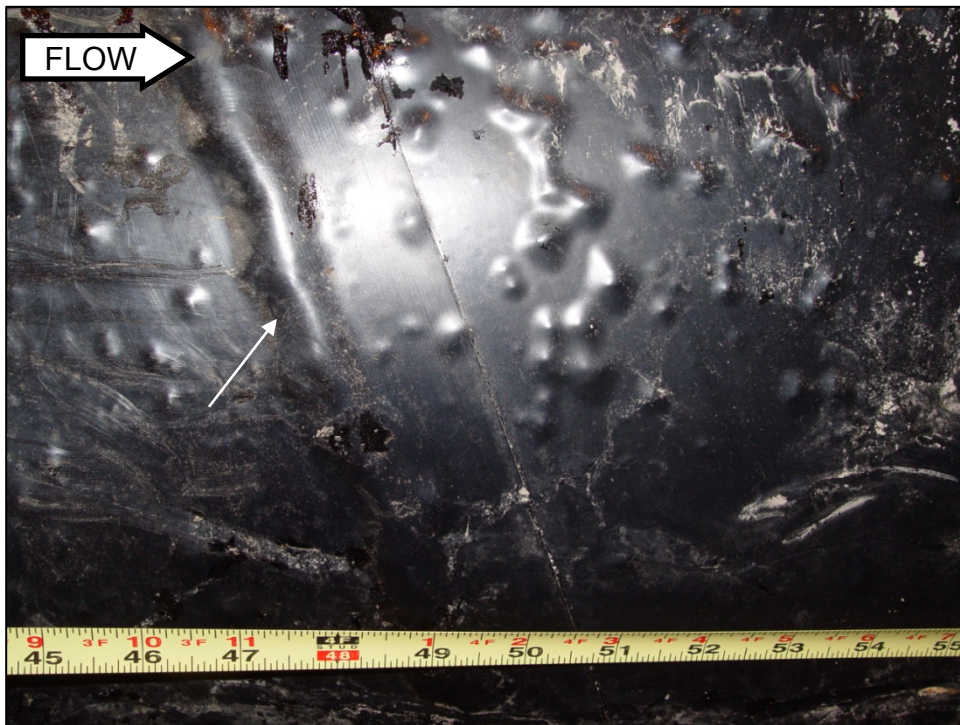


Figure 6. View of piece B showing a wrinkle at the upstream edge of a tape overlap as indicated by an arrow.

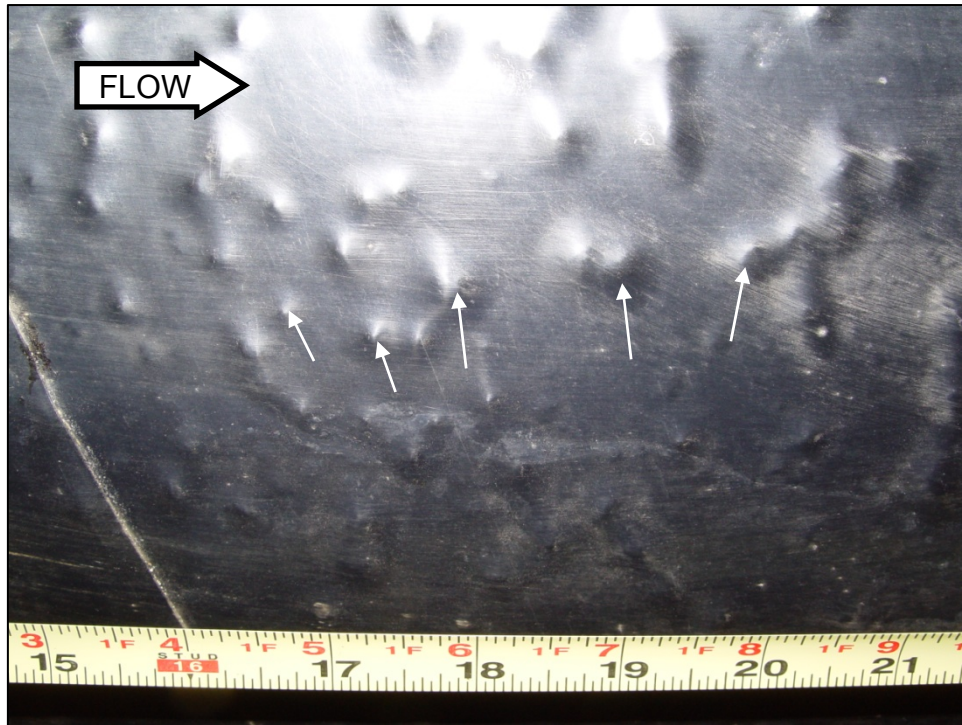


Figure 7. View of typical nodule features observed at the lower portion of the pipe. Arrows point to several of these nodules.

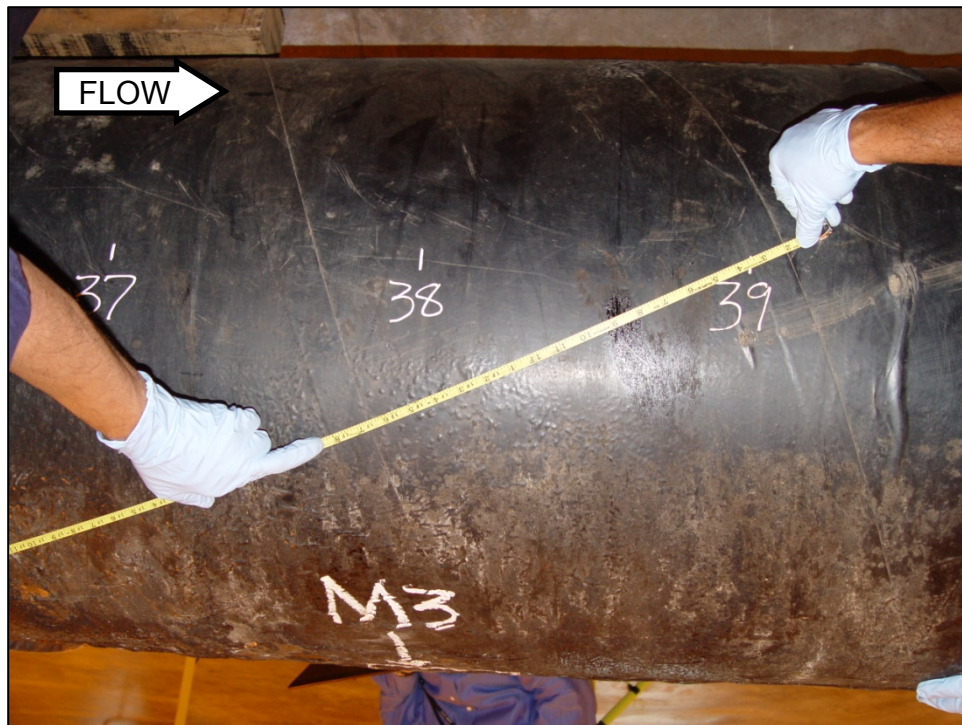


Figure 8. 12 o'clock position on pipe piece B showing relatively smooth coating features with smaller bulges near the 1 to 2 o'clock positions.

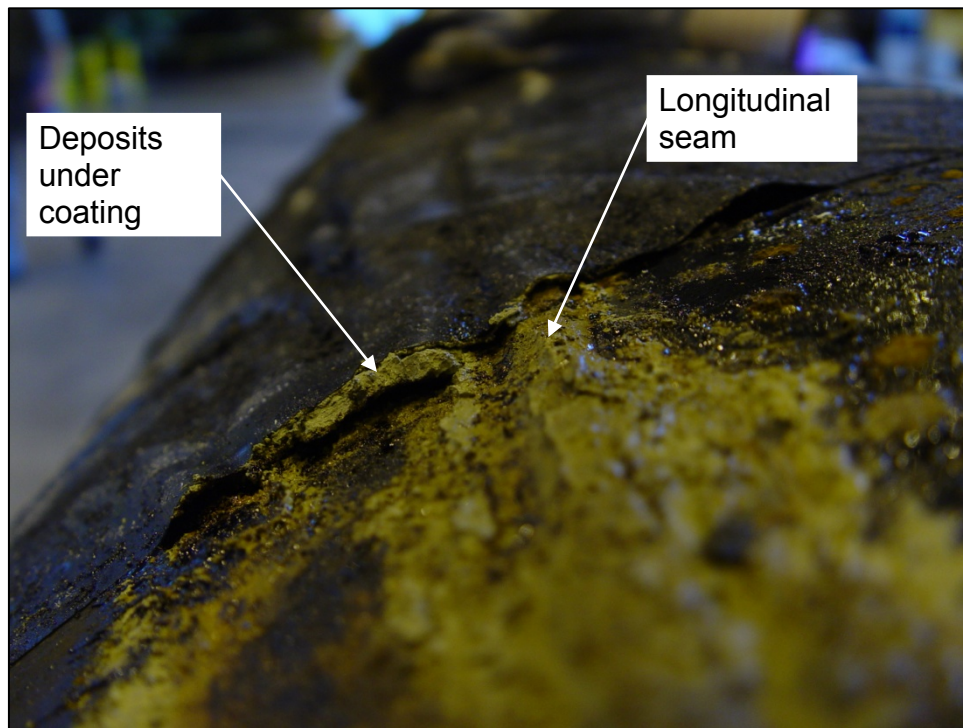


Figure 9. Views of corrosion deposits on and near the longitudinal seam of piece B upstream of the rupture location.

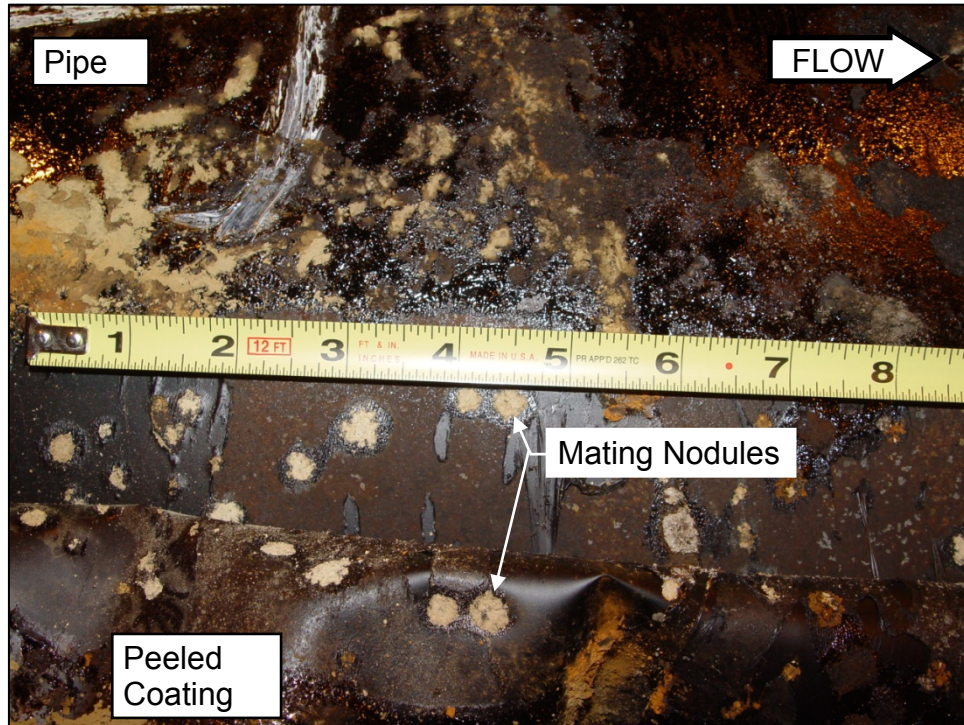


Figure 10. View of corrosion nodules as coating was peeled from the pipe surface near the rupture area.

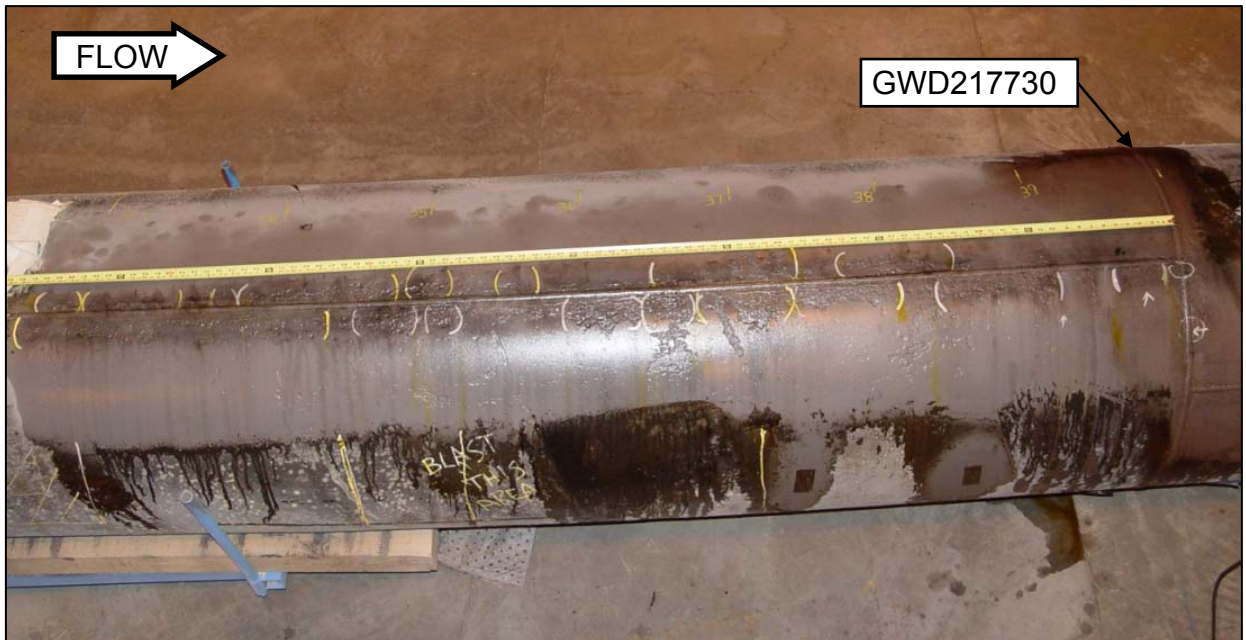


Figure 11. Overall view of the pipe with coating removed and abrasively cleaned showing areas of crack indications detected near the longitudinal seam downstream of the rupture location on joint 217720. Areas where crack indications were observed are bounded by parenthesis marks, and areas of faint indications on GWD217730 are circled.

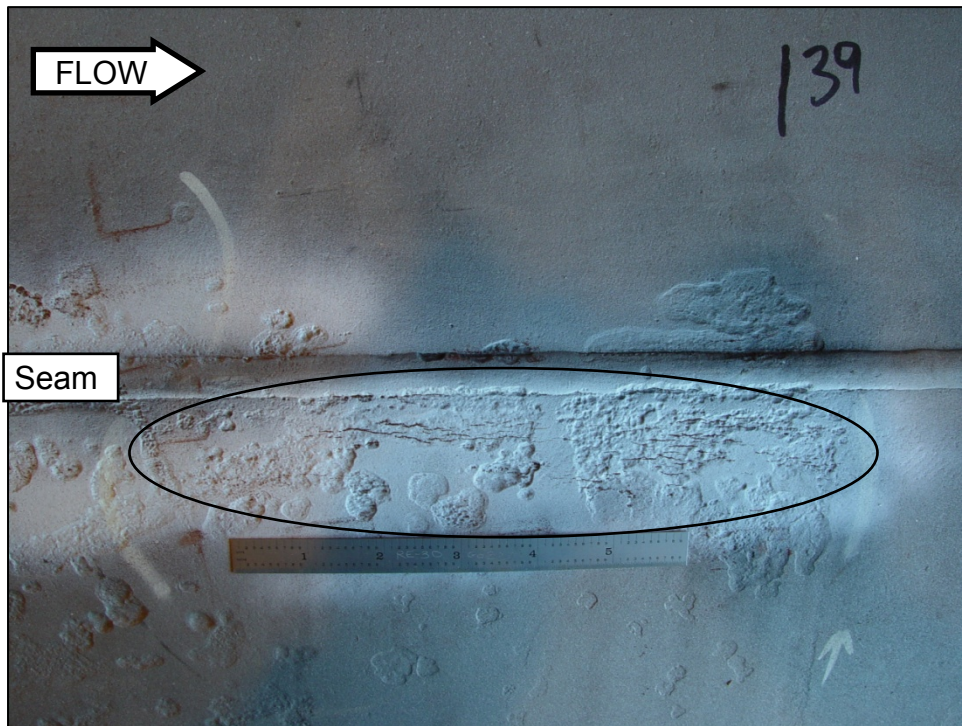
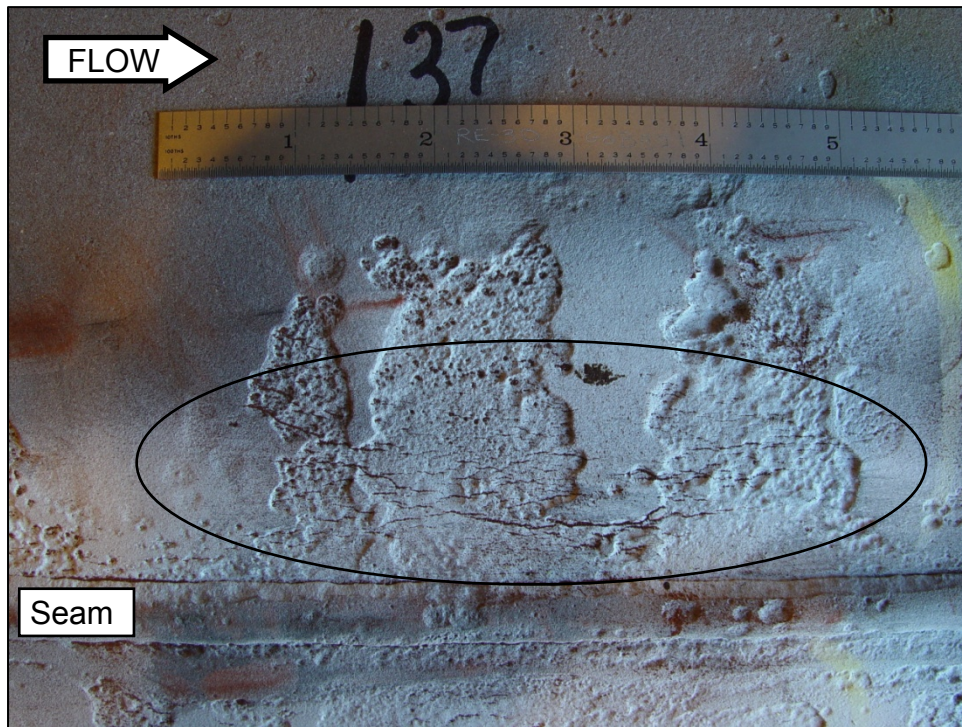


Figure 12. Views of clusters of crack indications at two locations on joint 217720 downstream of the rupture location. Crack clusters were located within the circled areas.

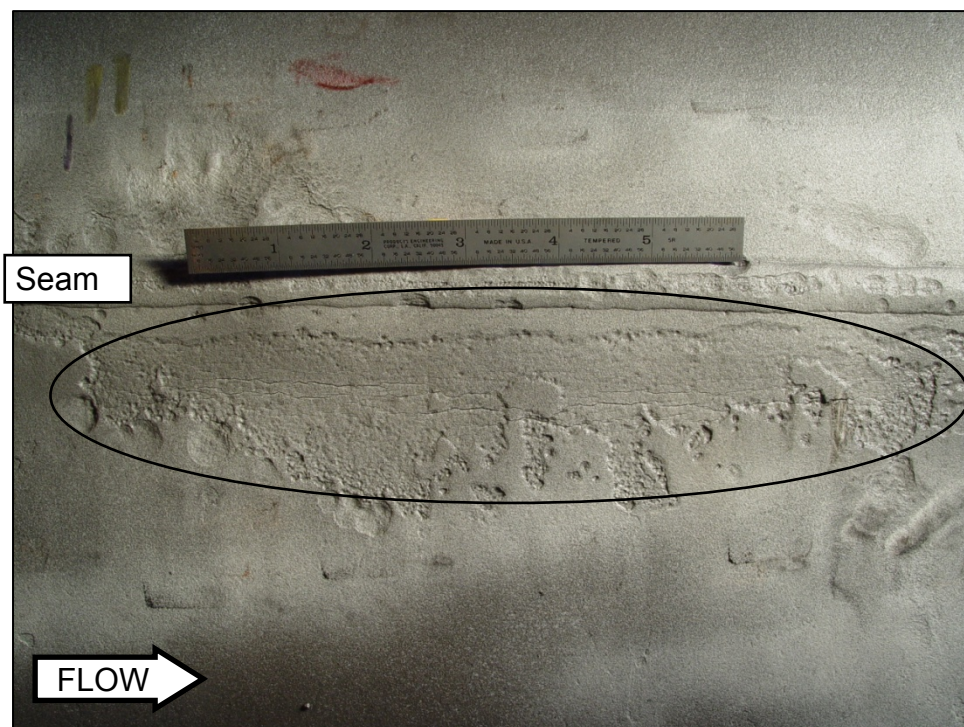


Figure 13. Close view of a crack cluster on piece A located between 11 and 12 feet downstream of girth weld GWD217720. Crack clusters were located within the circled area.

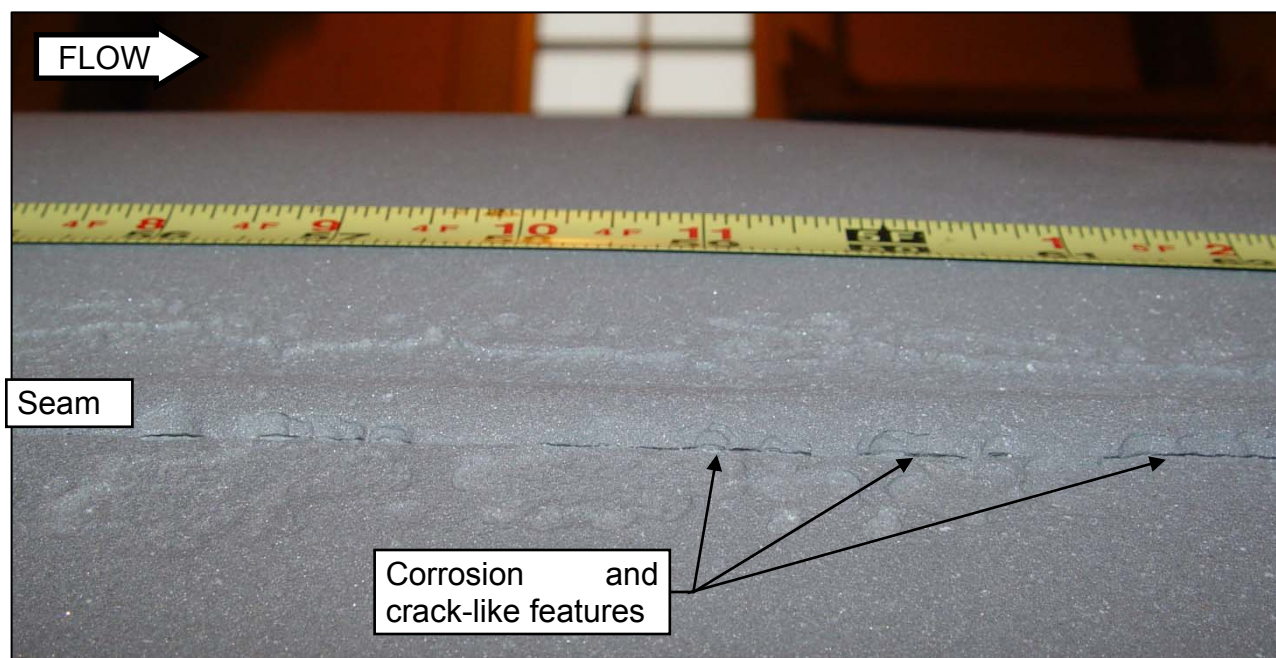


Figure 14. Oblique view of the longitudinal seam in joint 217730 showing typical corrosion and crack-like features at the toe of the weld.

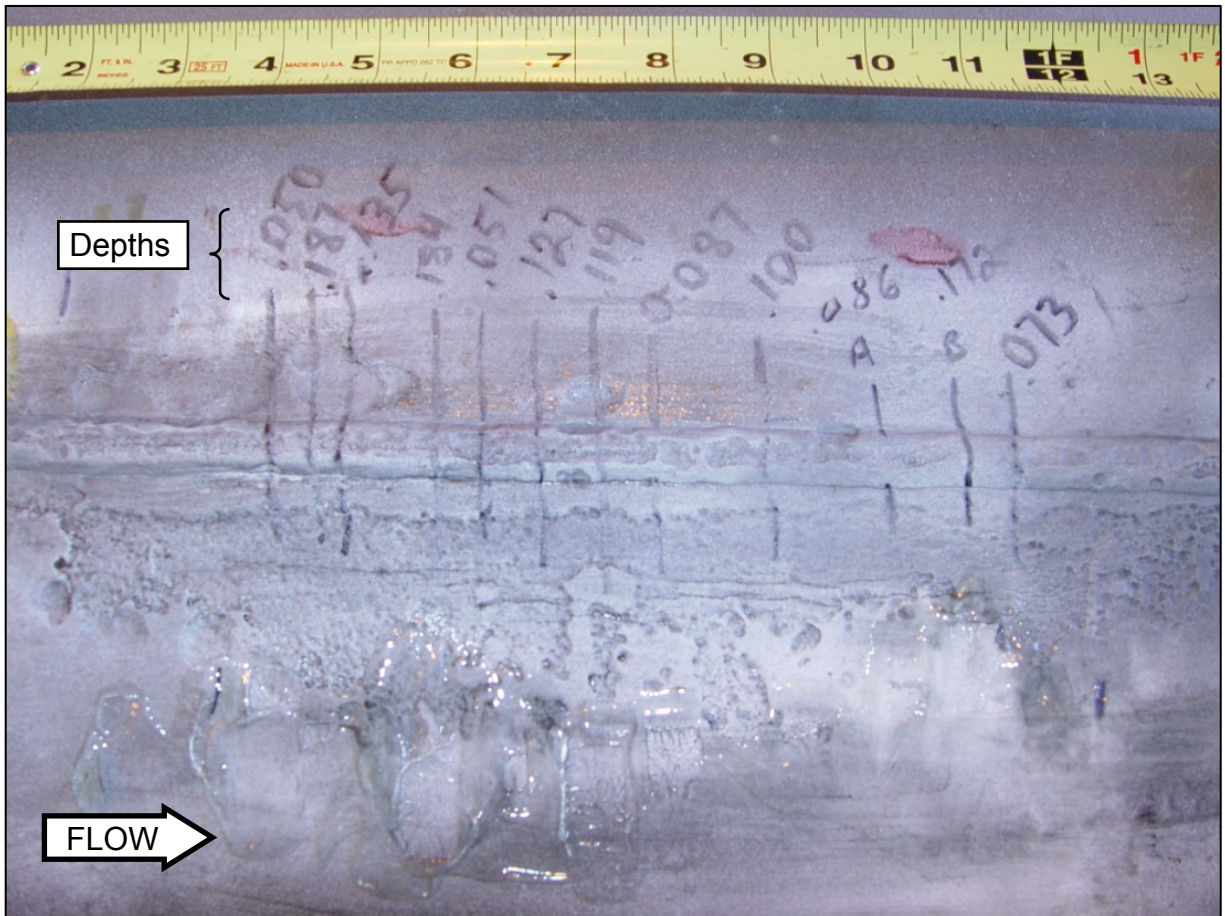


Figure 15. View of area shown in figure 13 after inspection using an ultrasonic flaw detector to estimate crack depths. Depth indications in units of inches are marked directly on the pipe surface with a line pointing to the location where the depth reading was obtained.



Figure 16. Overall views of the exterior (upper photo) and interior (lower photo) surfaces of piece B4 after coating removal and cleaning.

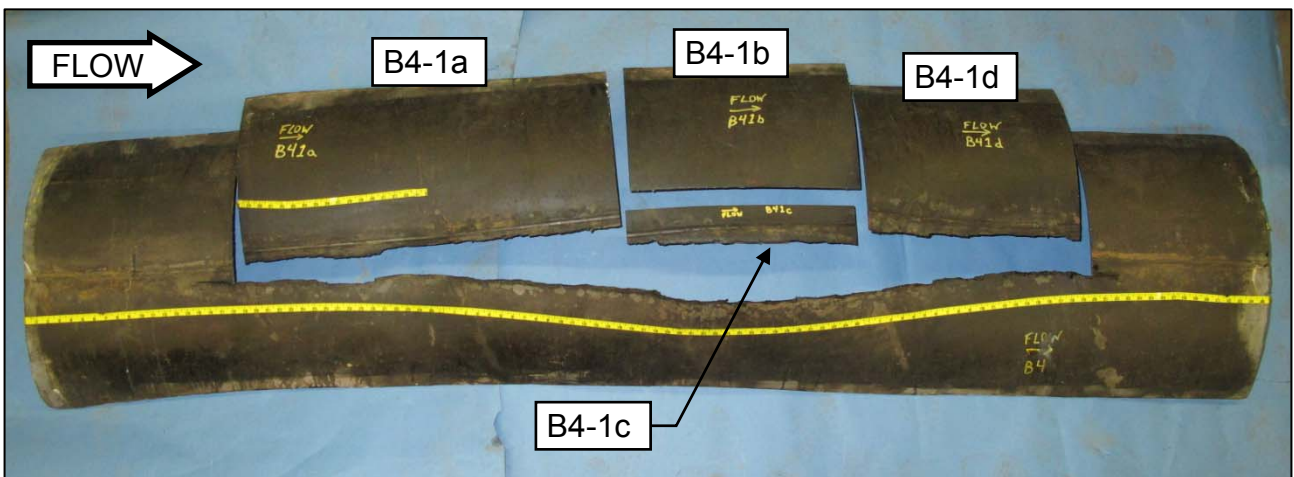


Figure 17. Piece B4 after sectioning for closer examination of the fracture surface on piece B4-1c.



Figure 18. Close view of the fracture surface after cleaning with solvents and Alconox/water solution. Image is stitched together from 3 individual images using Stream Enterprise software by Olympus, Center Valley, Pennsylvania.



Figure 19. Overall view of the outer surfaces of pieces B4-1c-i, B4-1c-ii, and B4-1c-iii after cutting and cleaning with oxide-removing chemicals. Locations where metallurgical samples MM1 and MM2 were taken are marked on piece B4-1c-iii.



Figure 20. Close view of the fracture surface at the area of deepest crack penetration after cleaning with oxide-removing chemicals.

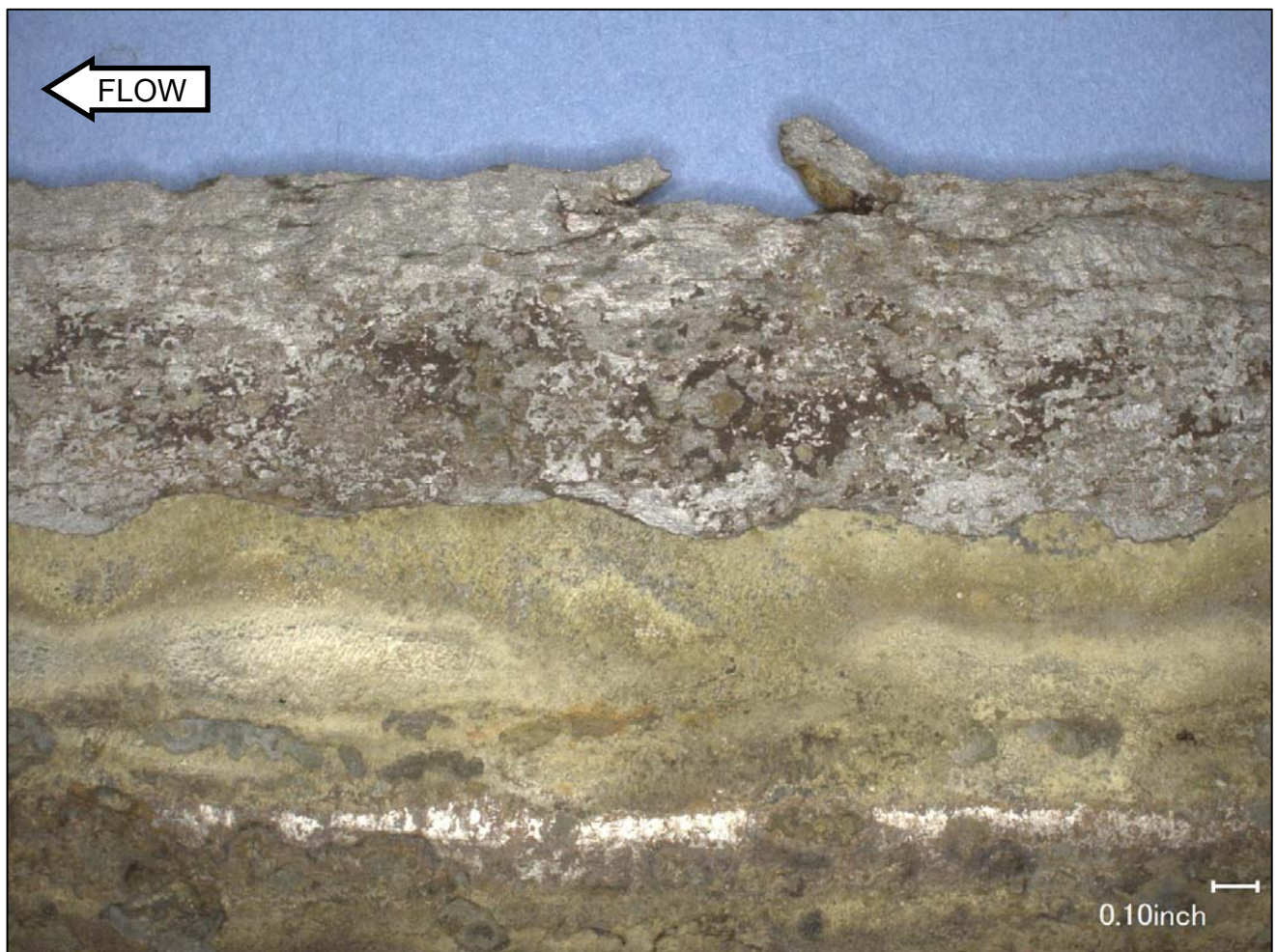


Figure 21. View of exterior surface of the pipe at the area of deepest crack penetration after cleaning with oxide-removing chemicals.



Figure 22. Close view of the fracture surface in the area of deepest crack penetration. A dashed line indicates the extent of the preexisting crack penetration.

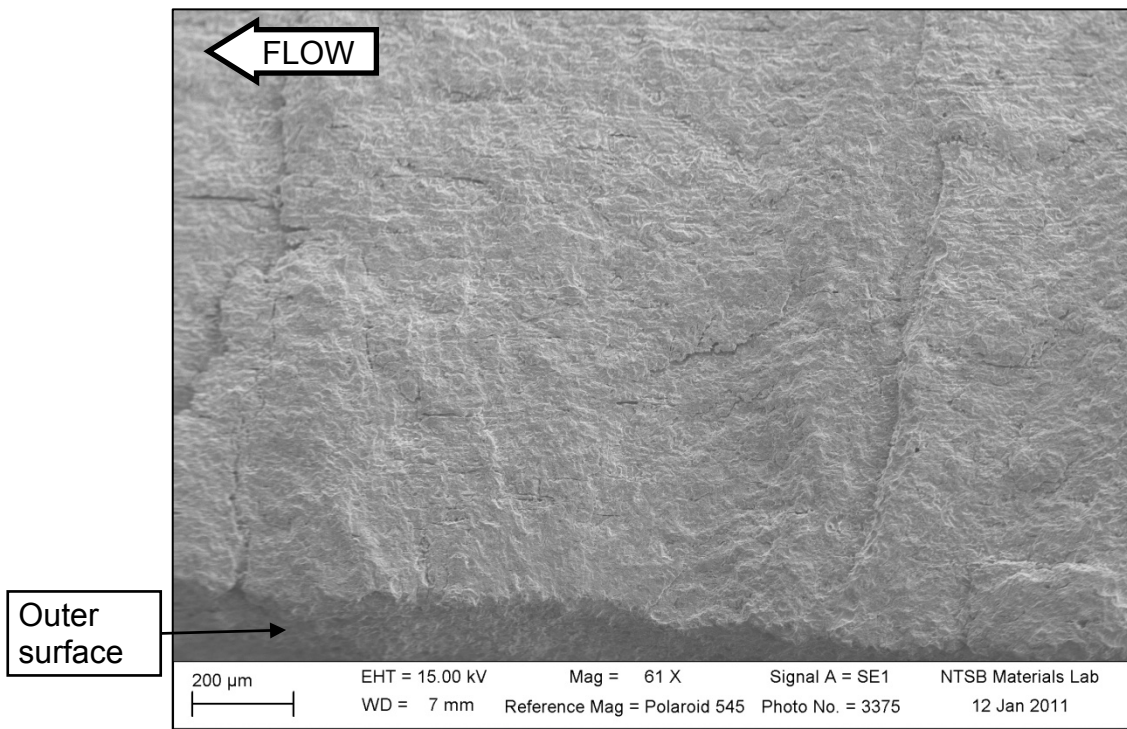


Figure 23. Overall SEM view of an origin area near the area of deepest penetration.

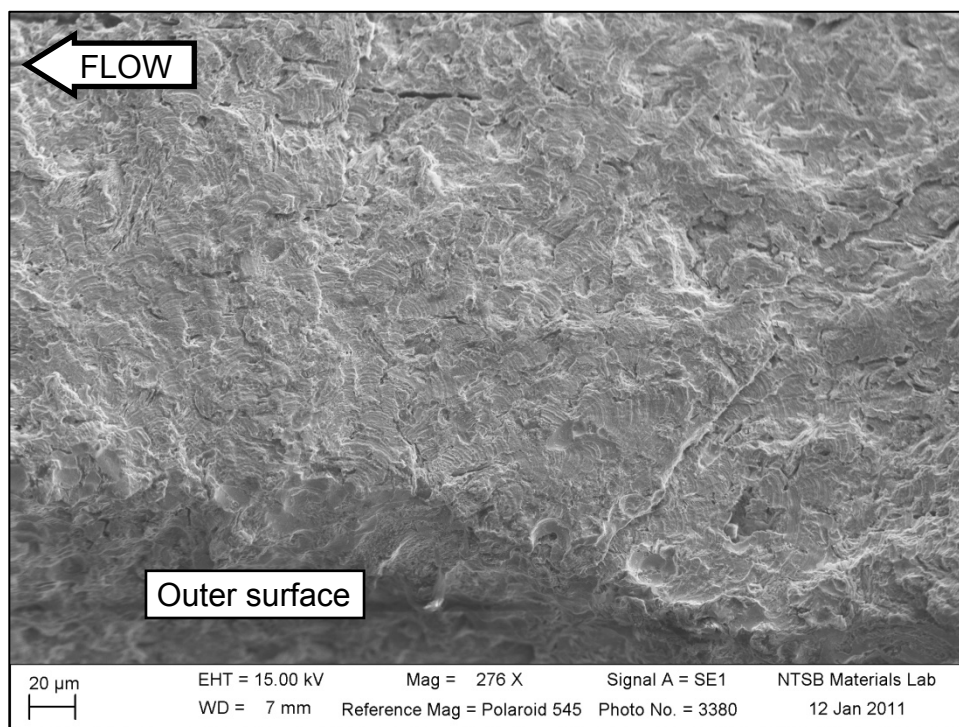


Figure 24. Close view of crack arrest features near the origin of the crack shown in figure 23.

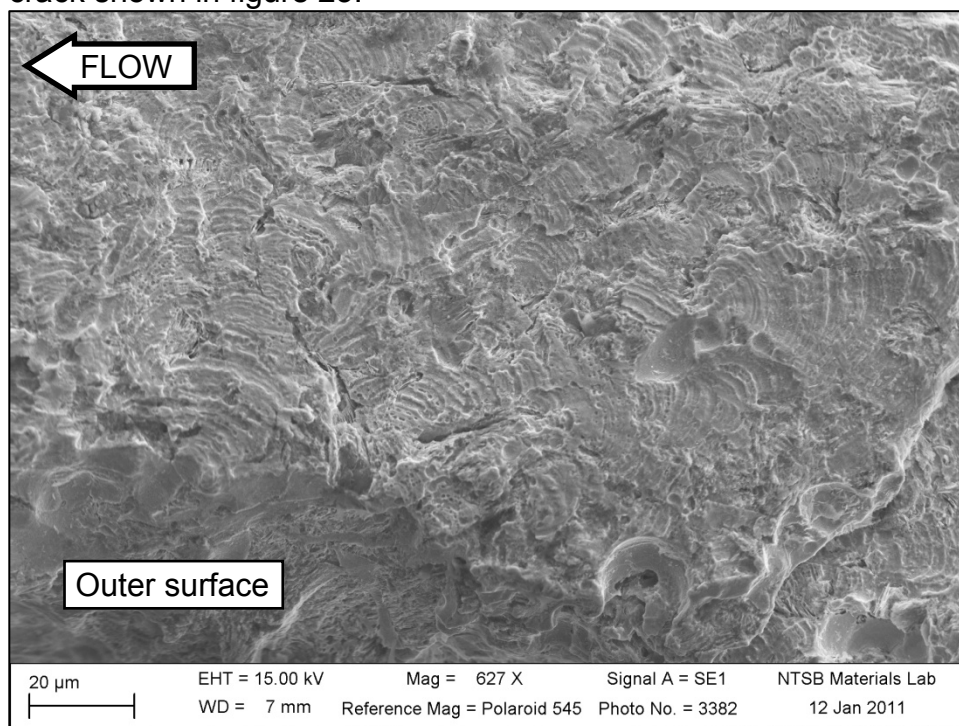


Figure 25. Closer view of crack arrest features at the origin shown in figure 24.

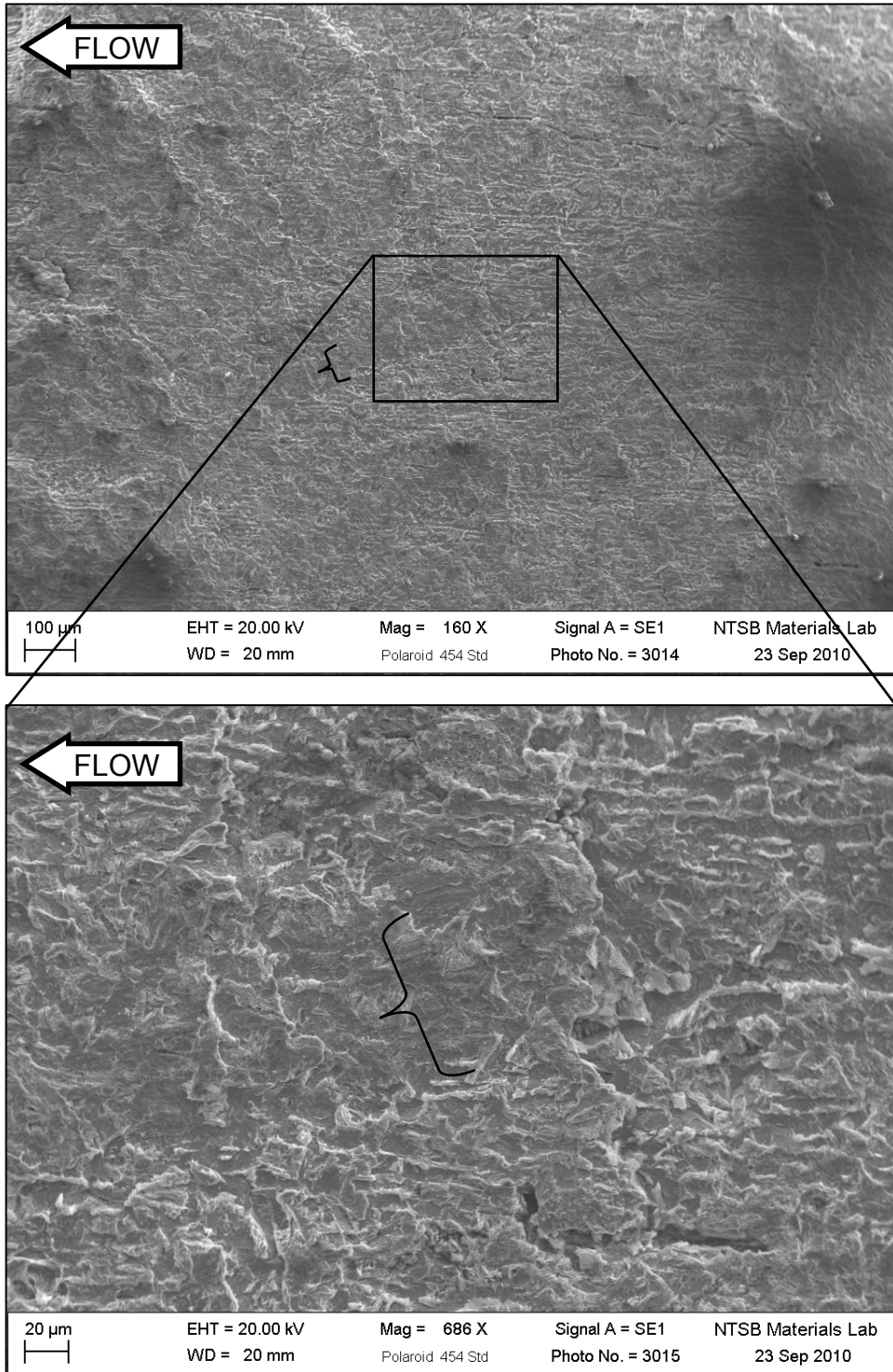


Figure 26. Views of broad crack arrest features further from the origin at a site near the area of deepest penetration. Brackets indicate the location of this feature appearing as a darker curving area on the fracture surface.

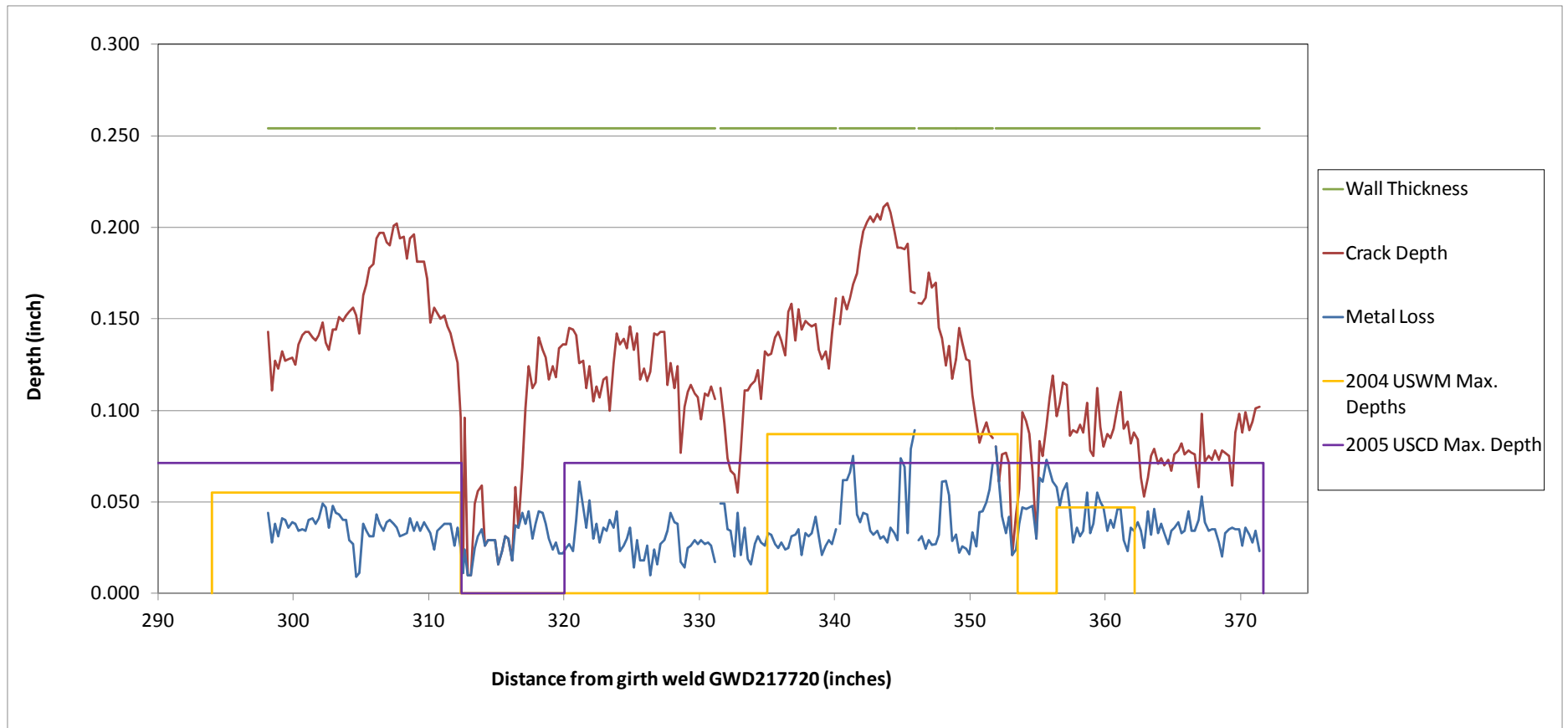


Figure 27. Crack profile data for the rupture at the area of deepest crack penetration showing metal loss depth and crack penetration depth along the length of the rupture at $\frac{1}{4}$ -inch increments. Breaks in the data indicate locations where cuts were made. Metal loss depth and crack penetration depth are referenced to the estimated original wall exterior surface as determined using an average of micrometer measurements in adjacent areas that appeared free from corrosion features. The wall thickness in this plot represents the wall thickness determined from the micrometer measurements. The yellow and purple lines indicate results from the 2004 ultrasound wall measurement (USWM) and the 2005 ultrasound crack detection (USCD) in-line inspection (ILI) tool inspection reports, respectively, showing locations and maximum depths for features reported in this area. (Additional details of the ILI inspections are included in Section D.15 of this report.)

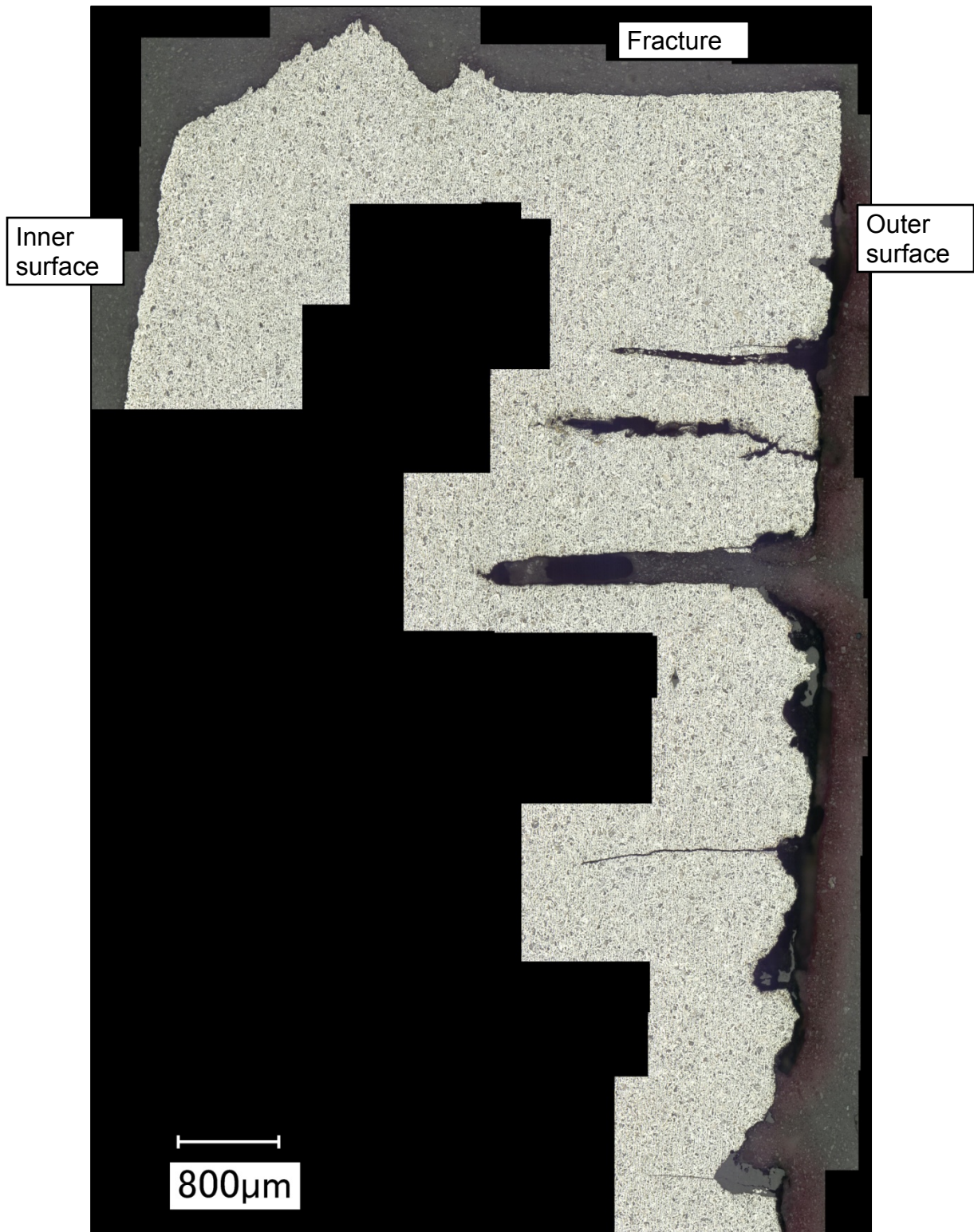


Figure 28. Montage of a polished and etched transverse cross-section (mount MM1) showing the fracture surface and multiple secondary cracks.

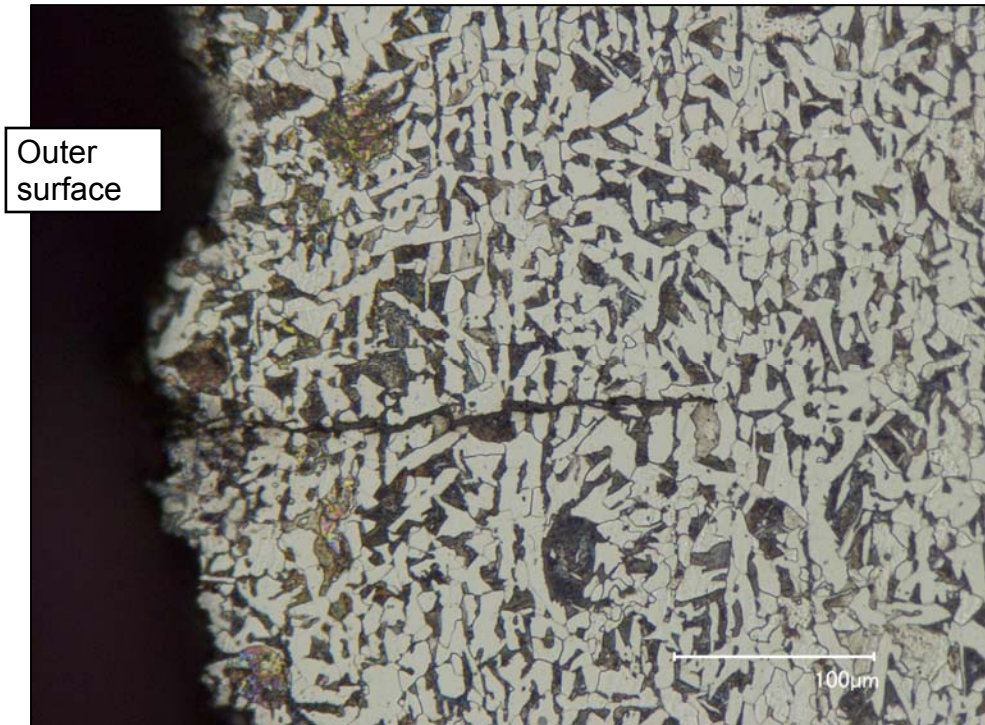


Figure 29. Close view of one of the smaller secondary cracks in a polished and etched transverse cross-section (mount MM2).

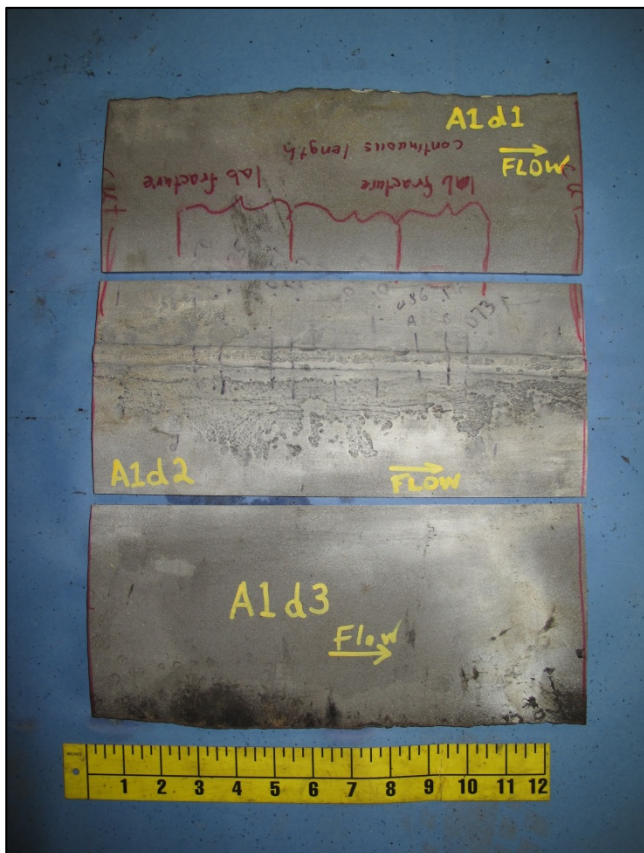


Figure 30. View of piece A1d2 cut from piece A1 to conduct lab fractures of crack indications detected by NDI.



Figure 31. View of piece B2b2 cut from piece B2 to conduct lab fractures of crack indications detected by NDI.

Figure 32. View of piece B2d2 cut from piece B2 to conduct lab fractures of crack indications detected by NDI.



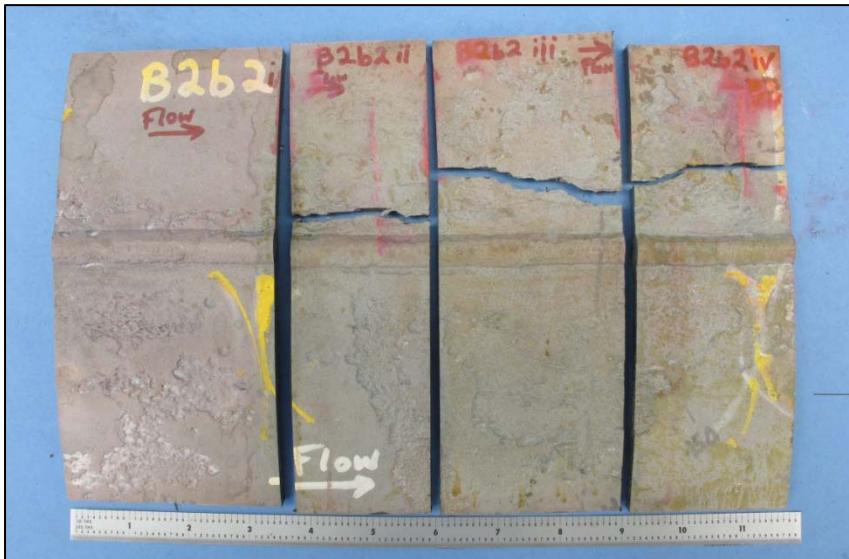
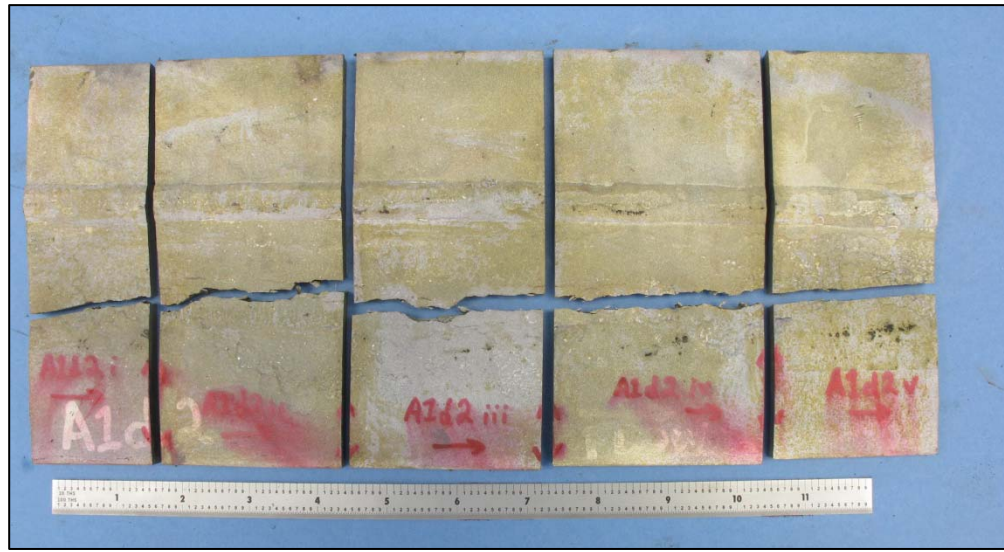
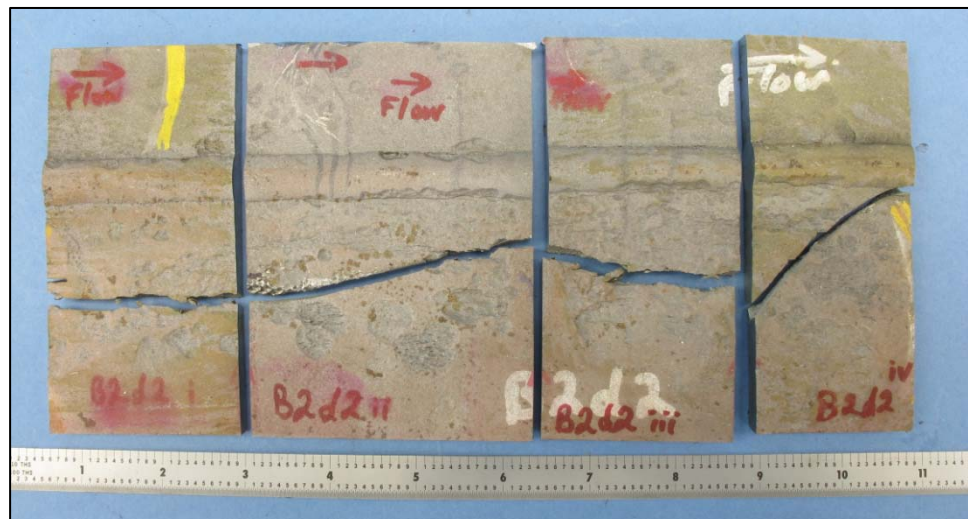


Figure 33. Post-fracture overall views of lab fracture samples.



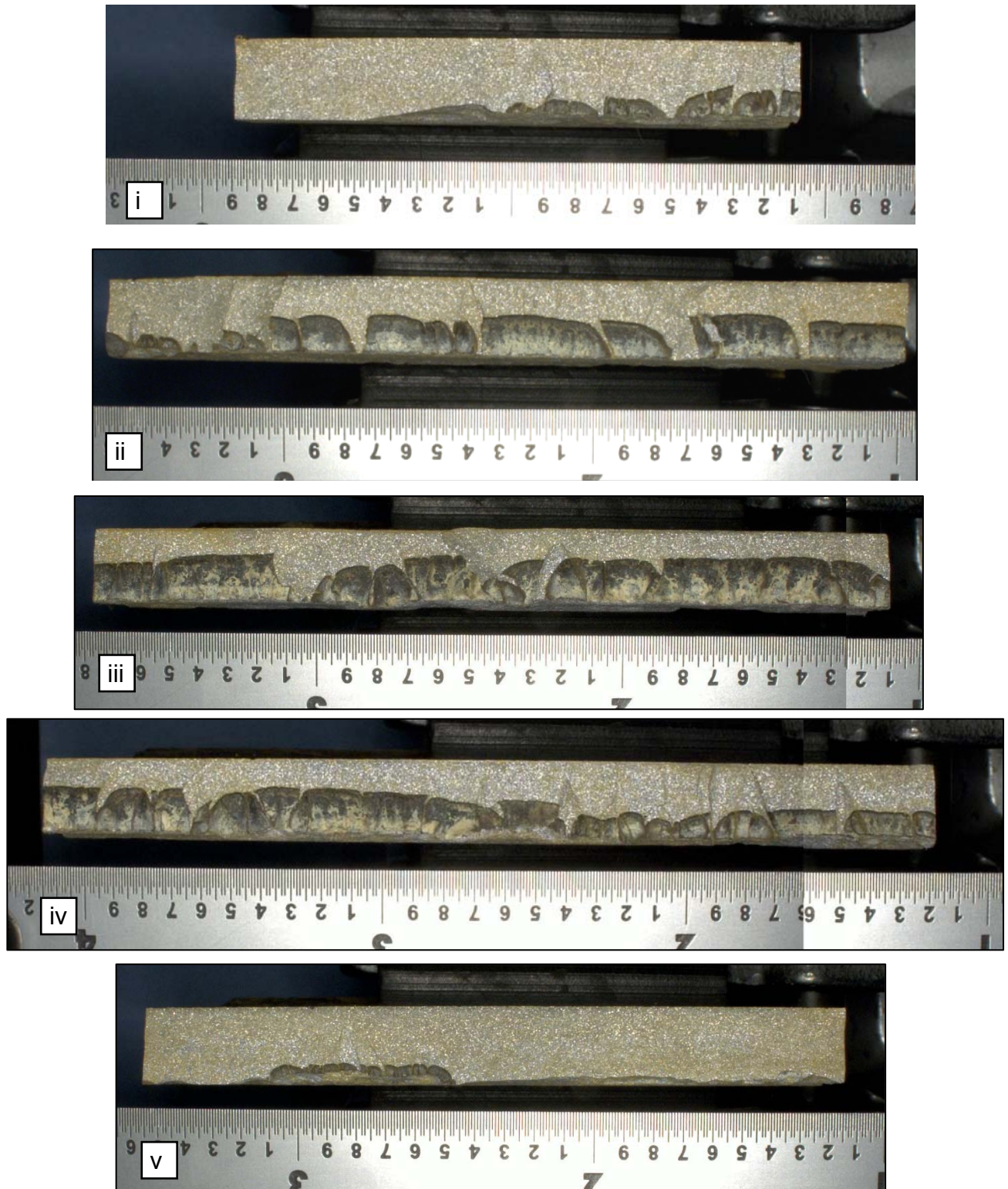


Figure 34. Overall views of lab fracture surfaces of samples A1d2i-v. The ruler is adjacent to the outer surface in each photo, and the pipe flow direction is from left to right.

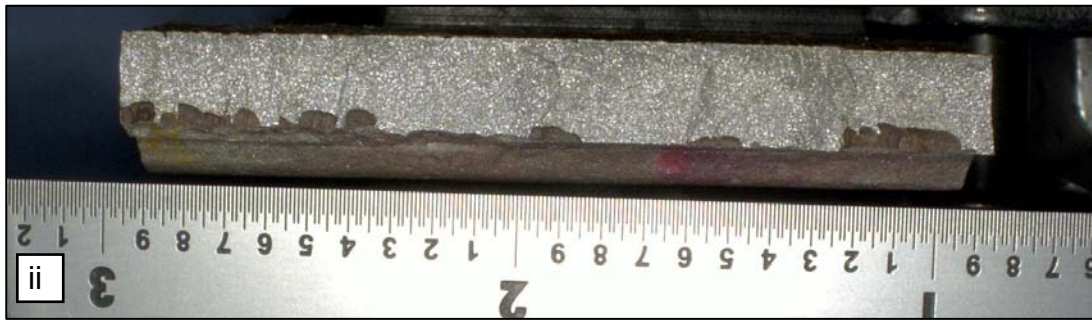


Figure 35. Overall views of lab fracture surfaces of samples B2b2ii-iv. The ruler is adjacent to the outer surface in each photo, and the pipe flow direction is from left to right.

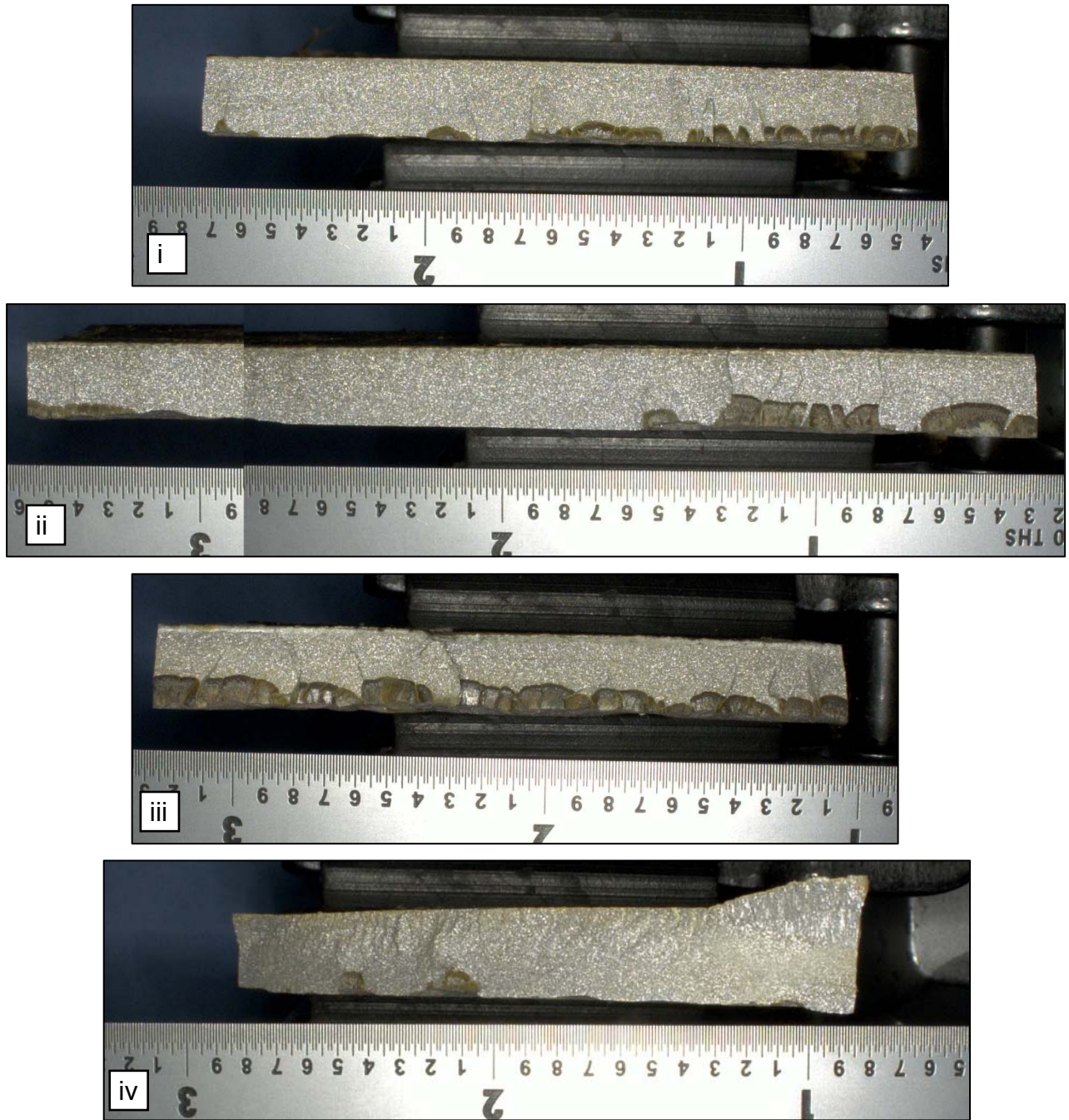


Figure 36. Overall views of lab fracture surfaces of samples B2d2i-iv. The ruler is adjacent to the outer surface in each photo, and the pipe flow direction is from left to right.

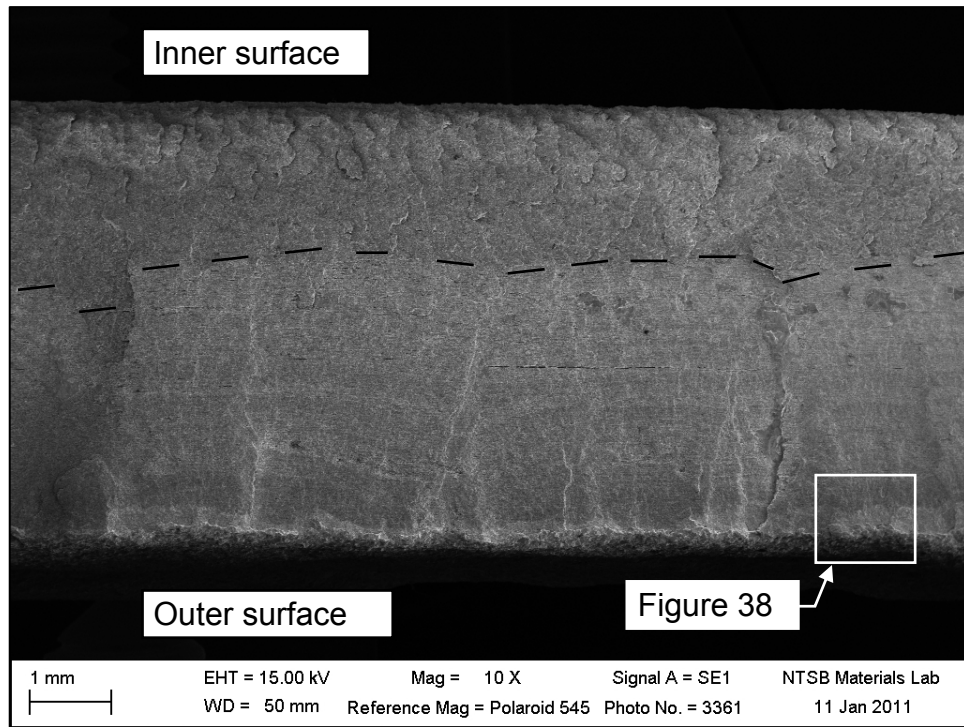


Figure 37. Overall view of deepest crack features in piece A1d2iii. A dashed line indicates the crack boundary.

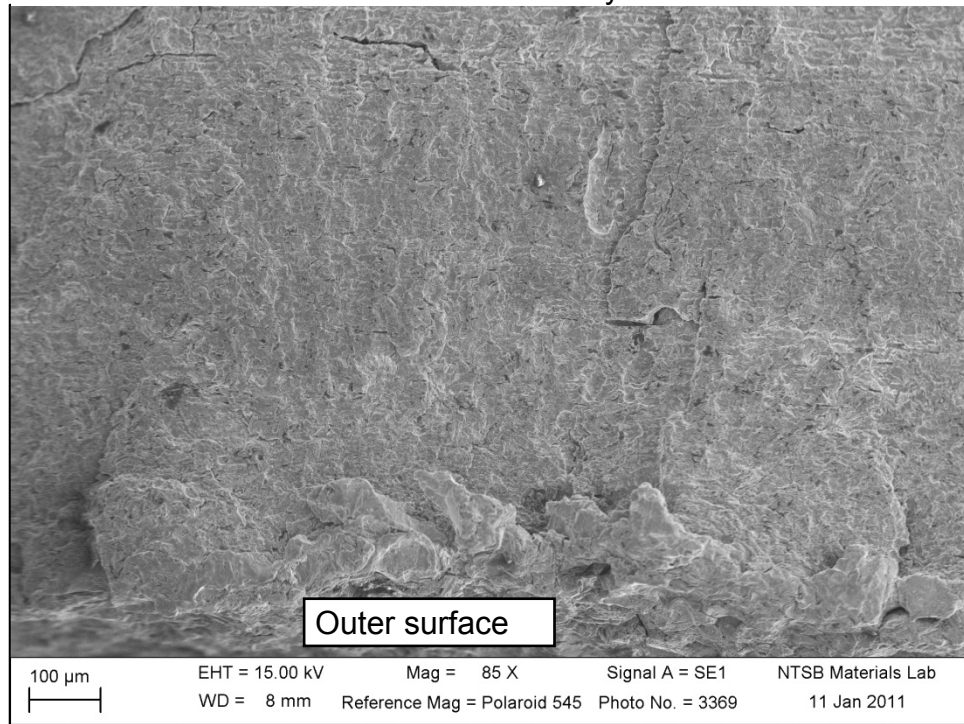


Figure 38. Closer view of the crack origin in the area indicated in figure 37.

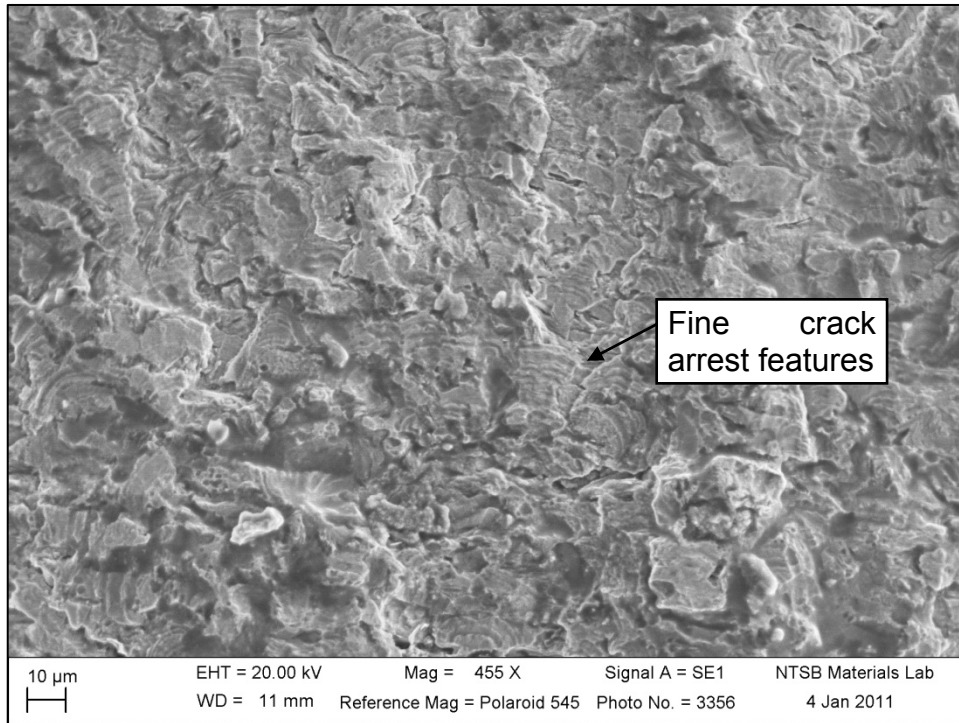


Figure 39. SEM view of fine crack arrest features observed within approximately 0.032 inches of an origin area on piece A1d2iii.

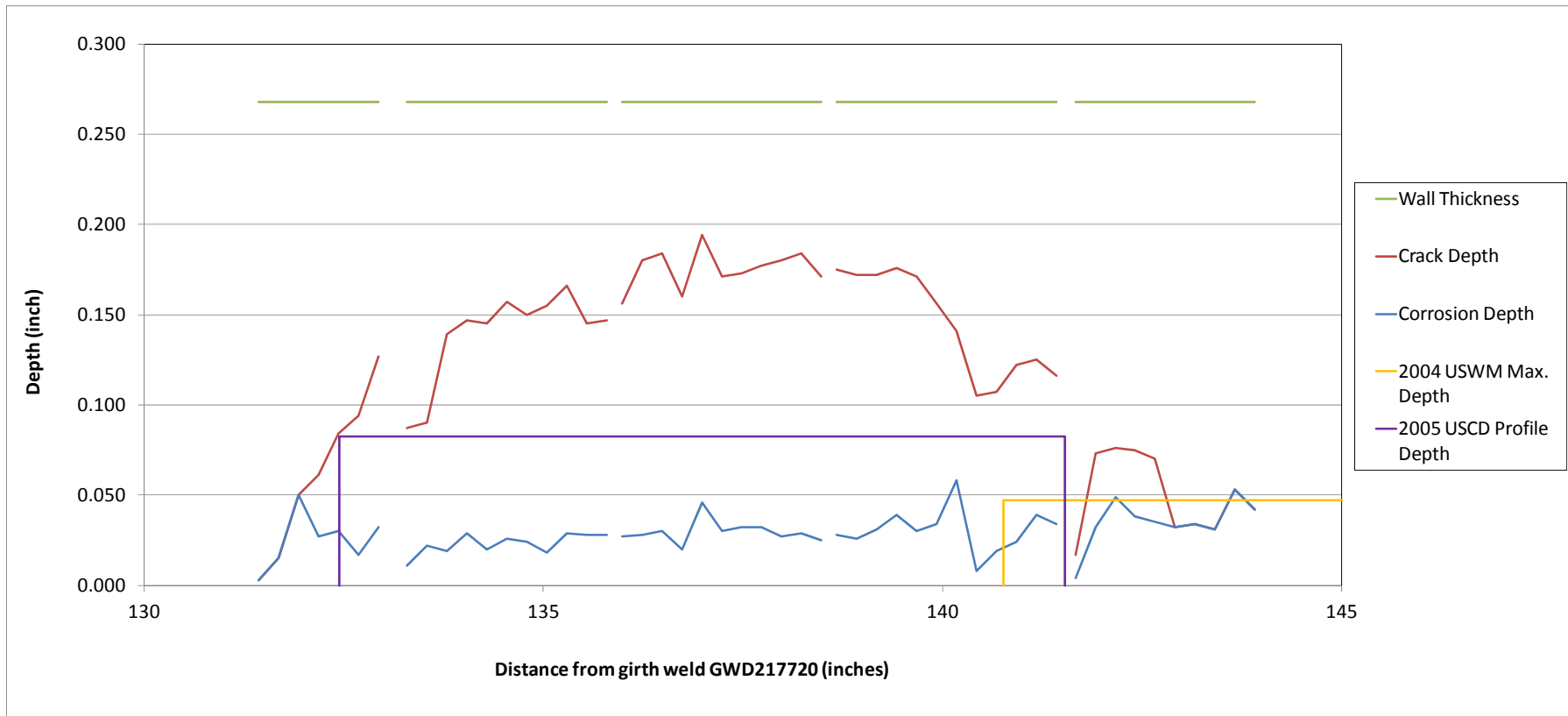


Figure 40. Crack profile data for the lab fractures from sample A1d2 showing metal loss depth and crack penetration depth along the length of the rupture at $\frac{1}{4}$ -inch increments. Breaks in the data indicate locations where cuts were made. Metal loss depth and crack penetration depth are referenced to the estimated original wall exterior surface as determined using an average of micrometer measurements in adjacent areas that appeared free from corrosion features. The wall thickness in this plot represents the wall thickness determined from the micrometer measurements. Results from the 2004 ultrasound wall measurement tool (USWM) and the 2005 ultrasound crack detection tool (USCD) in-line inspection (ILI) data for features intersecting the profiled crack. The line for the 2004 USWM data represents the location and maximum depth of that feature, which continues beyond 145 inches. The line for the 2005 USCD depth represents the profile depth provided at Enbridge's request during Enbridge's remaining strength assessment of the line using the 2005 USCD inspection report. (Additional details of the ILI inspections are included in Section D.15 of this report.)

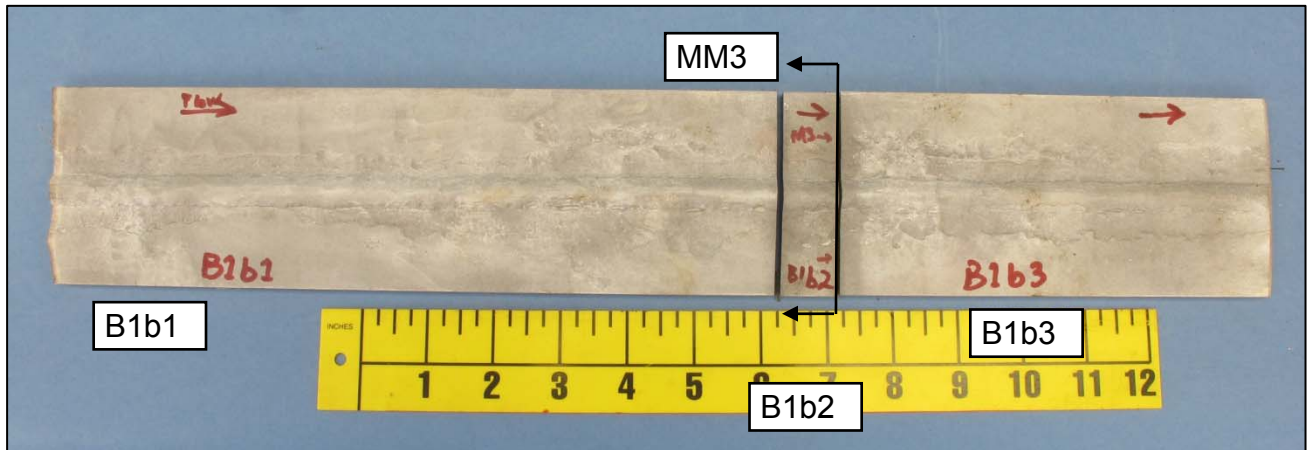


Figure 41. View of sample MM3 prepared from piece B1 for metallographic examination of the crack-like features at the weld toe in the longitudinal seam in joint 217730.

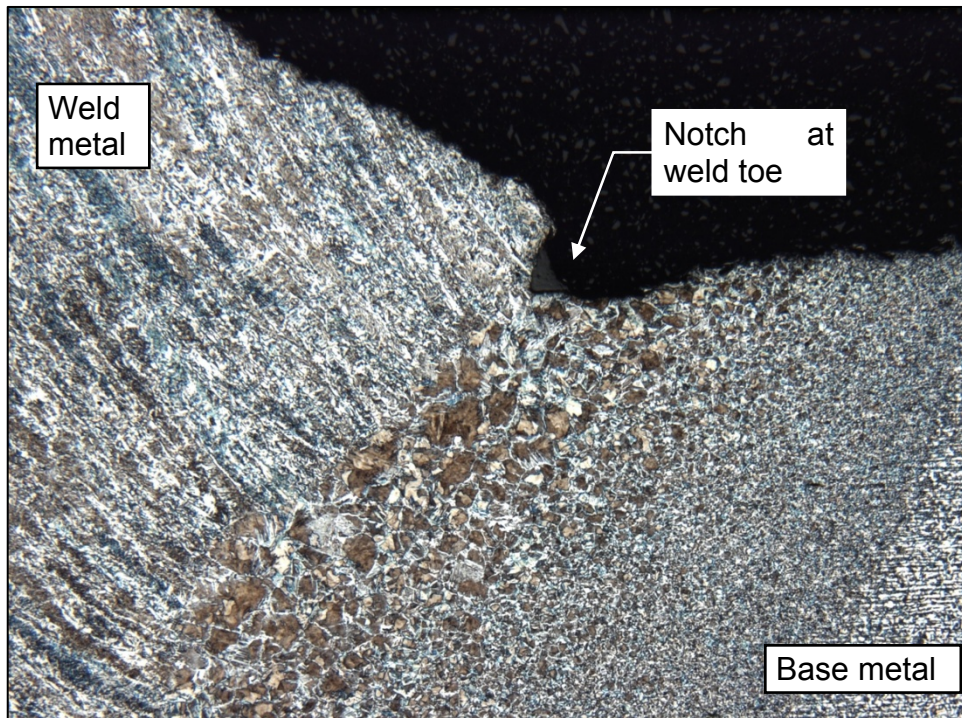
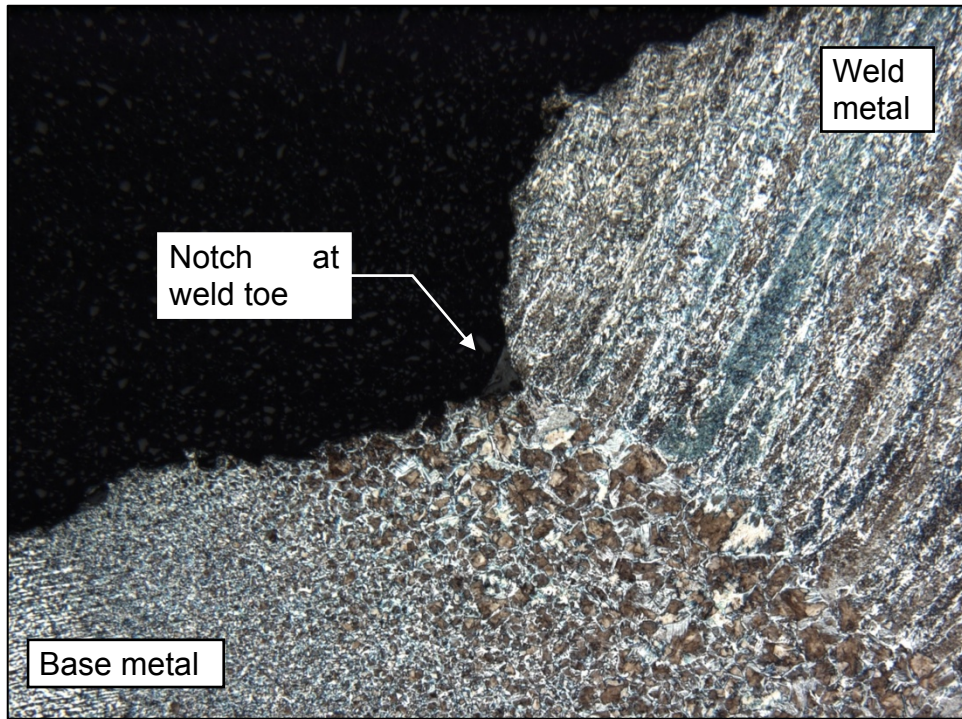


Figure 42. Views of etched specimen MM3 showing metallographic features at the weld toes of the longitudinal seam in joint 217730.

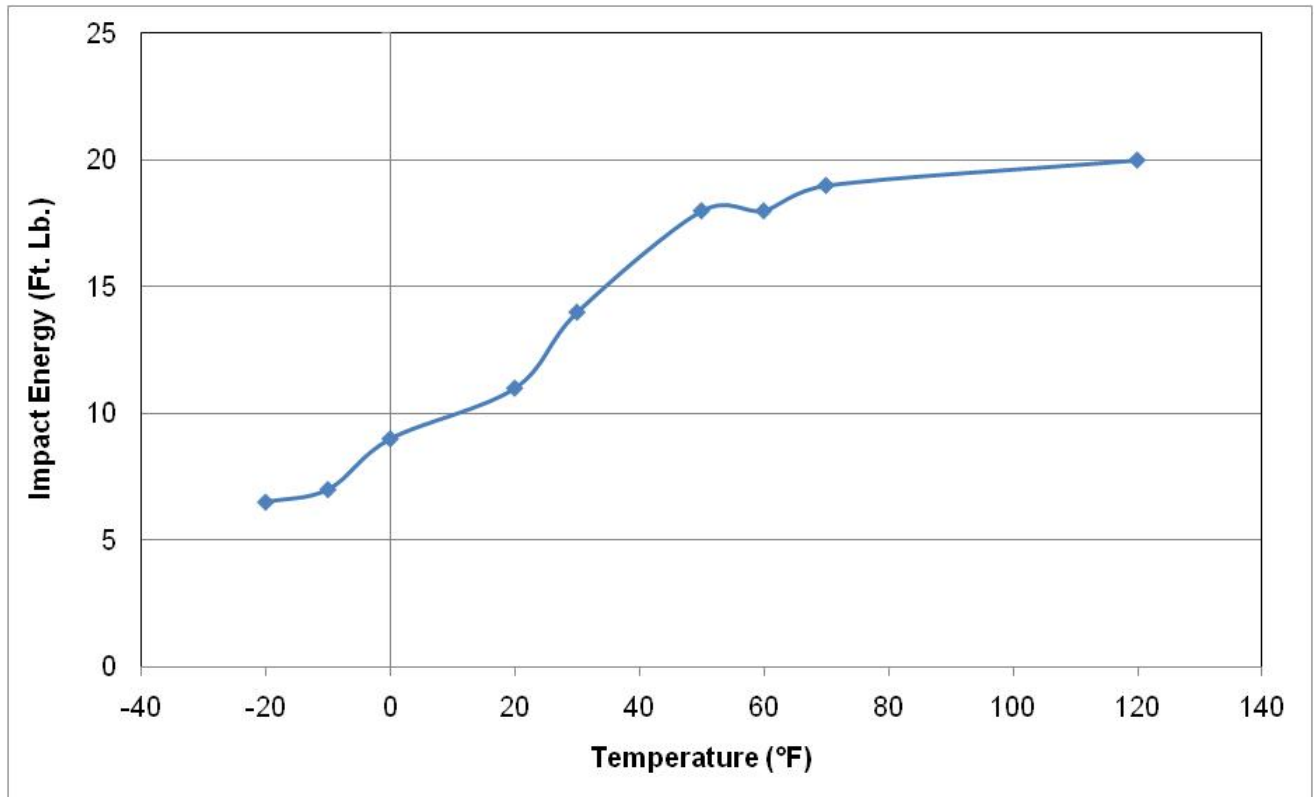


Figure 43. Plot of impact energies of Charpy specimens machined from the pipe wall of joint 217720 and tested at temperatures ranging from -20 °F to 120 °F. Each data point represents the average of two tests.

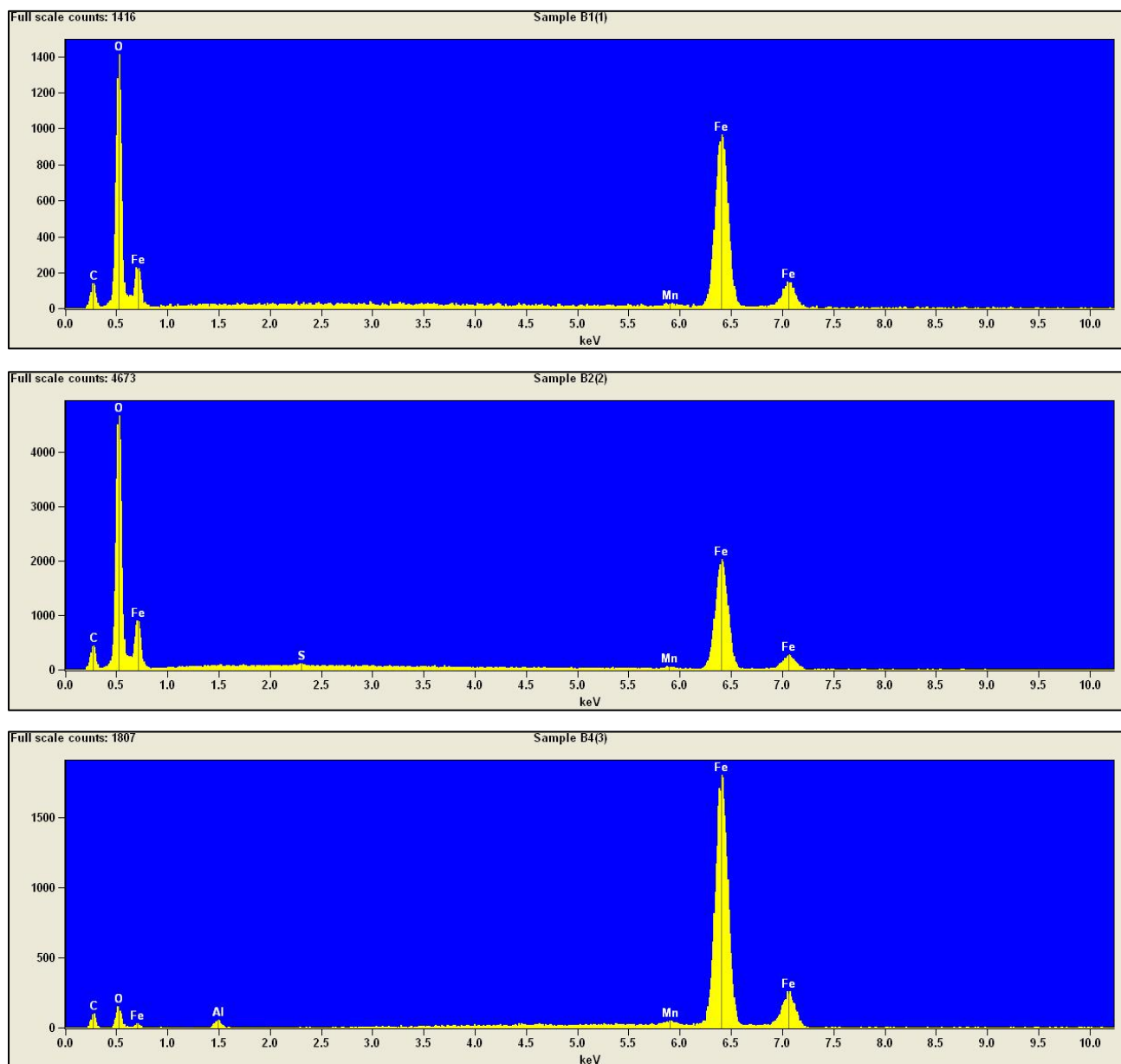


Figure 44. Typical EDS spectra obtained from corrosion samples. The upper spectrum shows results typical for most of the area of each sample. The middle spectrum shows results of an area analyzed on sample B2 showing a small peak of sulfur. The lower spectrum shows results for an area analyzed on sample B4 with a small peak of aluminum.

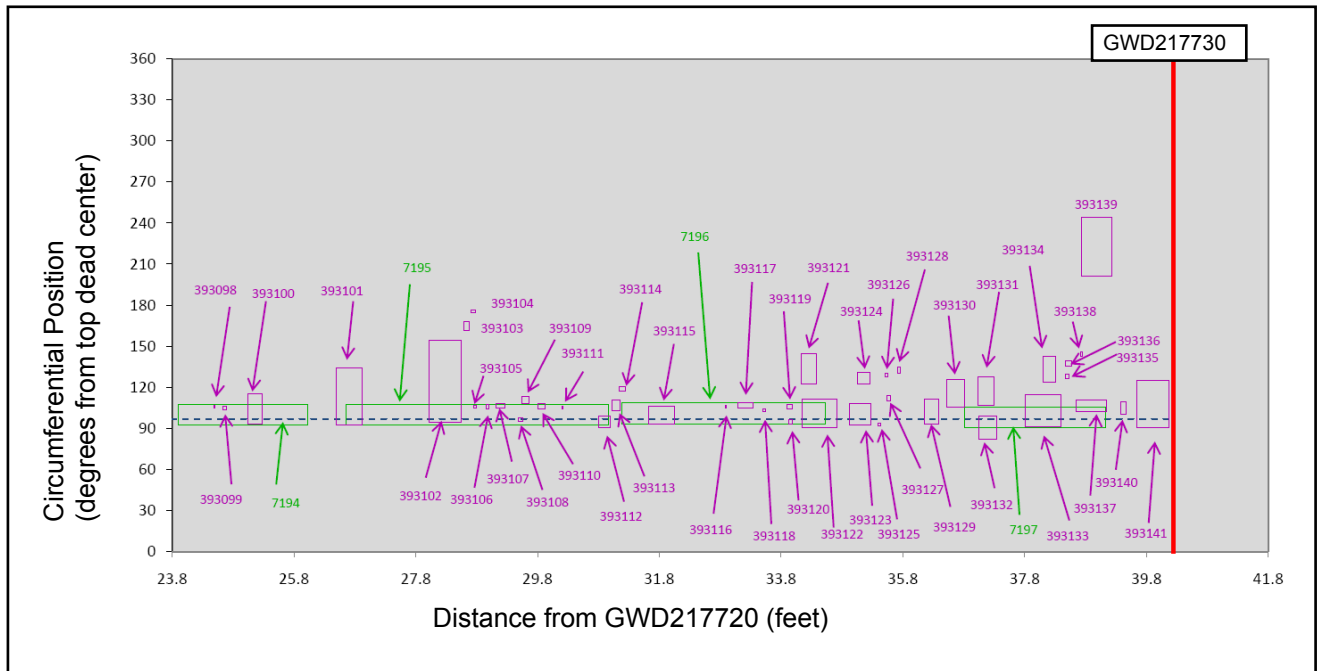
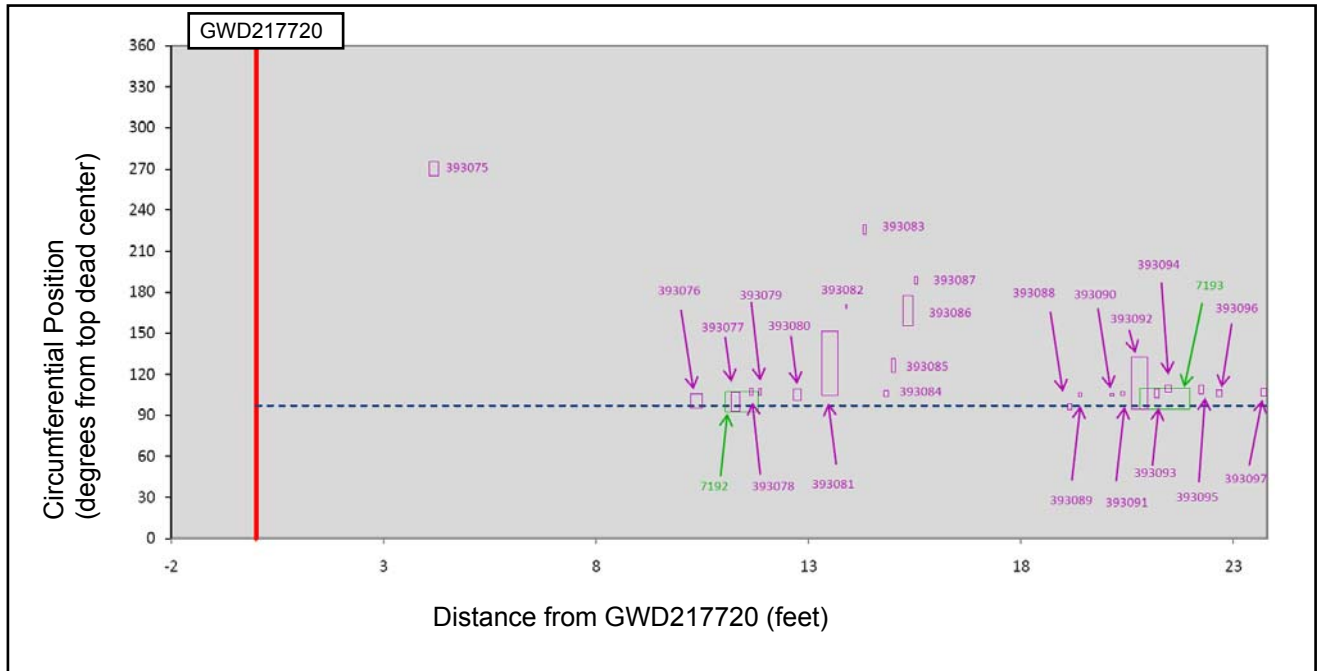


Figure 45. Plot of inspection data for joint 217720 showing locations of crack-like features from the 2005 USCD tool (green boxes) and locations of metal loss from the 2007 MFL tool (pink boxes). Red lines indicate girth weld locations, and a dashed blue line indicates the location of the seam weld.

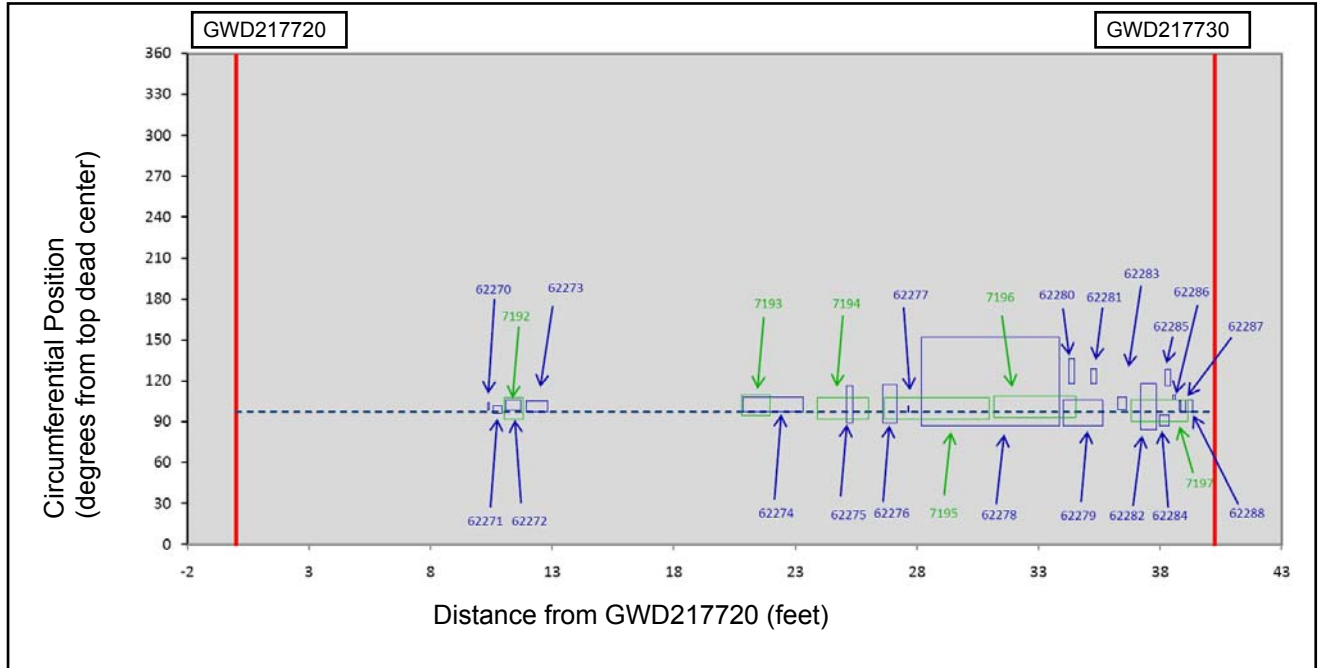


Figure 46. Plot of inspection data for joint 217720 showing locations of crack-like features from the 2005 USCD tool (green boxes) and locations of metal loss from the 2009 USWM tool (blue boxes). Red lines indicate girth weld locations, and a dashed blue line indicates the location of the seam weld.

E. APPENDIX A. COATING ANALYSIS FINAL REPORT



Final Report

National Transportation Safety Board
Mr. Michael Budinski

Date: 10/03/2011

Prepared by:
Dr. Mark Jordi
President
Jordi Labs LLC

Report Number: J6025

NTSB Confidential





October 3, 2011

Michael Budinski
National Transportation Safety Board

E: michael.budinski@ntsb.gov

Dear Michael,

Please find enclosed the test results for your samples described as:

1. *Line 6B Sample A2 DCA10MP007*
2. *Florida Gas Coating Sample*

The following tests were performed:

1. Pyrolysis Gas Chromatography Mass Spectroscopy (GC/MS) (JRC)
2. Fourier Transform Infrared Spectroscopy (FTIR) (JRC)
3. Nuclear Magnetic Resonance Spectroscopy (NMR) (JRC)
4. Liquid Chromatography Mass Spectroscopy (LCMS)
5. Temperature Rising Elution Fractionation (TREF)
6. Thermogravimetric Analysis (TGA)

Objective

The objective of this work was to investigate the chemistry of two (2) polyethylene tape samples with adhesive backing. Each sample consists of a PE tape with an attached adhesive backing. We understand one (1) material contains more low density polyethylene (LDPE) while the other consists of a blend of high density polyethylene (HDPE) and LDPE.

Summary of Results

The tape and adhesive materials were analyzed using a variety of techniques in order to identify their chemistry. Both tape polymers were found to be consistent with polyethylene. TREF analysis indicates that *Line 6B Sample A2* contains approximately 38% HDPE, while the *Florida Gas Coating Sample* was only found to contain LDPE. The PYMS behavior of the samples was consistent with the typical behavior of polyolefins, showing a large number of peaks consistent with various alkane fragments.

LCMS analysis of the extracts from the tape showed significantly large number of extractable components in the *Line 6B Sample A2* as compared to the *Florida Gas Coating Sample*. The compounds detected in *Line 6B Sample A2* include some common polymer additives; oleamide, stearic acid, Irgafos 38 and Ethyl Antioxidant 720. Additives detected in the *Florida Gas Coating Sample* are erucylamide and dioctyl phthalate. In general, the compounds which could be attributed to the adhesive layer could only be identified by mass alone. This generally indicates that they are nature products or degradation products and not commercially available pure compounds.

The tape material was analyzed by TGA in order determine the carbon black concentration in the samples. *Line 6B Sample A2* was found to contain 0.99% carbon black. The *Florida Gas Coating Sample* was found to contain 2.27% carbon black.

The adhesives were found to contain polyisoprene and polyisobutylene. These identifications were based on PYMS, FTIR and NMR analyses. A major pyrolysis product was identified as limonene, providing strong evidence of the presence of polyisoprene. The NMR and FTIR spectra also showed evidence of polyisoprene. Polyisobutylene was identified by NMR, while due to the structure of this compound FTIR and PYMS are not expected show obvious indication of its presence.

Individual Test Results

A summary of the individual test results is provided below. All accompanying data, including spectra, has been included in the data section of this report.

LCMS

In order to investigate the unique compounds present in the adhesive, samples containing the adhesive were compared to samples not containing the adhesive material. The analytical solutions were prepared by extracting the samples with a 50:50 mixture of methanol/Isopropanol at 80°C for one hour. The resulting solution collected from the *Florida Gas Coating Sample* (with adhesive) required filtration before analysis.

Line 6B Sample 2A was found to contain a variety of compounds. The majority of these compounds are present in both the sample containing the adhesive and the sample with only the tape. While many of these compounds could only be identified by their mass alone, a number of common polymer additives were identified.

The *Florida Gas Coating Sample* also showed a large number of components most of which were seen only in adhesive containing region. In general, these compounds could only be identified by mass alone.

Table 1				
LCMS Results - Line 6B Sample A2				
RT	MW	ID/Comments	No Adhesive	With Adhesive
1.0	129	C ₈ amine	x	x
5.2	213	Likely C ₁₂ H ₂₃ NO ₂	x	x
7.0	266		x	x
7.0	374		x	x
7.8	386		x	
8.3	356		x	x
8.3	384		x	x
8.6	368		x	x
9.0	528+	Ethoxylated nonyl phenol		x
9.6	354		x	x
9.6	370		x	x
9.9	234		x	x
9.9	358			x
10.3	398		x	x
10.6	340	C ₂₃ H ₃₂ O ₂ ; likely Ethyl antioxidant 720	x	x
10.8	254	Acidic/Phenolic; likely C ₁₇ H ₁₈ O ₂		x
10.9	281	Oleamide	x	x
11.5	460	Dinonylnaphthalenesulfonic acid		x
12.0	385			x
12.1	311		x	
12.2	337	Erucylamide		x
12.3	284	Stearic acid	x	x
12.8	393		x	x
12.8	367		x	x
13.2	619		x	x
13.4	395		x	x
14.0	514	Irgafos 38	x	x

Table 2				
LCMS Results - Florida Gas Coating Sample				
RT	MW	ID/Comments	No Adhesive	With Adhesive
1.3		Mixture		x
1.4	200		x	
1.4	228		x	x
3.1	62	nitrate anion		x
3.1	112			x
3.4	140			x
6.7	286			x
7.0	266			x
7.1	342	Dipropyleneglycol dibenzoate	x	
7.5	278			x
7.5	378			x
8.2	292			x
8.2	304			x
8.5	292			x
8.7	251			x
9.7	446			x
10.8	281	Oleamide		x
11.5	624	EDA-di(hydroxystearamide)	x	
11.5	390	Diocetyl phthalate	x	
12.2	337	Erucylamide	x	x
12.8	393			x
13.9	304			x
14.8	693			x
15.1	648			x

PYMS

Analysis by PY-GCMS was conducted using a double shot technique. The double shot experiment consists of heating the sample to release volatiles which were then cryogenically trapped and then analyzed by GCMS. Following completion of the 1st pass analysis, the remaining portion of the sample was then heated above the decomposition temperature rapidly and pyrolyzed components were passed into a gas chromatography column and analyzed by mass spectroscopy.

Prominent peaks found in PY-GCMS typically include fragments of the polymer as well as monomer, antioxidants and other additives. Sample peaks were compared with over 796,613 reference compounds using the NIST/EPA/NIH mass spectral search program.

Results

Both adhesives show relatively complex chromatograms. A major degradation product observed during the 1st pass is identified as limonene. The presence of this component provides strong evidence that polyisoprene is present as limonene is a major degradation product of polyisoprene. The major component in latex (natural rubber) is cis-1,4-polyisoprene. Data collected from a natural latex standard have been provided for comparison.

The additional components detected are consistent with logical degradation products. Degradation products observed are generally unsaturated hydrocarbons which are expected from polyisoprene.

While the PYMS behavior of the samples is similar they do show some differences. Specifically, we observe a group of large mass ions (>300 amu) detected during the 1st pass in *Line 6B Sample A2* which are not detected in the *Florida Gas Coating Sample*. These materials show relatively poor chromatography and are not well matched by the NIST spectral database. This provides some evidence that the compounds present are a variety of natural products. Natural products are often the most difficult to identify, as they generally are present as a large number of specific chemical species.

The PYMS data collected from the bulk polymeric material sampled away from the adhesive material is consistent with a polyolefin, such as polyethylene. PYMS of these materials generally show a large number of equally spaced chromatographic peaks. These peaks are consistent with incrementally higher molecular weight alkanes.

TGA

The sample was subjected to TGA analysis over the temperature range from ambient to 1000°C. The sample was kept under a nitrogen atmosphere during the heating ramp. Upon reaching 1000°C the gas flow was changed to air. The sample was held at 1000°C under air for 10 minutes. This method is designed to determine the carbon black content in a sample as carbon black will not show TGA weight loss under nitrogen. However, carbon black will burn when exposed to oxygen. Therefore, the weight loss that occurs after switching to air represents the carbon black content of the sample.

Table 3				
TGA Results				
Sample	Run	Weight Loss N ₂ (%)	Weight Loss Air (%)	Carbon Black (Avg. %)
<i>Line 6B Sample A2</i>	1	98.91	1.012	0.990
	2	98.07	0.9675	
<i>Florida Gas Coating Sample</i>	1	95.35	2.179	2.27
	2	96.23	2.361	

FTIR

In order to further compare the two adhesive materials, they were both analyzed by FTIR. While the spectra are similar, the *Line 6B Sample A2* adhesive is found to contain a strong peak near 1000 cm^{-1} . Peaks in this region are generally attributed to C-O-C stretching in ethers, or Si-O stretching in silicates. This band is not observed in the *Florida Gas Coating Sample* adhesive.

Other than this peak in the *Line 6B Sample A2* adhesive, both spectra are consistent with polyisoprene. **Table 4** contains a summary of the peaks observed as well as their identifications.

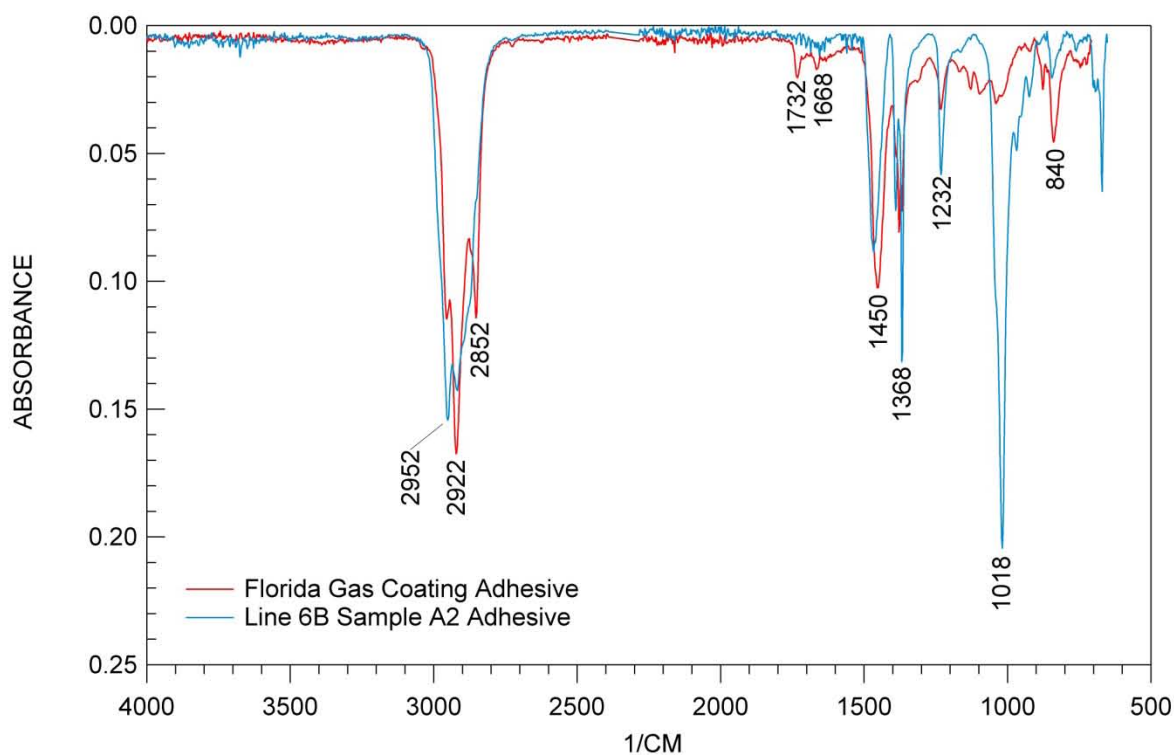


Figure 1 - Overlay of FTIR spectra collected from the adhesive portion of the samples.

Table 4 FTIR Results	
IR Frequency (cm ⁻¹)	Functional Group
2952, 2922, 2852	CH stretch
1732*	C=O
1668	C=C
1450	-CH ₂ - bend
1368	-CH ₃ bend
1232	Unknown
1018*	Si-O or C-O-C
840	CH Wag, Tri-substituted olefin

* - Only detected in the *Line 6B Sample A2 Sample*.

NMR

The adhesive portion of the samples was removed and dissolved in CDCl₃ for analysis by NMR. It was noted during dissolution that a black particulate material remained insoluble. This material most likely represents carbon black which was also detected in the tape.

The NMR spectra collected are consistent with a mixture or co-polymer of polyisoprene and polyisobutylene. Due to the fact that polyisobutylene is a saturated hydrocarbon, it could not be identified based on PYMS or FTIR data alone. This polymer will tend to pyrolyze to a variety of alkanes which can be difficult to relate directly to a specific polymer. FTIR spectra of this polymer will generally show a limited number of peaks useful for identification. **Tables 5** and **6** include identification of the NMR peaks observed with respect to polyisobutylene and polyisoprene.

Table 5 Polyisobutylene	
Identification	Chemical Shift (ppm)
A1	59.5
A2	38.1
B1	31.2

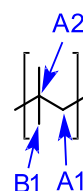
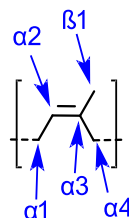


Table 6 Polyisoprene	
Identification	Chemical Shift (ppm)
$\alpha 1$	26.4
$\alpha 2$	125.0
$\alpha 3$	135.2
$\alpha 4$	31.2
$\beta 1$	22.7



When compared, the samples show different monomer ratios. The *Florida Gas Coating Sample* is found to contain a significantly lower fraction of polyisobutylene. The ratio of the monomers can be calculated using the peak areas observed as follows:

$$\%Polyisoprene = \frac{Area_{\alpha 3}}{Area_{\alpha 1} + Area_{\alpha 3}} \times 100$$

Using this equation, the *Florida Gas Coating Sample* adhesive is found to contain 69% polyisoprene, while *Line 6B Sample 2A* adhesive contains 16% polyisoprene. It should be noted that these percentages represent only the ratio of these two monomers, and not the overall content in the adhesive. The chloroform soluble portion of the *Florida Gas Coating Sample* adhesive shows some additional unidentified peaks. Due to the complexity of the NMR spectrum collected they cannot be specifically identified. These peaks could be due to another component or could represent the polymer end groups.

TREF

TREF is a technique for the analysis of polyolefins (primarily polyethylene) which allows the separation of components with different branching structures. High density and low density polyethylene can be resolved by this method. The experiment consists of placing the sample into a suitable solvent and loading it onto a GPC column. The temperature of the system is then lowered and the polyolefin precipitates onto the GPC packing as a function of its branching structure. The temperature is then raised in a controlled manner, causing elution of the polymer as a function of its branching structure. The most highly branched material generally elutes first.

The two samples show a clear difference in HDPE/LDPE ratio. Peak 1, observed at approximately 79°C can be identified as LDPE while the peak eluting at approximately 100°C represents the HDPE fraction. The *Florida Gas Coating Sample* is not found to contain a significant HDPE fraction. On the other hand, *Line 6B Sample A2* shows approximately 38.1% HDPE. There is also a fairly significant difference in soluble fractions (low molecular weight oligomers). Specifically the *Florida Gas Coating Sample* contains more soluble material.

Table 7					
TREF Results					
Sample	T ^a (°C) Peak 1	Peak 1 Area (%)	T ^a (°C) Peak 2	Peak 2 Area (%)	Soluble Fraction (%) (35°C)
<i>Florida Gas Coating</i>	79.3	87.4	--	--	12
<i>Line 6B Sample A2</i>	79.6	57.8	99.7	38.1	4

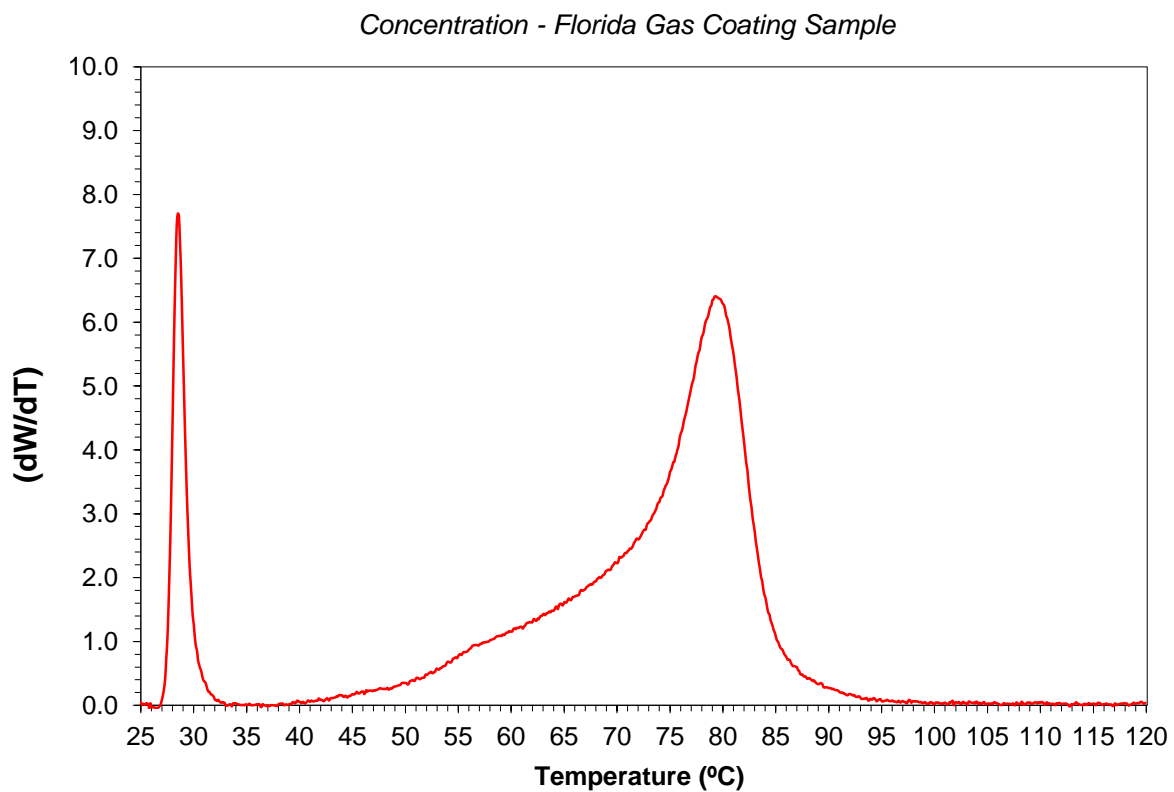


Figure 2 - Elution profile *Florida Gas Coating Sample*.

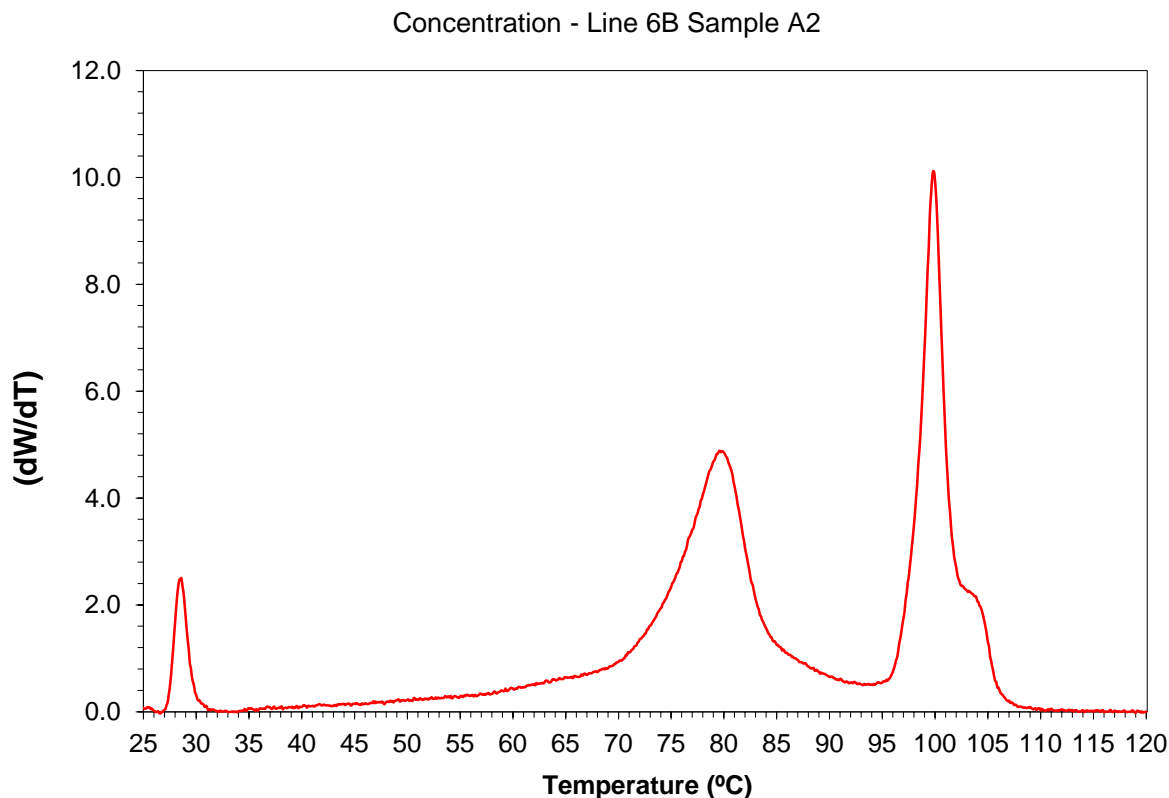


Figure 3 - Elution profile for *Line 6B Sample A2*.

Analysis Conditions

PY-GCMS (Adhesive)

Solid samples were analyzed using a Hewlet 6890 gas chromatograph in conjunction with a 5975B mass selective detector using a Frontier Laboratories double shot Pyrolyzer model PY2020ID. Data acquisition was accomplished using chemstation software. Sample peaks were compared with over 796,613 reference compounds using the NIST/EPA/NIH mass spectral search program.

The following run conditions were applied for Gas Chromatographic analysis:

Sample Size = ~.1mg

Initial Delay = 2.0 minutes

Initial Temperature: 50°C

Final Temperature: 350°C

Temperature Ramp Rate 1: 20°C per minute

Hold Time: 15 minutes

Pyrolysis Temperature: 1st pass = 100-350 2nd pass = 550°C

Detector Temperature: 315°C

Injector Split = 80:1

Mass Range: Low Mass = 30 High Mass = 700
Column = Ultra Alloy –PBDE

PY-GCMS (Bulk Polymer)

Solid samples were analyzed using a Hewlet 6890 gas chromatograph in conjunction with a 5975B mass selective detector using a Frontier Laboratories double shot Pyrolyzer model PY2020ID. Data acquisition was accomplished using chemstation software. Sample peaks were compared with over 796,613 reference compounds using the NIST/EPA/NIH mass spectral search program.

The following run conditions were applied for Gas Chromatographic analysis:

Sample Size = ~.1mg
Initial Delay = 2.0 minutes
Initial Temperature: 50°C
Final Temperature: 350°C
Temperature Ramp Rate 1: 20°C per minute
Hold Time: 15 minutes
Pyrolysis Temperature: 1st pass =100-300 2nd pass = 550°C
Detector Temperature: 315°C
Injector Split = 80:1
Mass Range: Low Mass = 30 High Mass = 700
Column = Ultra Alloy –PBDE

TGA

Analysis of samples was accomplished using a TA 500 Thermogravimetric Analyzer in combination with TA Universal Analysis software. Approximately 8-12mg of the sample was weighed into a platinum weigh boat for each analysis. Samples were run under a nitrogen atmosphere and heated from ambient to 1000°C at a rate of 20°C per minute. After reaching 1000°C the sample purge gas was switched to air and held isothermally for 10 minutes.

LCMS

LCMS analyses were performed under the following conditions:

Column:	Waters Symmetry C18 5 μ
Column Temperature:	30°C
Initial Mobile Phase:	40% water (0.005% HOAc) / 60% methanol
Final Mobile Phase A:	100% methanol
Gradient Time A:	10 minutes
Final Mobile Phase B:	50% methanol / 50% isopropyl alcohol
Gradient Time B:	5 minutes

Final Hold Time:	1 minute
Ionization Mode:	ESI, APCI
Polarity:	Positive and negative
Vaporizer Temp.:	220°C, 400°C
Mass Range:	50 – 1200
Scan Period:	2.2 seconds

ESI is electrospray ionization. Positive ion analyses give strong signals for compounds that are easily protonated or sodiated. Negative ion analyses give strong signals for acidic compounds. APCI is atmospheric pressure chemical ionization. Positive ion analyses give strong signals for compounds that are easily protonated. Negative ion analyses give strong signals for phenolic compounds.

The analytical solutions were prepared by extracting the samples with a 50:50 mixture of methanol/Isopropanol at 80°C for one hour. The resulting solution from sample 4 required filtration before analysis.

TREF

Analysis Parameters			Method: Default		
	Dis.	Stab.	Cryst:	Elution	
Rate (°C /min)	40.00	40.00	0.50	1.0	
Temp. (°C)	150	95	35	35	120
Time (min)	90	45	10		10
Filling Vol. (ml).	20.00	Detector Mode:2 Wavelength Baseline: Traditional			
Sample Vol. (ml)	0.30				
Column Load Vol.	1.90				
Pump Flow (ml/min)	0.50				
Concentration: mg/ml	3.0				

Closing Comments

Deformulation of an unknown material is intended to provide a best estimate of the chemical nature of the sample. All chemical structures are supported by the evidence presented but are subject to revision upon receipt of additional evidence. Additional factors such as material processing conditions may also affect final material properties.

Jordi Labs' reports are issued solely for the use of the clients to whom they are addressed. No quotations from reports or use of the Jordi name is permitted except as authorized in writing. The liability of Jordi Labs with respect to the services rendered shall be limited to the amount of consideration paid for such services and do not include any consequential damages.

Jordi Labs specializes in polymer testing and has 30 years experience doing complete polymer reformulations. We are one of the few labs in the country specialized in this type of testing. We will work closely with you to help explain your test results and solve your problem. We appreciate your business and are looking forward to speaking with you concerning these results.

Sincerely,

^(R)
(R)

Kevin Rowland, M.S.
Senior Chemist
Jordi Labs LLC

^(R)
(R)

Mark Jordi, Ph. D.
President
Jordi Labs LLC

Appendix

Table of Contents

- Pages -1 – PYMS Data
- Pages 97- – FTIR Data
- Pages - – NMR Data
- Pages - – LCMS Data
- Pages - – TGA Data

**F. APPENDIX B. PIPE MECHANICAL PROPERTIES AND CHEMICAL ANALYSIS
REPORT**



Lehigh Testing Laboratories, Inc.

A Subsidiary of THE MMR GROUP, INC.

308 WEST BASIN ROAD • P.O. BOX 903 • NEW CASTLE, DE 19720
(302) 328-0500 • FAX (302) 328-0417



TEST REPORT

NATIONAL TRANSPORTATION SAFETY BOARD
ATTENTION: MATTHEW FOX
490 L'ENFANT PLAZA EAST
WASHINGTON, DC 20594

DATE: November 10, 2010

PO NO: Verbal

LEHIGH NO: **K-33-33**
Sample 1

PAGE: 1 of 1

MATERIAL: API 5L GRADE X52
SAMPLE DESIGNATION: (1) SAMPLE: SECTION OF PIPE 30" OD X 0.25" WALL
PIECE B3a (BASE MATERIAL WITHOUT A WELD)
IS 20" IN THE LONGITUDINAL DIRECTION AND
20" IN THE CIRCUMFERENTIAL DIRECTION
NTSB ACCIDENT NUMBER: DCA10MP007

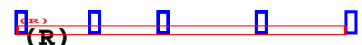
CHEMICAL ANALYSIS (%)

Carbon	0.23
Sulfur	0.013
Phosphorus	0.007
Silicon	<0.01
Manganese	1.16
Chromium	0.01
Nitrogen	0.004

Results are for information only.

LTL Procedure: *QA-CH-P-048 Rev 1 (Leco C&S)*
QA-CH-P-124 Rev 1 (ICP)
QA-CH-P-122 Rev 1 (Leco N)

Lehigh Testing Laboratories, Inc.


(R)

Peter M. Engelgau, Principal Chemist



TEST REPORT

NATIONAL TRANSPORTATION SAFETY BOARD
ATTENTION: MATTHEW FOX
490 L'ENFANT PLAZA EAST
WASHINGTON, DC 20594

DATE: November 10, 2010

PO NO: Verbal

LEHIGH NO: **K-33-33**
Sample 1

PAGE: 1 of 1

MATERIAL: API 5L GRADE X52
SAMPLE DESIGNATION: (1) SAMPLE: SECTION OF PIPE 30" OD X 0.25" WALL
PIECE B3a (BASE MATERIAL WITHOUT A WELD)
IS 20" IN THE LONGITUDINAL DIRECTION AND
20" IN THE CIRCUMFERENTIAL DIRECTION
NTSB ACCIDENT NUMBER: DCA10MP007

MECHANICAL PROPERTIES (Per ASTM A370-07)

#1 – PIECE B3a

BASE METAL

TRANSVERSE TENSILES

	<u>1-1</u>	<u>1-2</u>	<u>1-3</u>
Width (inches):	1.504	1.512	1.513
Thickness (inches):	0.258	0.261	0.261
Area (square inches):	0.3880	0.3946	0.3949
Yield Point (psi): 0.5% EUL	59,400	61,900	63,000
Yield Point (psi): 0.2% Offset	55,800	58,600	61,700
Ultimate Tensile Strength (psi):	83,100	81,900	82,100
Elongation (%) in 2":	27	25	25

Results are for information only.

Lehigh Testing Laboratories, Inc.


(R)

Kenneth M. Petito, Supvr., Mechanical Testing



TEST REPORT

NATIONAL TRANSPORTATION SAFETY BOARD
ATTENTION: MATTHEW FOX
490 L'ENFANT PLAZA EAST
WASHINGTON, DC 20594

DATE: November 10, 2010

PO NO: Verbal

LEHIGH NO: **K-33-33**
Sample 1

PAGE: 1 of 1

MATERIAL: API 5L GRADE X52
SAMPLE DESIGNATION: (1) SAMPLE: SECTION OF PIPE 30" OD X 0.25" WALL
PIECE B3a (BASE MATERIAL WITHOUT A WELD)
IS 20" IN THE LONGITUDINAL DIRECTION AND
20" IN THE CIRCUMFERENTIAL DIRECTION
NTSB ACCIDENT NUMBER: DCA10MP007

IMPACT PROPERTIES (Per ASTM A370-07)

<u>LTL #</u>	<u>Customer ID</u>	<u>Test Temp</u>	<u>Impact Energy (Ft/Lbs)</u>	<u>Lateral Expansion (Mils)</u>	<u>Shear (%)</u>
K-33-33-1	Piece B3a	70° F	19	33	100
K-33-33-1	Piece B3a	70° F	19	32	100
K-33-33-2	Piece B3a	0° F	9	16	25
K-33-33-2	Piece B3a	0° F	9	17	25
K-33-33-3	Piece B3a	120° F	20	42	100
K-33-33-3	Piece B3a	120° F	20	43	100
K-33-33-4	Piece B3a	20° F	11	27	50
K-33-33-4	Piece B3a	20° F	11	26	50
K-33-33-5	Piece B3a	30° F	14	31	60
K-33-33-5	Piece B3a	30° F	14	32	60
K-33-33-6	Piece B3a	50° F	18	36	90
K-33-33-6	Piece B3a	50° F	18	35	90
K-33-33-7	Piece B3a	-20° F	7	15	0
K-33-33-7	Piece B3a	-20° F	6	13	0
K-33-33-8	Piece B3a	-10° F	7	16	15
K-33-33-8	Piece B3a	-10° F	7	17	15
K-33-33-9	Not Tested				
K-33-33-9	Not Tested				
K-33-33-10	Piece B3a	60° F	18	38	95
K-33-33-10	Piece B3a	60° F	18	39	95

Results are for information only.

Specimen Size: 5mm X 10mm

Lehigh Testing Laboratories, Inc.


(R)

Kenneth M. Petito, Supvr., Mechanical Testing



TEST REPORT

NATIONAL TRANSPORTATION SAFETY BOARD
ATTENTION: MATTHEW FOX
490 L'ENFANT PLAZA EAST
WASHINGTON, DC 20594

DATE: November 10, 2010

PO NO: Verbal

LEHIGH NO: **K-33-33**
Sample 2

PAGE: 1 of 1

MATERIAL: API 5L GRADE X52
SAMPLE DESIGNATION: (1) SAMPLE: SECTION FROM A PIPE 30" OD X 0.25" WALL
PIECE A1a (CONTAINING THE WELD)
IS 8" IN THE LONGITUDINAL DIRECTION AND
16" IN THE CIRCUMFERENTIAL DIRECTION
NTSB ACCIDENT NUMBER: DCA10MP007

MECHANICAL PROPERTIES (Per ASTM A370-07)

#2 – PIECE A1a

CONTAINING THE WELD

TRANSVERSE TENSILES

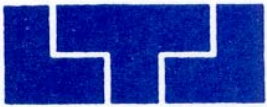
	<u>2-1</u>	<u>2-2</u>	<u>2-3</u>
Width (inches):	1.525	1.525	1.518
Thickness (inches):	0.258	0.260	0.263
Area (square inches):	0.3935	0.3965	0.3992
Yield Point (psi): 0.5% EUL	63,900	63,000	64,200
Yield Point (psi): 0.2% Offset	63,200	62,000	62,700
Ultimate Tensile Strength (psi):	83,200	82,400	81,700
Elongation (%) in 2":	22	19	22
Location of Fracture:	Base	Base	Base

Results are for information only.

Lehigh Testing Laboratories, Inc.



Kenneth M. Petito, Supvr., Mechanical Testing



Lehigh Testing Laboratories, Inc.

A Subsidiary of THE MMR GROUP, INC.

308 WEST BASIN ROAD • P.O. BOX 903 • NEW CASTLE, DE 19720
(302) 328-0500 • FAX (302) 328-0417



TEST REPORT

NATIONAL TRANSPORTATION SAFETY BOARD
ATTENTION: MATTHEW FOX
490 L'ENFANT PLAZA EAST
WASHINGTON, DC 20594

DATE: November 10, 2010

PO NO: Verbal

LEHIGH NO: **K-33-33**
Sample 3

PAGE: 1 of 1

MATERIAL: API 5L GRADE X52
SAMPLE DESIGNATION: (1) SAMPLE: PIECE B1a (APPROX 2-1/2" SQUARE X 1/4" THICK)
NTSB ACCIDENT NUMBER: DCA10MP007

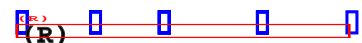
CHEMICAL ANALYSIS (%)

Carbon	0.26
Sulfur	0.014
Phosphorus	0.008
Silicon	<0.01
Manganese	1.18
Nitrogen	0.004

Results are for information only.

LTL Procedure: *QA-CH-P-048 Rev 1 (Leco C&S)*
QA-CH-P-124 Rev 1 (ICP)
QA-CH-P-122 Rev 1 (Leco N)

Lehigh Testing Laboratories, Inc.



Peter M. Engelgau, Principal Chemist

G. APPENDIX C. PIPE RESIDUAL STRESS ANALYSIS REPORT



Lambda Research, Inc

part of the Lambda Technologies Group

5521 Fair Lane
Cincinnati, OH 45227
Phone: (513)561-0883
Fax: (513)561-0886
www.lambdatechs.com

March 11, 2011

Dr. Matthew R. Fox
National Transportation Safety Board
490 L'Enfant Plaza East, SW
Washington, DC 20594

Dear Matt:

The final report covering the determination of the principal subsurface residual stress distributions by the ring core method in two carbon steel pipe sections is enclosed. Locations RS1 and RS4 had relatively low residual stresses.

This completes the work authorized under your credit card purchase. We will close this project and return the test materials to you under separate cover. If you have not received them within a reasonable period of time, please contact us, and a tracer will be placed immediately.

I am also enclosing a client reply card designed to help us improve our service and better meet your needs. Please take a moment to give us your thoughts and return the card by e-mail.

Lambda Technologies provides engineering design services to optimize surface enhancement technologies including conventional shot peening, ultrasonic peening, low plasticity burnishing, deep rolling, and laser peening, for specific applications. Our residual stress measurement and modeling capabilities are combined with decades of experience with these technologies to solve fatigue and stress corrosion problems. Service lives of components damaged by fretting, FOD, corrosion pitting, etc. can often be restored or extended with an appropriate surface treatment. Publications describing a variety of alloys, damage mechanisms, and applications are available on our web site at www.lambdatechs.com. Please contact me, or our Surface Enhancement division, for further information on surface enhancement solutions .

Should you have any questions, or if we can be of further service, please call me.

Sincerely,

Thomas P. Lachtrupp
Project Engineer

TPL:tlb

Enclosure



National Transportation Safety Board
490 L'Enfant Plaza East, SW
Washington, DC 20594

**DETERMINATION OF THE PRINCIPAL SUBSURFACE
RESIDUAL STRESS DISTRIBUTIONS BY THE
RING CORE METHOD IN TWO CARBON STEEL PIPE SECTIONS**

REPORT: 995-16203
DATE: March 11, 2011

ATTN: Dr. Matthew R. Fox
AUTHORIZATION: Credit Card
REF.: PO#NTSBV392

SPECIFICATIONS: N/A
LRI PROCEDURES: 3P1051

INTRODUCTION

Two pipe sections were received from National Transportation Safety Board for the purpose of determining the principal subsurface residual stress distributions. The pipe sections, identified as A3 and B5, were manufactured from carbon steel and were nominally 14.0 in. long with a 30.0 in. diameter and a 0.3 in. wall thickness (356 mm long with a 762 mm diameter and a 6 mm wall thickness).

Thomas P. Lachtrupp
Project Engineer

Quality Assurance



Testing
Cert.
#0138.01

This report shall not be reproduced, except in full, without the approval of Lambda Research, Inc. The results reported apply only to the specific sample/s submitted for analysis. Measurement uncertainties are reported as one standard deviation (1σ) assuming a Gaussian distribution. Multiply the uncertainty shown by a factor of 2 to determine the expanded 2σ uncertainty, providing nominally 95% confidence ($k=2$), per ISO/IEC 17025-2005. Lambda Research is accredited in accordance with ISO/IEC 17025-2005 by the American Association for Laboratory Accreditation in the field of Mechanical Testing, Certificate Number 0138.01.



Testing
Cert.
#0138.01

TECHNIQUE

The principal residual stresses were measured as functions of depth at a total of three locations on Specimen A3 and two locations on Specimen B5 on the outside diameter as marked by the client and shown in Figures 6 through 10.

The principal residual stresses were calculated using an incremental ring coring (mechanical dissection) method. The method consists of applying a strain gage rosette to each area of interest and dissecting a plug containing the strain gages. During the sectioning operation, the residual strain in the part is relieved. The relieved strain is recorded and is used to calculate the residual stress as a function of depth.

Rectangular electrical resistance strain gage rosettes were installed at the measurement location on each specimen. The strain gage rosettes were placed with the No. 1 gage reference direction oriented as indicated in the attached tables of data. A plug containing the strain gage was then cut at the depth increments shown in the attached data.

RESULTS AND DISCUSSION

The residual stress values were resolved in the three directions shown in the attached data. The data are presented in the Appendix and are shown graphically in Figures 1 through 5. Compressive stresses are shown as negative values, tensile as positive, in units of ksi (10^3 psi) and MPa.

In each table the column titled STRESS 1, lists the residual stresses in the reference direction. The reference direction is in the hoop direction. The columns titled STRESS 2 and STRESS 3 are the residual stresses in the 45 degree and axial directions, respectively, rotated counterclockwise from the No. 1 direction. All three stresses lie in a plane which is parallel to the plane of the surface. The maximum stress, minimum stress and phi are calculated using Mohr's Circle for stress. The maximum stress direction is defined by the angle phi, which is taken to be a positive angle counterclockwise from the No. 1 gage reference direction.

In each figure the residual stresses calculated in the three measurement directions are plotted along with the maximum and minimum residual stresses. A plot of phi as a function of depth is also shown.

CONCLUSIONS

The residual stress depth profiles are presented in Figures 1 through 5. It should be noted that the data near the surface has the highest error due to assumptions made pertaining to the slope of the strain relaxation near the surface and the sensitivity of the strain gage to near surface relaxation. The highest overall tension was measured at location RS2 on specimen A3. Location RS3 on specimen A3 and location RS5 on specimen B5 were collectively the most compressive locations measured with location RS5 being the more compressive of the two.

(ircore.doc.0603)

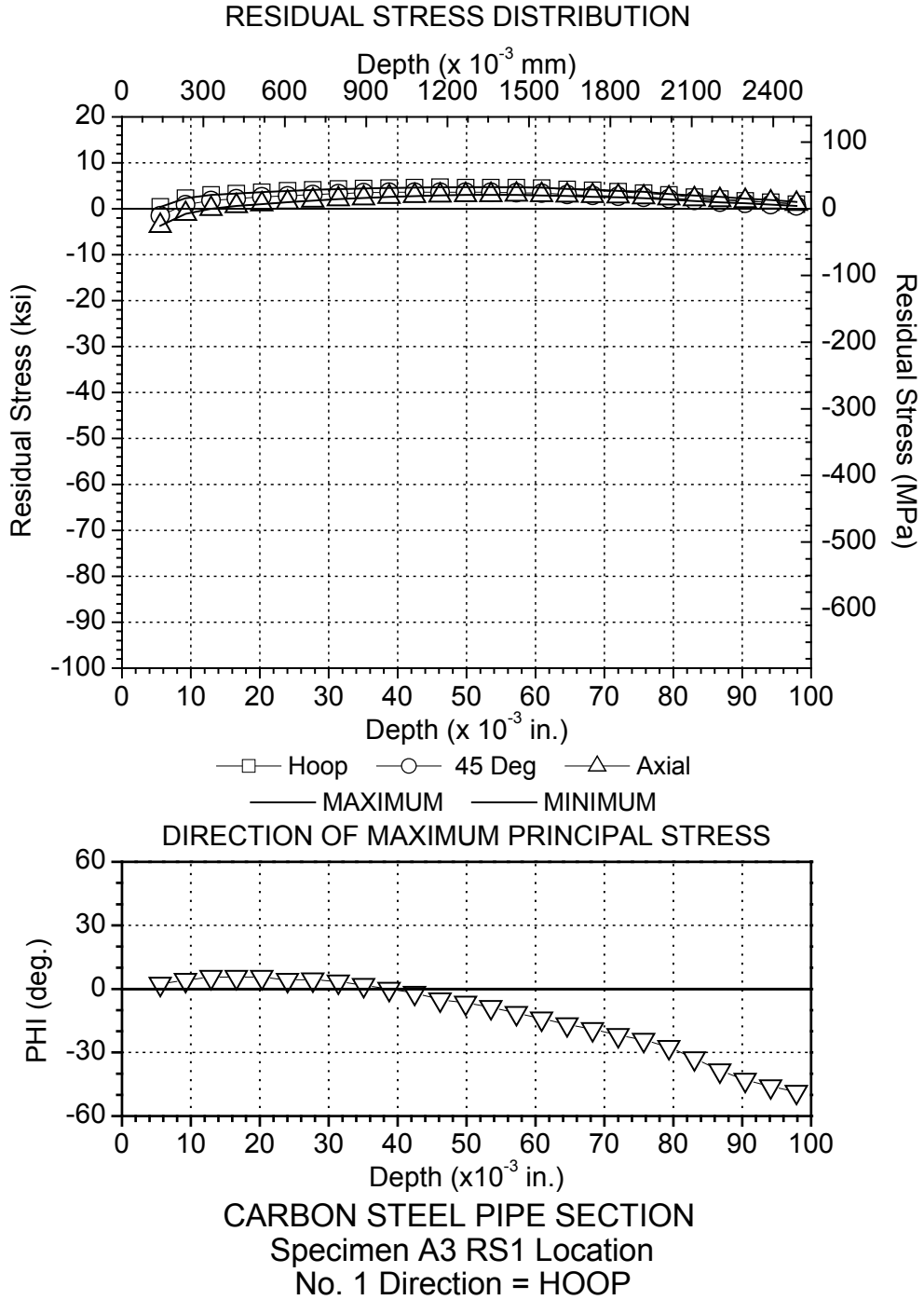


Figure 1

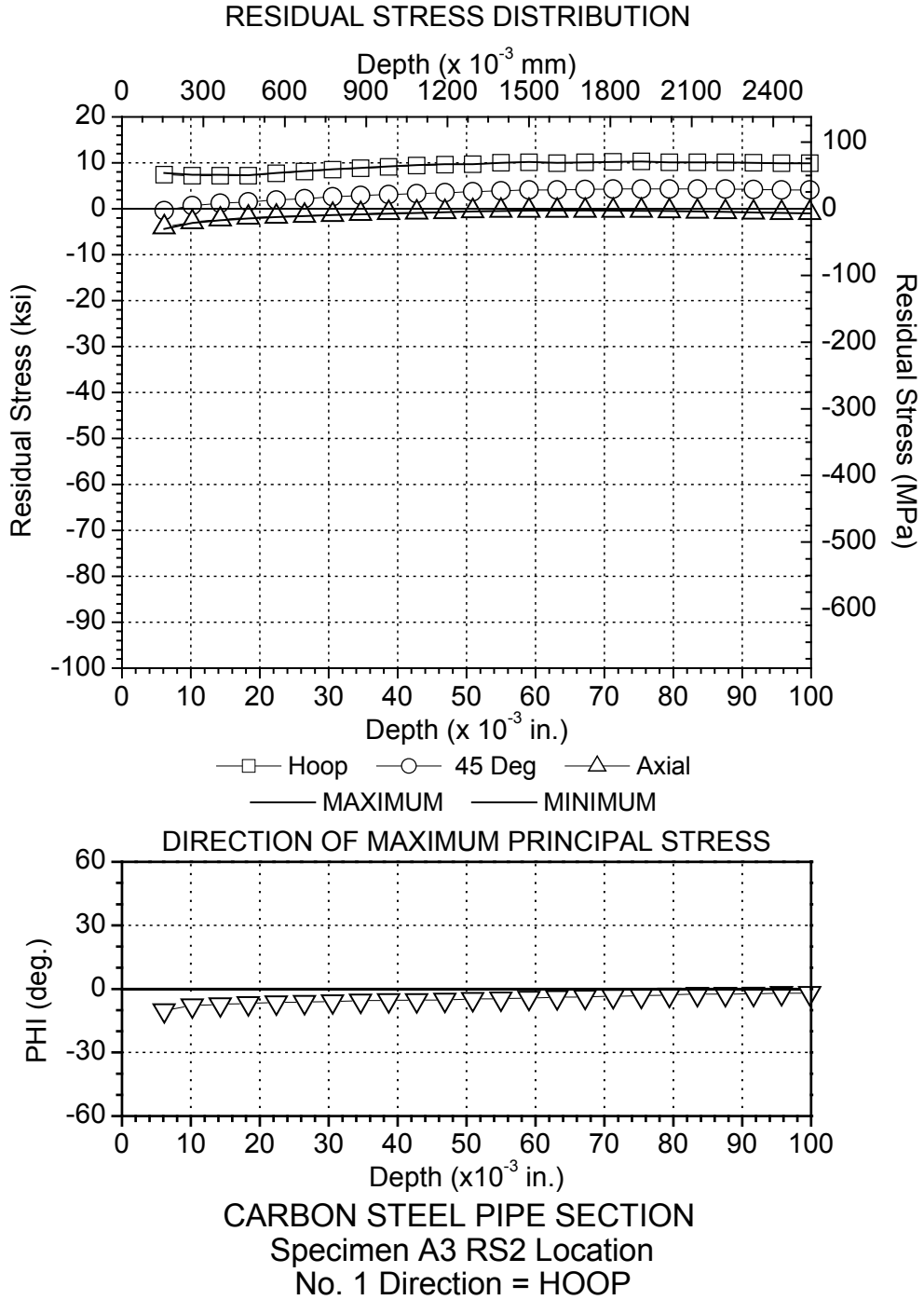


Figure 2

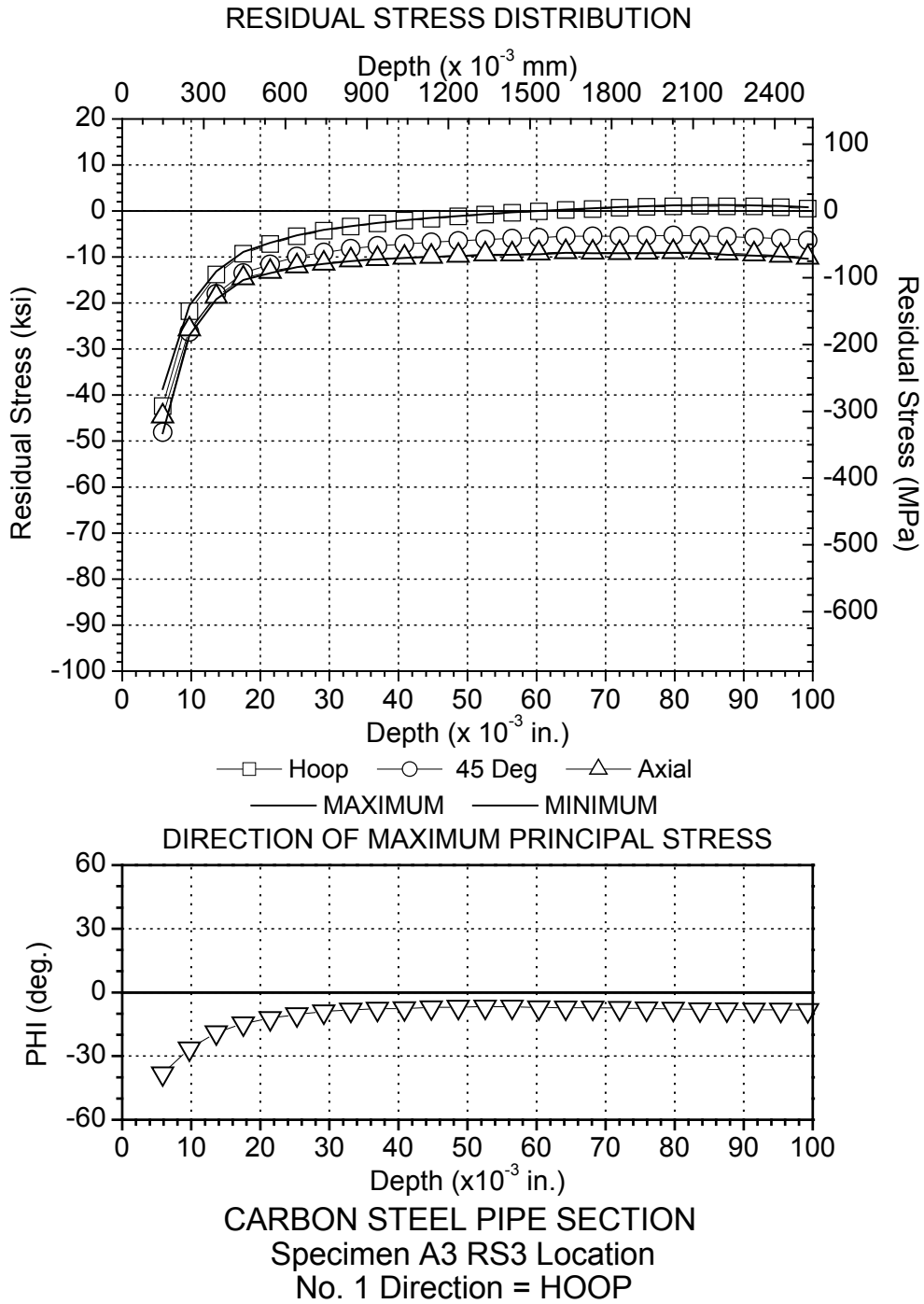


Figure 3

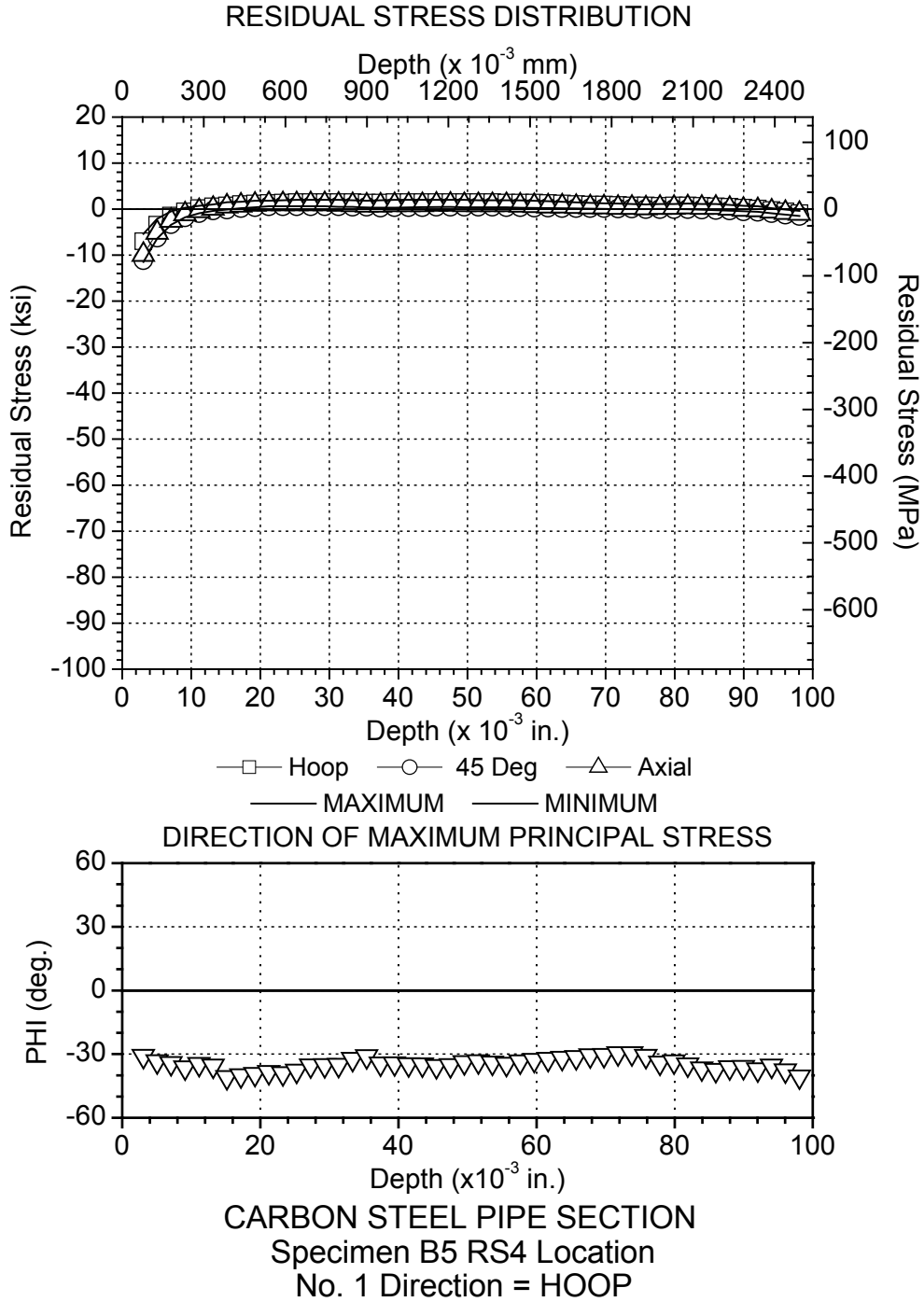
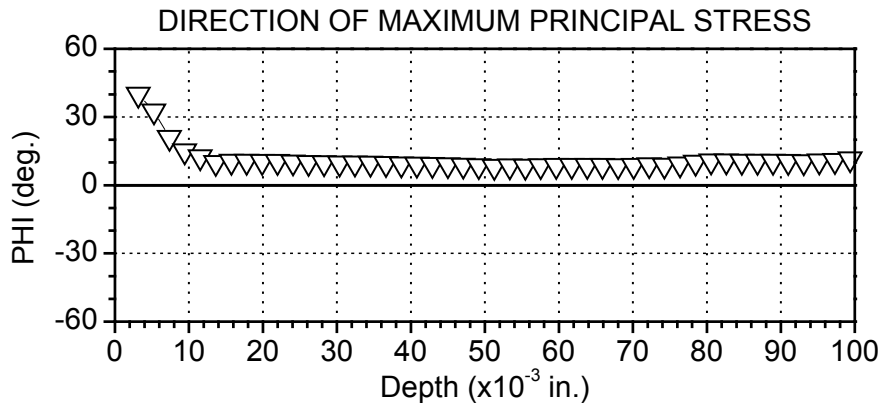
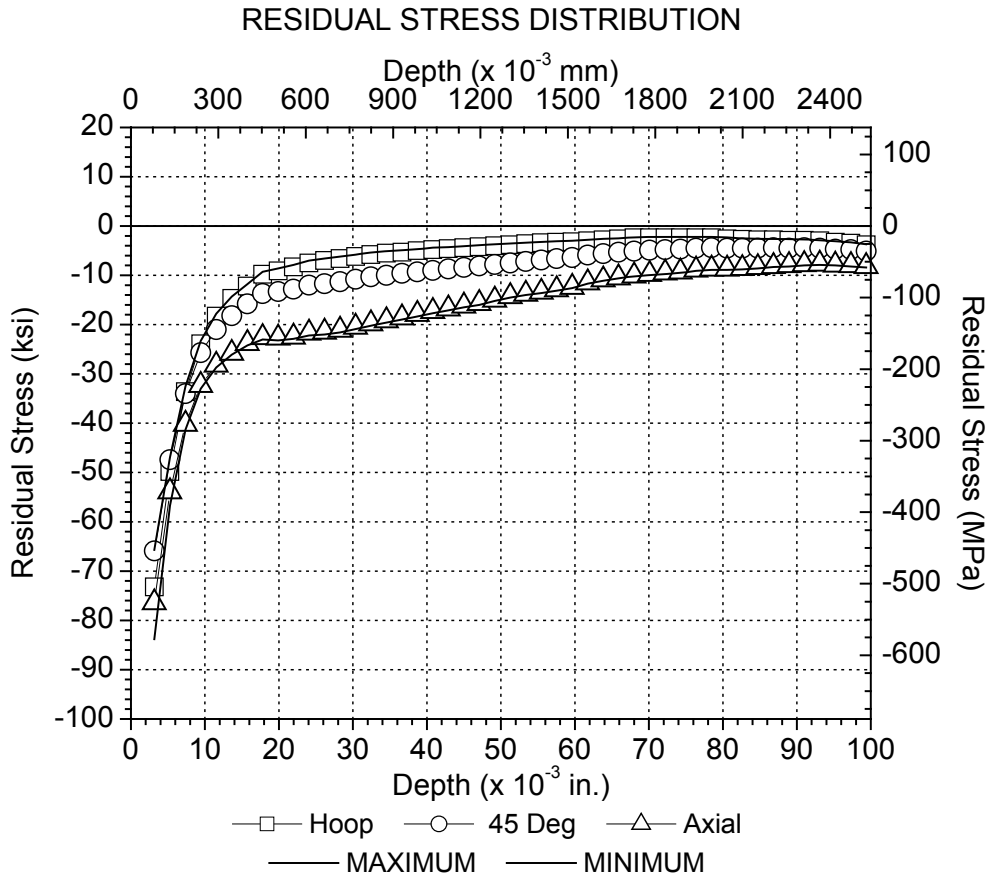


Figure 4



CARBON STEEL PIPE SECTION
Specimen B5 RS5 Location
No. 1 Direction = HOOP

Figure 5

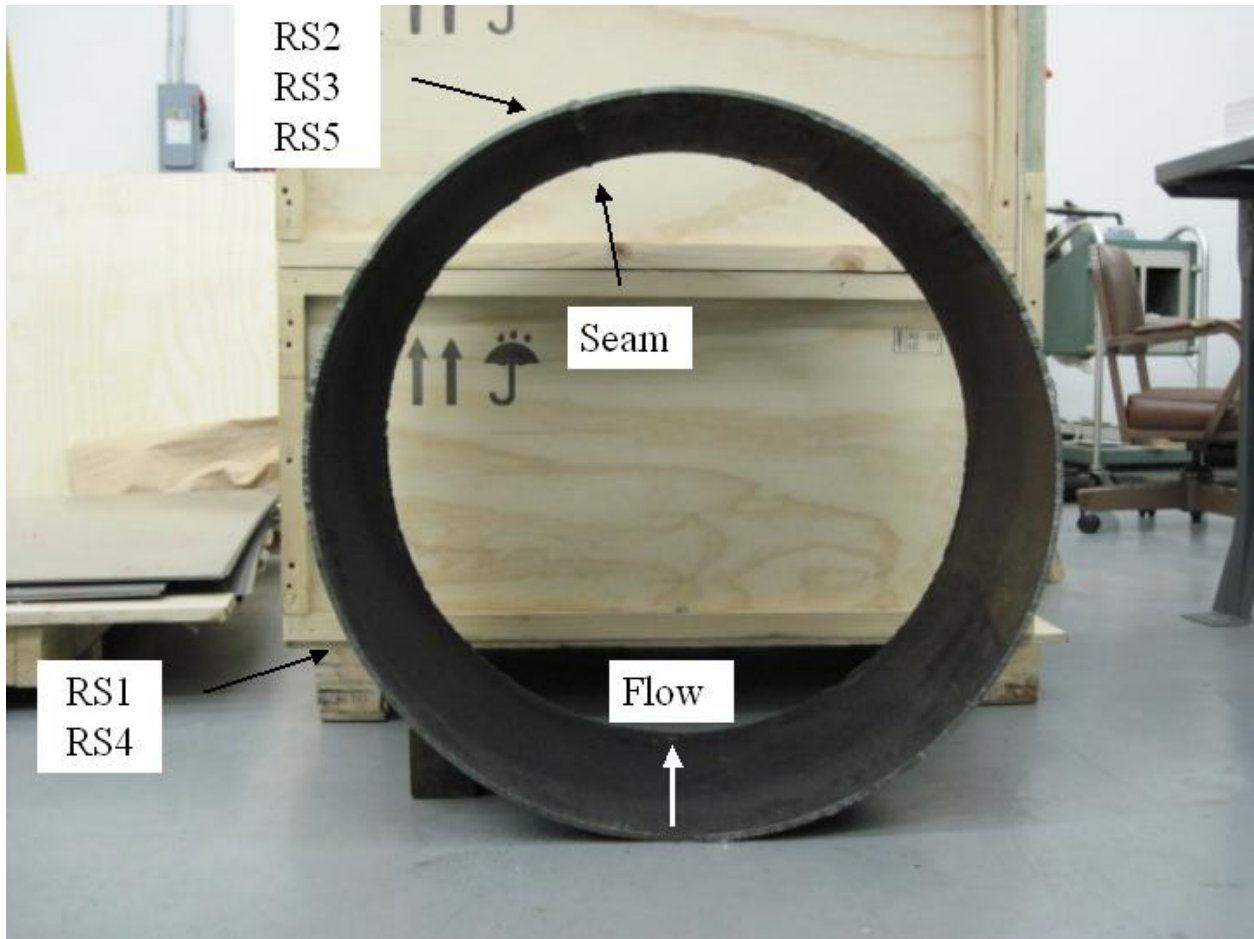


Figure 6

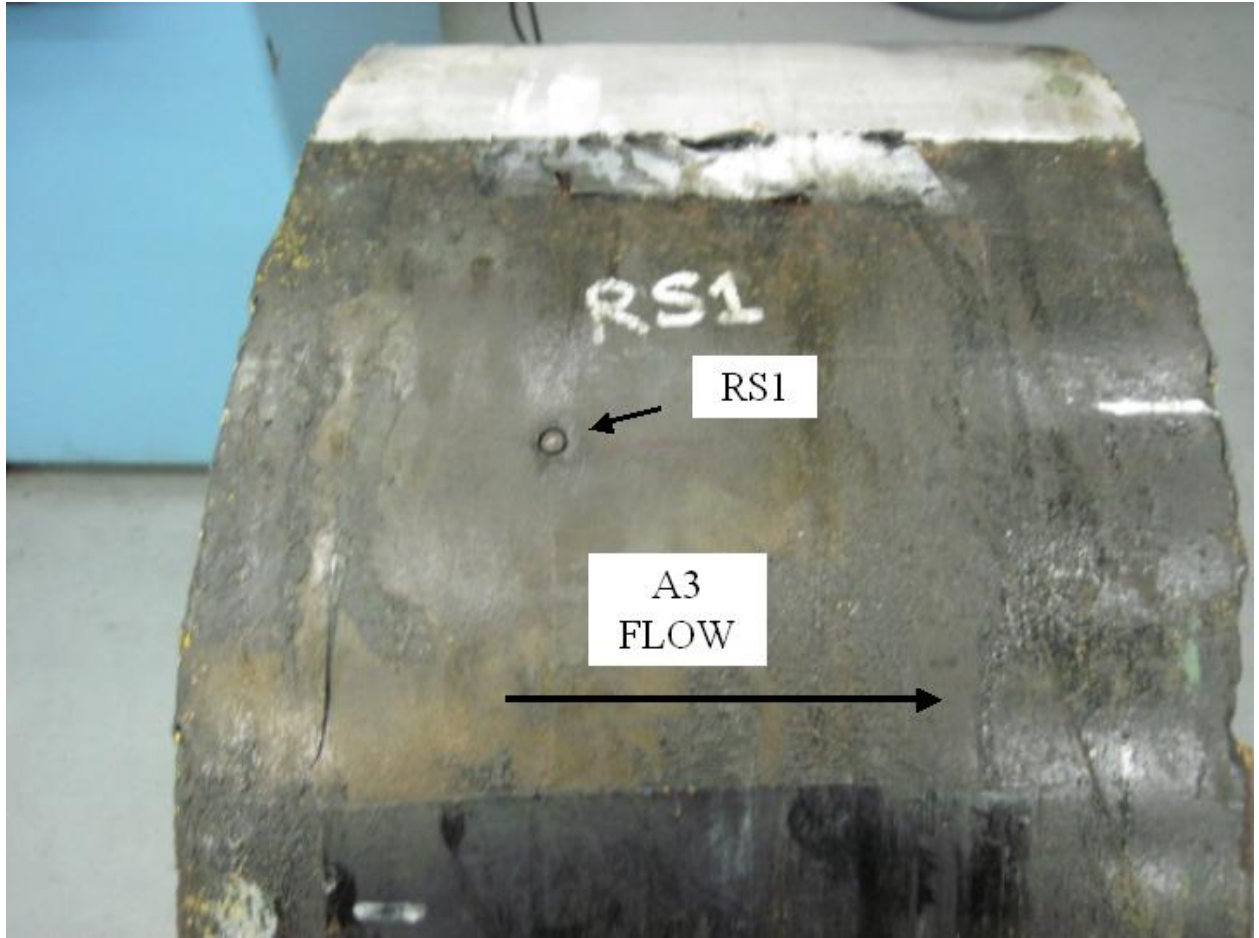


Figure 7

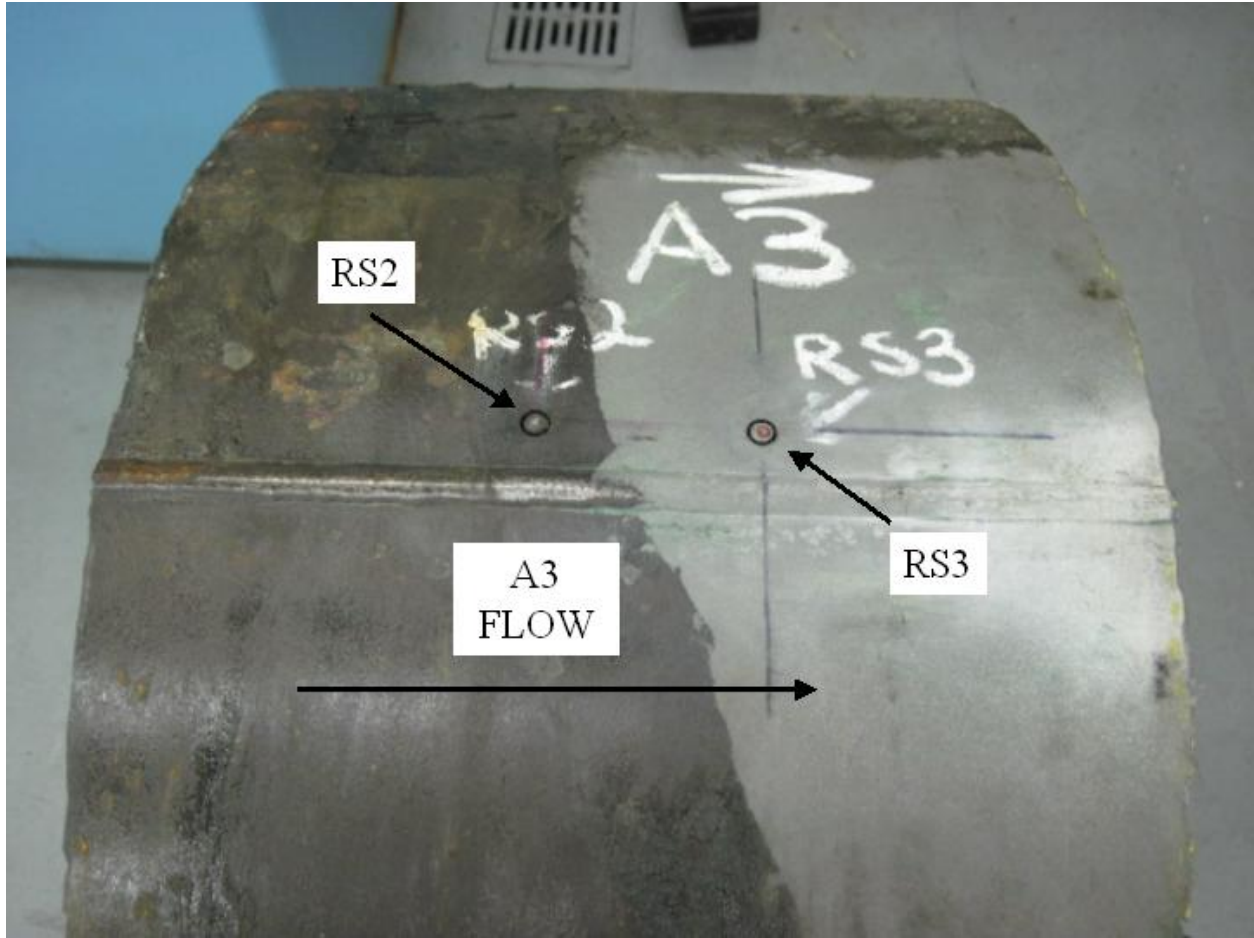


Figure 8

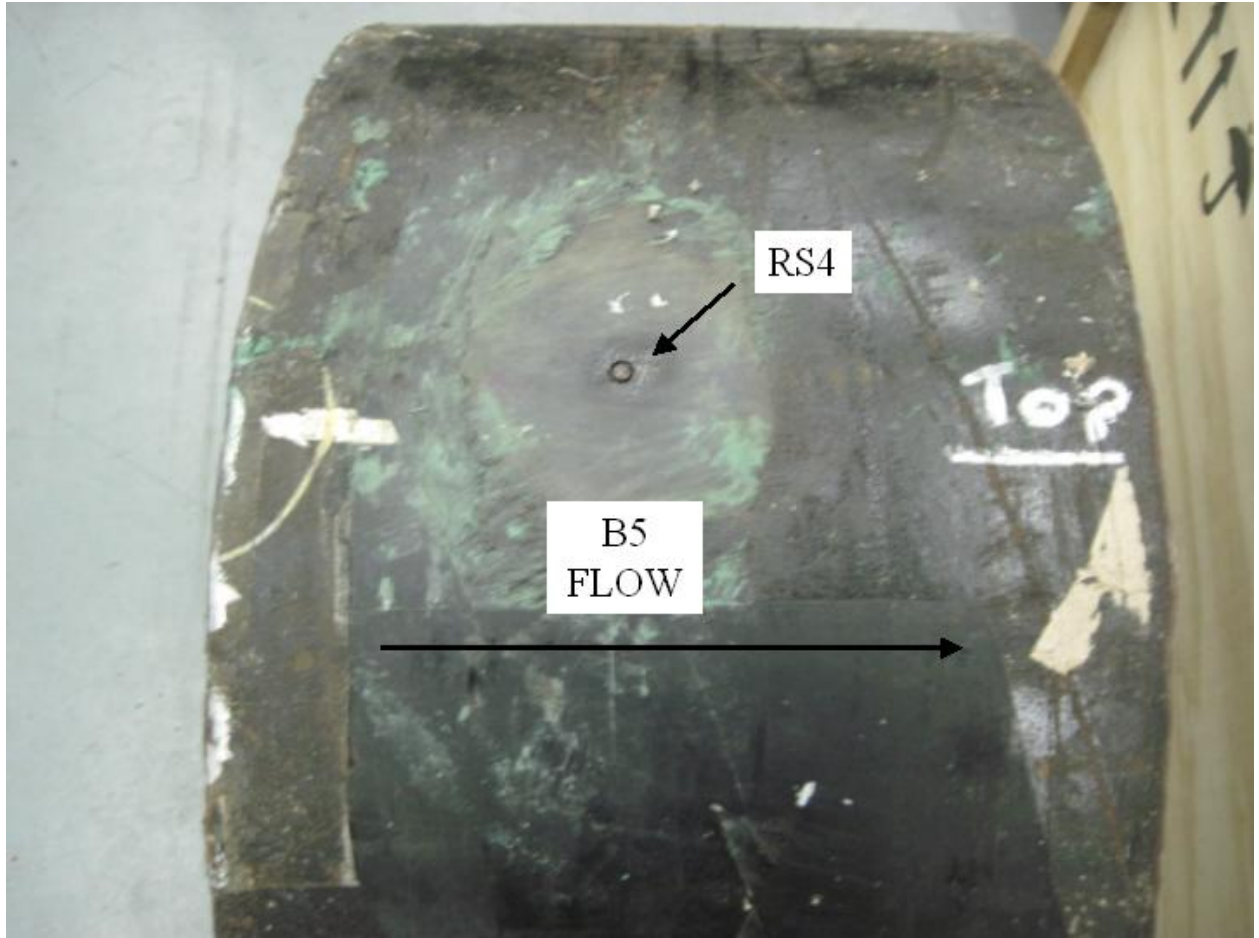


Figure 9

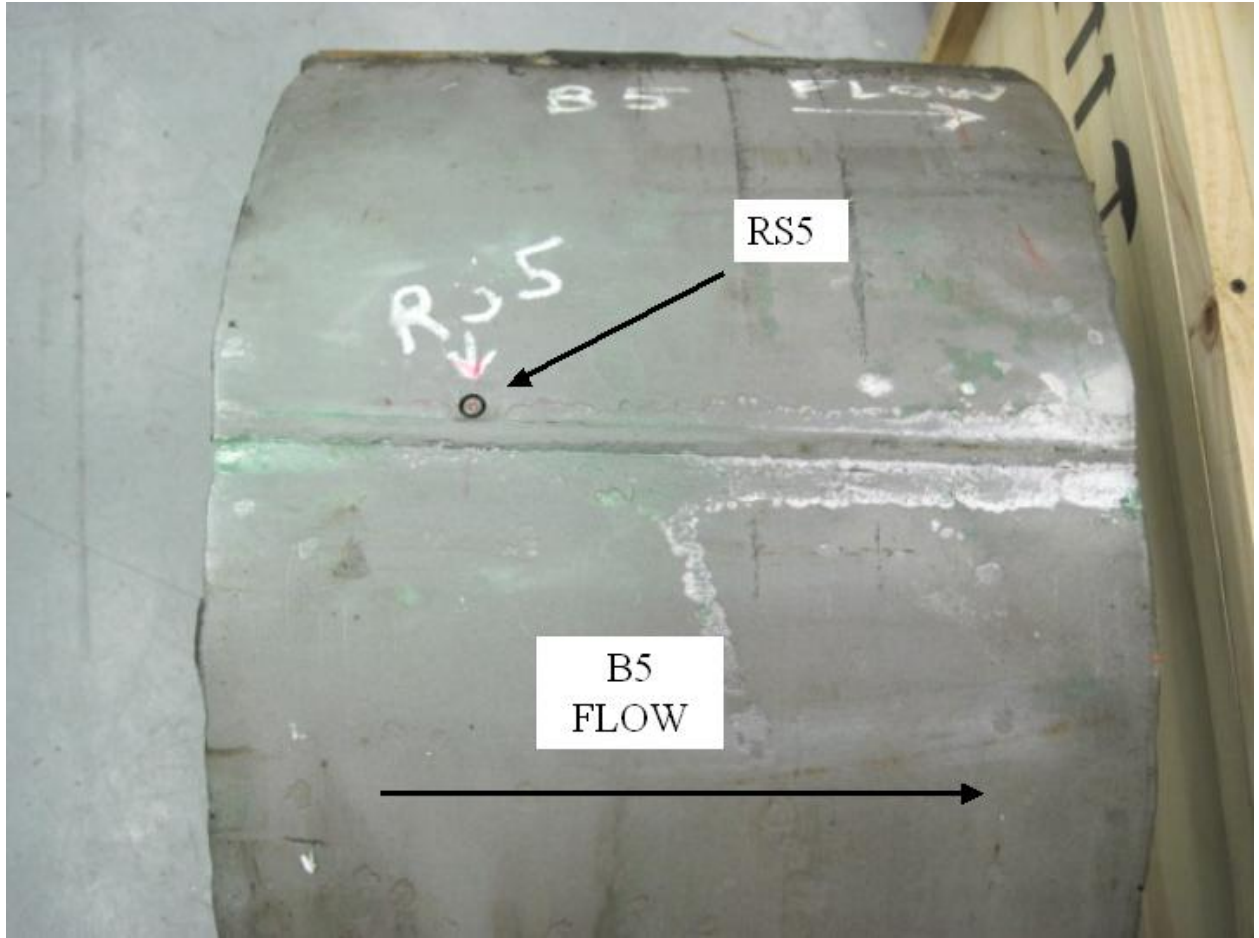


Figure 10

APPENDIX

STRAIN READINGS TAKEN FROM STRAIN GAGE ROSETTE.

MODULUS OF ELASTICITY = 29.7 (X10⁶ PSI) POISSON RATIO = 0.29

CARBON STEEL PIPE SECTION No. 1 Direction = HOOP
Specimen A3 RS1 Location

	DEPTH		STRAIN A	STRAIN B	STRAIN C
	in.	(mm)	microinch/inch	microinch/inch	microinch/inch
1	0.0056	(0.141)	-6	-8	-6
2	0.0092	(0.235)	-4	-8	-7
3	0.0129	(0.328)	-1	-6	-7
4	0.0166	(0.422)	3	-3	-5
5	0.0203	(0.516)	7	0	-4
6	0.0240	(0.610)	13	4	-2
7	0.0277	(0.704)	19	9	0
8	0.0314	(0.797)	26	15	3
9	0.0351	(0.891)	33	19	6
10	0.0388	(0.985)	39	25	10
11	0.0425	(1.079)	46	29	14
12	0.0462	(1.172)	53	36	18
13	0.0499	(1.266)	61	41	22
14	0.0535	(1.360)	69	47	26
15	0.0572	(1.454)	74	51	30
16	0.0609	(1.547)	79	54	33
17	0.0646	(1.641)	86	58	36
18	0.0683	(1.735)	92	62	38
19	0.0720	(1.829)	96	64	40
20	0.0757	(1.923)	100	66	43
21	0.0794	(2.016)	102	66	44
22	0.0831	(2.110)	105	69	45
23	0.0868	(2.204)	106	68	47
24	0.0904	(2.297)	108	69	48
25	0.0941	(2.391)	107	70	49
26	0.0979	(2.485)	108	68	48

STRESS RESOLVED ALONG GAGE AXES.

MODULUS OF ELASTICITY = 29.7 (X10⁶ PSI) POISSON RATIO = 0.29

CARBON STEEL PIPE SECTION No. 1 Direction = HOOP
Specimen A3 RS1 Location

	DEPTH		STRESS 1		STRESS 2		STRESS 3	
	in.	(mm)	ksi	(MPa)	ksi	(MPa)	ksi	(MPa)
1	0.0056	(0.141)	0.4	(2)	-1.5	(-10)	-3.7	(-25)
2	0.0092	(0.235)	2.3	(16)	0.9	(6)	-1.1	(-7)
3	0.0129	(0.328)	3.0	(20)	1.8	(12)	0.0	(0)
4	0.0166	(0.422)	3.3	(23)	2.2	(15)	0.6	(4)
5	0.0203	(0.516)	3.6	(25)	2.6	(18)	1.0	(7)
6	0.0240	(0.610)	3.9	(27)	2.8	(19)	1.4	(10)
7	0.0277	(0.704)	4.1	(28)	3.1	(22)	1.8	(12)
8	0.0314	(0.797)	4.3	(29)	3.3	(23)	2.1	(14)
9	0.0351	(0.891)	4.4	(31)	3.5	(24)	2.3	(16)
10	0.0388	(0.985)	4.5	(31)	3.6	(25)	2.6	(18)
11	0.0425	(1.079)	4.6	(32)	3.6	(25)	2.8	(19)
12	0.0462	(1.172)	4.7	(32)	3.6	(25)	2.9	(20)
13	0.0499	(1.266)	4.6	(32)	3.6	(25)	3.0	(21)
14	0.0535	(1.360)	4.6	(32)	3.6	(25)	3.0	(21)
15	0.0572	(1.454)	4.6	(32)	3.5	(24)	3.1	(21)
16	0.0609	(1.547)	4.5	(31)	3.4	(23)	3.0	(21)
17	0.0646	(1.641)	4.2	(29)	3.1	(22)	2.9	(20)
18	0.0683	(1.735)	4.0	(28)	2.9	(20)	2.8	(19)
19	0.0720	(1.829)	3.7	(26)	2.7	(19)	2.7	(19)
20	0.0757	(1.923)	3.4	(24)	2.5	(17)	2.5	(18)
21	0.0794	(2.016)	3.0	(21)	2.2	(15)	2.3	(16)
22	0.0831	(2.110)	2.5	(18)	1.8	(12)	2.1	(14)
23	0.0868	(2.204)	2.1	(15)	1.4	(10)	1.9	(13)
24	0.0904	(2.297)	1.7	(12)	1.2	(8)	1.7	(12)
25	0.0941	(2.391)	1.4	(10)	0.9	(6)	1.4	(10)
26	0.0979	(2.485)	1.0	(7)	0.6	(4)	1.1	(8)

PRINCIPAL STRESSES AND PRINCIPAL DIRECTION.

MODULUS OF ELASTICITY = 29.7 (X10⁶ PSI) POISSON RATIO = 0.29CARBON STEEL PIPE SECTION No. 1 Direction = HOOP
Specimen A3 RS1 Location

	DEPTH		MAXIMUM STRESS		MINIMUM STRESS		PHI
	in.	(mm)	ksi	(MPa)	ksi	(MPa)	(Deg.)
1	0.0056	(0.141)	0.4	(3)	-3.7	(-25)	2.3
2	0.0092	(0.235)	2.3	(16)	-1.1	(-7)	4.2
3	0.0129	(0.328)	3.0	(21)	0.0	(0)	5.6
4	0.0166	(0.422)	3.3	(23)	0.6	(4)	5.6
5	0.0203	(0.516)	3.6	(25)	1.0	(7)	5.6
6	0.0240	(0.610)	3.9	(27)	1.4	(10)	4.2
7	0.0277	(0.704)	4.1	(28)	1.8	(12)	4.4
8	0.0314	(0.797)	4.3	(29)	2.1	(14)	3.4
9	0.0351	(0.891)	4.4	(31)	2.3	(16)	1.8
10	0.0388	(0.985)	4.5	(31)	2.6	(18)	0.0
11	0.0425	(1.079)	4.6	(32)	2.8	(19)	-1.9
12	0.0462	(1.172)	4.7	(32)	2.9	(20)	-5.0
13	0.0499	(1.266)	4.7	(32)	3.0	(20)	-6.6
14	0.0535	(1.360)	4.7	(32)	3.0	(21)	-8.6
15	0.0572	(1.454)	4.7	(33)	3.0	(21)	-11.4
16	0.0609	(1.547)	4.6	(31)	2.9	(20)	-14.0
17	0.0646	(1.641)	4.3	(30)	2.8	(19)	-16.7
18	0.0683	(1.735)	4.2	(29)	2.6	(18)	-19.0
19	0.0720	(1.829)	3.9	(27)	2.5	(17)	-21.8
20	0.0757	(1.923)	3.7	(25)	2.3	(16)	-24.1
21	0.0794	(2.016)	3.2	(22)	2.0	(14)	-27.5
22	0.0831	(2.110)	2.9	(20)	1.7	(12)	-32.8
23	0.0868	(2.204)	2.6	(18)	1.4	(10)	-38.5
24	0.0904	(2.297)	2.2	(15)	1.2	(8)	-43.0
25	0.0941	(2.391)	1.9	(13)	0.9	(6)	-46.0
26	0.0979	(2.485)	1.5	(11)	0.6	(4)	-48.6

STRAIN READINGS TAKEN FROM STRAIN GAGE ROSETTE.

MODULUS OF ELASTICITY = 29.7 (X10⁶ PSI) POISSON RATIO = 0.29

CARBON STEEL PIPE SECTION No. 1 Direction = HOOP
Specimen A3 RS2 Location

	DEPTH		STRAIN A	STRAIN B	STRAIN C
	in.	(mm)	microinch/inch	microinch/inch	microinch/inch
1	0.0061	(0.156)	-5	-7	-6
2	0.0102	(0.259)	-1	-6	-8
3	0.0143	(0.363)	7	-4	-10
4	0.0183	(0.466)	16	-3	-12
5	0.0224	(0.569)	27	0	-14
6	0.0265	(0.673)	40	3	-17
7	0.0306	(0.776)	54	7	-19
8	0.0346	(0.879)	69	12	-22
9	0.0387	(0.983)	86	17	-25
10	0.0428	(1.086)	103	23	-27
11	0.0469	(1.190)	121	27	-31
12	0.0509	(1.293)	139	33	-34
13	0.0550	(1.397)	157	39	-38
14	0.0591	(1.500)	174	43	-43
15	0.0631	(1.604)	191	46	-47
16	0.0672	(1.707)	208	52	-52
17	0.0713	(1.811)	224	58	-55
18	0.0754	(1.914)	239	62	-60
19	0.0794	(2.017)	253	65	-65
20	0.0835	(2.121)	266	68	-71
21	0.0876	(2.225)	279	70	-77
22	0.0916	(2.328)	290	73	-82
23	0.0957	(2.431)	300	73	-87
24	0.0998	(2.535)	310	77	-92

STRESS RESOLVED ALONG GAGE AXES.

MODULUS OF ELASTICITY = 29.7 (X10⁶ PSI) POISSON RATIO = 0.29

CARBON STEEL PIPE SECTION No. 1 Direction = HOOP
Specimen A3 RS2 Location

	DEPTH		STRESS 1		STRESS 2		STRESS 3	
	in.	(mm)	ksi	(MPa)	ksi	(MPa)	ksi	(MPa)
1	0.0061	(0.156)	7.4	(51)	-0.4	(-3)	-4.0	(-28)
2	0.0102	(0.259)	7.2	(50)	0.7	(5)	-2.9	(-20)
3	0.0143	(0.363)	7.2	(50)	1.2	(8)	-2.3	(-16)
4	0.0183	(0.466)	7.2	(50)	1.5	(10)	-1.9	(-13)
5	0.0224	(0.569)	7.7	(53)	1.9	(13)	-1.7	(-12)
6	0.0265	(0.673)	8.1	(56)	2.2	(15)	-1.5	(-10)
7	0.0306	(0.776)	8.5	(59)	2.6	(18)	-1.3	(-9)
8	0.0346	(0.879)	8.8	(61)	2.9	(20)	-1.1	(-8)
9	0.0387	(0.983)	9.1	(63)	3.1	(22)	-0.9	(-6)
10	0.0428	(1.086)	9.4	(65)	3.3	(23)	-0.8	(-5)
11	0.0469	(1.190)	9.6	(67)	3.5	(24)	-0.7	(-5)
12	0.0509	(1.293)	9.7	(67)	3.7	(26)	-0.5	(-4)
13	0.0550	(1.397)	10.0	(69)	3.9	(27)	-0.4	(-3)
14	0.0591	(1.500)	10.1	(70)	4.1	(28)	-0.4	(-3)
15	0.0631	(1.604)	9.9	(68)	4.1	(28)	-0.4	(-3)
16	0.0672	(1.707)	10.1	(70)	4.2	(29)	-0.4	(-3)
17	0.0713	(1.811)	10.2	(70)	4.3	(29)	-0.4	(-3)
18	0.0754	(1.914)	10.3	(71)	4.3	(30)	-0.4	(-3)
19	0.0794	(2.017)	10.1	(70)	4.3	(30)	-0.5	(-3)
20	0.0835	(2.121)	10.1	(70)	4.3	(30)	-0.6	(-4)
21	0.0876	(2.225)	10.1	(70)	4.3	(30)	-0.7	(-5)
22	0.0916	(2.328)	10.0	(69)	4.2	(29)	-0.8	(-6)
23	0.0957	(2.431)	9.9	(68)	4.1	(28)	-0.9	(-6)
24	0.0998	(2.535)	9.9	(68)	4.1	(28)	-0.9	(-7)

PRINCIPAL STRESSES AND PRINCIPAL DIRECTION.

MODULUS OF ELASTICITY = 29.7 (X10⁶ PSI)

POISSON RATIO = 0.29

CARBON STEEL PIPE SECTION No. 1 Direction = HOOP
Specimen A3 RS2 Location

	DEPTH		MAXIMUM STRESS		MINIMUM STRESS		PHI
	in.	(mm)	ksi	(MPa)	ksi	(MPa)	(Deg.)
1	0.0061	(0.156)	7.8	(54)	-4.4	(-30)	-10.1
2	0.0102	(0.259)	7.4	(51)	-3.1	(-22)	-7.9
3	0.0143	(0.363)	7.4	(51)	-2.5	(-17)	-7.3
4	0.0183	(0.466)	7.3	(50)	-2.1	(-14)	-6.8
5	0.0224	(0.569)	7.8	(54)	-1.8	(-13)	-6.4
6	0.0265	(0.673)	8.2	(57)	-1.6	(-11)	-6.2
7	0.0306	(0.776)	8.6	(59)	-1.4	(-10)	-5.9
8	0.0346	(0.879)	8.9	(61)	-1.2	(-8)	-5.6
9	0.0387	(0.983)	9.2	(63)	-1.0	(-7)	-5.4
10	0.0428	(1.086)	9.5	(65)	-0.9	(-6)	-5.4
11	0.0469	(1.190)	9.7	(67)	-0.8	(-5)	-5.2
12	0.0509	(1.293)	9.7	(67)	-0.6	(-4)	-4.8
13	0.0550	(1.397)	10.0	(69)	-0.5	(-4)	-4.6
14	0.0591	(1.500)	10.2	(70)	-0.4	(-3)	-4.3
15	0.0631	(1.604)	10.0	(69)	-0.4	(-3)	-4.0
16	0.0672	(1.707)	10.1	(70)	-0.4	(-3)	-3.7
17	0.0713	(1.811)	10.2	(71)	-0.4	(-3)	-3.4
18	0.0754	(1.914)	10.3	(71)	-0.4	(-3)	-3.3
19	0.0794	(2.017)	10.1	(70)	-0.5	(-3)	-2.8
20	0.0835	(2.121)	10.1	(70)	-0.6	(-4)	-2.4
21	0.0876	(2.225)	10.1	(70)	-0.7	(-5)	-2.4
22	0.0916	(2.328)	10.0	(69)	-0.8	(-6)	-2.3
23	0.0957	(2.431)	9.9	(68)	-0.9	(-6)	-2.0
24	0.0998	(2.535)	9.9	(68)	-1.0	(-7)	-2.0

STRAIN READINGS TAKEN FROM STRAIN GAGE ROSETTE.

MODULUS OF ELASTICITY = 29.7 (X10⁶ PSI) POISSON RATIO = 0.29

CARBON STEEL PIPE SECTION NO. 1 DIRECTION = HOOP
Specimen A3 RS3 Location

	DEPTH		STRAIN A	STRAIN B	STRAIN C
	in.	(mm)	microinch/inch	microinch/inch	microinch/inch
1	0.0059	(0.149)	-27	-30	-31
2	0.0097	(0.247)	-49	-52	-51
3	0.0136	(0.347)	-63	-71	-70
4	0.0175	(0.446)	-77	-89	-89
5	0.0214	(0.544)	-87	-105	-107
6	0.0253	(0.643)	-96	-120	-125
7	0.0292	(0.742)	-102	-134	-143
8	0.0331	(0.840)	-107	-146	-159
9	0.0370	(0.939)	-110	-159	-176
10	0.0409	(1.038)	-113	-171	-194
11	0.0448	(1.137)	-114	-181	-212
12	0.0487	(1.236)	-114	-192	-228
13	0.0526	(1.335)	-113	-201	-243
14	0.0565	(1.434)	-111	-210	-258
15	0.0603	(1.532)	-108	-218	-273
16	0.0642	(1.631)	-104	-225	-287
17	0.0681	(1.730)	-100	-232	-301
18	0.0720	(1.829)	-95	-239	-314
19	0.0759	(1.929)	-91	-245	-327
20	0.0798	(2.027)	-85	-252	-339
21	0.0837	(2.126)	-80	-256	-351
22	0.0876	(2.225)	-75	-262	-362
23	0.0915	(2.324)	-69	-266	-371
24	0.0954	(2.423)	-64	-270	-379
25	0.0993	(2.521)	-60	-275	-389

STRESS RESOLVED ALONG GAGE AXES.

MODULUS OF ELASTICITY = 29.7 (X10⁶ PSI)

POISSON RATIO = 0.29

CARBON STEEL PIPE SECTION NO. 1 DIRECTION = HOOP

Specimen A3 RS3 Location

	DEPTH		STRESS 1		STRESS 2		STRESS 3	
	in.	(mm)	ksi	(MPa)	ksi	(MPa)	ksi	(MPa)
1	0.0059	(0.149)	-42.4	(-292)	-48.1	(-332)	-44.6	(-308)
2	0.0097	(0.247)	-21.8	(-150)	-26.3	(-182)	-25.7	(-177)
3	0.0136	(0.347)	-13.8	(-95)	-18.0	(-124)	-18.6	(-128)
4	0.0175	(0.446)	-9.3	(-64)	-13.5	(-93)	-14.6	(-101)
5	0.0214	(0.544)	-7.2	(-50)	-11.6	(-80)	-13.2	(-91)
6	0.0253	(0.643)	-5.5	(-38)	-9.9	(-69)	-12.0	(-83)
7	0.0292	(0.742)	-4.3	(-30)	-9.0	(-62)	-11.4	(-78)
8	0.0331	(0.840)	-3.4	(-24)	-8.2	(-56)	-10.7	(-74)
9	0.0370	(0.939)	-2.7	(-19)	-7.6	(-53)	-10.4	(-72)
10	0.0409	(1.038)	-2.1	(-15)	-7.2	(-49)	-10.1	(-70)
11	0.0448	(1.137)	-1.7	(-12)	-6.8	(-47)	-9.9	(-68)
12	0.0487	(1.236)	-1.2	(-9)	-6.5	(-45)	-9.7	(-67)
13	0.0526	(1.335)	-0.8	(-6)	-6.2	(-43)	-9.4	(-65)
14	0.0565	(1.434)	-0.4	(-3)	-6.0	(-41)	-9.4	(-65)
15	0.0603	(1.532)	-0.1	(-1)	-5.8	(-40)	-9.2	(-64)
16	0.0642	(1.631)	0.2	(1)	-5.5	(-38)	-8.9	(-62)
17	0.0681	(1.730)	0.4	(3)	-5.5	(-38)	-9.0	(-62)
18	0.0720	(1.829)	0.7	(5)	-5.5	(-38)	-9.1	(-63)
19	0.0759	(1.929)	0.9	(6)	-5.4	(-37)	-9.0	(-62)
20	0.0798	(2.027)	1.0	(7)	-5.3	(-37)	-8.9	(-61)
21	0.0837	(2.126)	1.1	(8)	-5.4	(-38)	-9.0	(-62)
22	0.0876	(2.225)	1.0	(7)	-5.6	(-39)	-9.2	(-64)
23	0.0915	(2.324)	1.0	(7)	-5.8	(-40)	-9.4	(-65)
24	0.0954	(2.423)	0.8	(6)	-6.0	(-41)	-9.7	(-67)
25	0.0993	(2.521)	0.5	(4)	-6.4	(-44)	-10.1	(-70)

PRINCIPAL STRESSES AND PRINCIPAL DIRECTION.

MODULUS OF ELASTICITY = 29.7 (X10⁶ PSI) POISSON RATIO = 0.29

CARBON STEEL PIPE SECTION NO. 1 DIRECTION = HOOP
Specimen A3 RS3 Location

	DEPTH		MAXIMUM STRESS		MINIMUM STRESS		PHI
	in.	(mm)	ksi	(MPa)	ksi	(MPa)	(Deg.)
1	0.0059	(0.149)	-38.7	(-267)	-48.3	(-333)	-38.2
2	0.0097	(0.247)	-20.5	(-141)	-27.0	(-186)	-26.5
3	0.0136	(0.347)	-13.1	(-90)	-19.2	(-133)	-18.9
4	0.0175	(0.446)	-8.9	(-61)	-15.0	(-104)	-14.7
5	0.0214	(0.544)	-6.9	(-48)	-13.5	(-93)	-12.2
6	0.0253	(0.643)	-5.3	(-36)	-12.2	(-84)	-10.3
7	0.0292	(0.742)	-4.1	(-29)	-11.5	(-80)	-9.0
8	0.0331	(0.840)	-3.3	(-22)	-10.9	(-75)	-8.2
9	0.0370	(0.939)	-2.6	(-18)	-10.5	(-73)	-7.7
10	0.0409	(1.038)	-2.0	(-14)	-10.2	(-70)	-7.5
11	0.0448	(1.137)	-1.5	(-11)	-10.0	(-69)	-7.1
12	0.0487	(1.236)	-1.1	(-8)	-9.8	(-68)	-6.9
13	0.0526	(1.335)	-0.7	(-5)	-9.6	(-66)	-6.8
14	0.0565	(1.434)	-0.3	(-2)	-9.5	(-65)	-6.8
15	0.0603	(1.532)	0.0	(0)	-9.4	(-65)	-7.1
16	0.0642	(1.631)	0.3	(2)	-9.1	(-63)	-7.2
17	0.0681	(1.730)	0.6	(4)	-9.2	(-63)	-7.2
18	0.0720	(1.829)	0.8	(6)	-9.2	(-64)	-7.4
19	0.0759	(1.929)	1.1	(7)	-9.2	(-63)	-7.6
20	0.0798	(2.027)	1.2	(8)	-9.1	(-63)	-7.8
21	0.0837	(2.126)	1.3	(9)	-9.2	(-64)	-8.1
22	0.0876	(2.225)	1.3	(9)	-9.5	(-65)	-8.1
23	0.0915	(2.324)	1.2	(8)	-9.7	(-67)	-8.2
24	0.0954	(2.423)	1.1	(7)	-9.9	(-68)	-8.2
25	0.0993	(2.521)	0.8	(5)	-10.4	(-71)	-8.4

STRESS RESOLVED ALONG GAGE AXES.

MODULUS OF ELASTICITY = 29.7 (X10⁶ PSI) POISSON RATIO = 0.29

CARBON STEEL PIPE SECTION No. 1 = HOOP
Specimen B5 RS4 Location

	DEPTH		STRESS 1		STRESS 2		STRESS 3	
	in.	(mm)	ksi	(MPa)	ksi	(MPa)	ksi	(MPa)
1	0.0031	(0.078)	-7.0	(-49)	-11.1	(-77)	-9.9	(-68)
2	0.0051	(0.129)	-3.4	(-23)	-6.2	(-43)	-5.1	(-35)
3	0.0071	(0.180)	-1.4	(-10)	-3.3	(-23)	-2.5	(-17)
4	0.0091	(0.231)	-0.5	(-3)	-1.8	(-12)	-1.1	(-8)
5	0.0111	(0.283)	0.2	(1)	-0.9	(-6)	-0.4	(-3)
6	0.0132	(0.334)	0.6	(4)	-0.3	(-2)	0.1	(1)
7	0.0152	(0.385)	0.8	(6)	-0.1	(-1)	0.6	(4)
8	0.0172	(0.437)	1.1	(7)	0.2	(2)	0.8	(6)
9	0.0192	(0.488)	1.2	(9)	0.4	(3)	1.0	(7)
10	0.0212	(0.539)	1.3	(9)	0.6	(4)	1.1	(7)
11	0.0233	(0.591)	1.4	(10)	0.6	(4)	1.1	(8)
12	0.0253	(0.642)	1.5	(10)	0.6	(4)	1.1	(8)
13	0.0273	(0.693)	1.5	(11)	0.6	(4)	1.1	(7)
14	0.0293	(0.745)	1.5	(11)	0.6	(4)	1.1	(7)
15	0.0313	(0.796)	1.5	(10)	0.6	(4)	1.0	(7)
16	0.0334	(0.848)	1.5	(10)	0.5	(4)	0.9	(6)
17	0.0354	(0.899)	1.4	(10)	0.5	(3)	0.8	(5)
18	0.0374	(0.950)	1.4	(10)	0.3	(2)	0.8	(6)
19	0.0394	(1.002)	1.5	(10)	0.4	(3)	0.9	(6)
20	0.0415	(1.053)	1.5	(10)	0.4	(3)	0.9	(6)
21	0.0435	(1.104)	1.5	(10)	0.4	(3)	0.9	(6)
22	0.0455	(1.156)	1.5	(10)	0.5	(3)	1.0	(7)
23	0.0475	(1.207)	1.5	(10)	0.5	(4)	1.0	(7)
24	0.0495	(1.258)	1.5	(10)	0.5	(3)	0.9	(6)
25	0.0516	(1.310)	1.5	(10)	0.5	(3)	0.9	(6)
26	0.0536	(1.361)	1.5	(10)	0.5	(3)	0.9	(6)
27	0.0556	(1.413)	1.4	(10)	0.4	(3)	0.9	(6)
28	0.0576	(1.464)	1.4	(10)	0.4	(3)	0.8	(6)
29	0.0597	(1.515)	1.4	(9)	0.3	(2)	0.7	(5)
30	0.0617	(1.567)	1.3	(9)	0.3	(2)	0.6	(4)
31	0.0637	(1.618)	1.2	(8)	0.2	(2)	0.6	(4)
32	0.0657	(1.669)	1.1	(8)	0.2	(1)	0.5	(3)
33	0.0678	(1.721)	1.0	(7)	0.2	(1)	0.4	(3)
34	0.0698	(1.772)	1.0	(7)	0.2	(1)	0.4	(3)

STRESS RESOLVED ALONG GAGE AXES.

MODULUS OF ELASTICITY = 29.7 (X10⁶ PSI) POISSON RATIO = 0.29

CARBON STEEL PIPE SECTION No. 1 = HOOP
Specimen B5 RS4 Location

	DEPTH		STRESS 1		STRESS 2		STRESS 3	
	in.	(mm)	ksi	(MPa)	ksi	(MPa)	ksi	(MPa)
35	0.0718	(1.824)	0.9	(6)	0.1	(1)	0.3	(2)
36	0.0738	(1.875)	0.8	(6)	0.1	(0)	0.3	(2)
37	0.0758	(1.926)	0.8	(5)	0.0	(0)	0.2	(2)
38	0.0779	(1.978)	0.7	(5)	0.0	(0)	0.3	(2)
39	0.0799	(2.029)	0.8	(5)	0.0	(0)	0.3	(2)
40	0.0819	(2.080)	0.8	(5)	0.0	(0)	0.4	(3)
41	0.0839	(2.132)	0.7	(5)	-0.1	(-1)	0.3	(2)
42	0.0860	(2.183)	0.6	(4)	-0.2	(-1)	0.3	(2)
43	0.0880	(2.234)	0.5	(3)	-0.3	(-2)	0.1	(1)
44	0.0900	(2.285)	0.3	(2)	-0.5	(-3)	-0.1	(-1)
45	0.0920	(2.337)	0.1	(1)	-0.6	(-4)	-0.2	(-1)
46	0.0940	(2.389)	-0.2	(-1)	-0.9	(-6)	-0.5	(-4)
47	0.0960	(2.440)	-0.5	(-4)	-1.2	(-8)	-0.8	(-6)
48	0.0981	(2.491)	-0.9	(-6)	-1.5	(-11)	-1.0	(-7)

PRINCIPAL STRESSES AND PRINCIPAL DIRECTION.

MODULUS OF ELASTICITY = 29.7 (X10⁶ PSI) POISSON RATIO = 0.29

CARBON STEEL PIPE SECTION No. 1 = HOOP
Specimen B5 RS4 Location

	DEPTH		MAXIMUM STRESS		MINIMUM STRESS		PHI (Deg.)
	in.	(mm)	ksi	(MPa)	ksi	(MPa)	
35	0.0718	(1.824)	1.2	(8)	0.0	(0)	-29.7
36	0.0738	(1.875)	1.1	(8)	0.0	(0)	-29.6
37	0.0758	(1.926)	1.0	(7)	0.0	(0)	-31.0
38	0.0779	(1.978)	1.1	(8)	0.0	(0)	-34.1
39	0.0799	(2.029)	1.1	(8)	0.0	(0)	-33.5
40	0.0819	(2.080)	1.2	(8)	0.0	(0)	-35.0
41	0.0839	(2.132)	1.1	(8)	-0.1	(-1)	-36.8
42	0.0860	(2.183)	1.1	(8)	-0.2	(-1)	-37.6
43	0.0880	(2.234)	0.9	(6)	-0.4	(-2)	-36.3
44	0.0900	(2.285)	0.7	(5)	-0.5	(-4)	-36.1
45	0.0920	(2.337)	0.6	(4)	-0.6	(-4)	-37.2
46	0.0940	(2.389)	0.2	(2)	-0.9	(-6)	-35.5
47	0.0960	(2.440)	-0.1	(-1)	-1.2	(-8)	-37.8
48	0.0981	(2.491)	-0.4	(-3)	-1.5	(-11)	-40.6

STRESS RESOLVED ALONG GAGE AXES.

MODULUS OF ELASTICITY = 29.7 (X10⁶ PSI)

POISSON RATIO = 0.29

CARBON STEEL PIPE SECTION No. 1 Direction = HOOP
Specimen B5 RS5 Location

	DEPTH		STRESS 1		STRESS 2		STRESS 3	
	in.	(mm)	ksi	(MPa)	ksi	(MPa)	ksi	(MPa)
1	0.0032	(0.080)	-73.2	(-504)	-65.9	(-454)	-76.4	(-527)
2	0.0053	(0.134)	-49.8	(-343)	-47.4	(-327)	-53.9	(-372)
3	0.0074	(0.187)	-33.6	(-232)	-34.0	(-234)	-40.2	(-277)
4	0.0094	(0.239)	-23.9	(-165)	-25.7	(-177)	-32.3	(-223)
5	0.0115	(0.293)	-18.3	(-126)	-21.0	(-145)	-28.2	(-195)
6	0.0136	(0.346)	-14.7	(-101)	-18.2	(-126)	-25.8	(-178)
7	0.0157	(0.399)	-12.2	(-84)	-15.8	(-109)	-23.8	(-164)
8	0.0178	(0.452)	-9.8	(-68)	-13.7	(-95)	-22.6	(-156)
9	0.0199	(0.505)	-9.1	(-63)	-13.3	(-92)	-22.7	(-156)
10	0.0220	(0.558)	-8.3	(-58)	-12.8	(-88)	-22.5	(-155)
11	0.0241	(0.612)	-7.5	(-52)	-12.0	(-83)	-21.7	(-150)
12	0.0262	(0.665)	-7.0	(-49)	-11.7	(-80)	-21.5	(-148)
13	0.0283	(0.718)	-6.6	(-46)	-11.3	(-78)	-21.1	(-146)
14	0.0304	(0.771)	-6.2	(-43)	-10.8	(-75)	-20.5	(-141)
15	0.0324	(0.824)	-5.8	(-40)	-10.3	(-71)	-19.8	(-136)
16	0.0345	(0.877)	-5.5	(-38)	-10.0	(-69)	-19.2	(-132)
17	0.0366	(0.930)	-5.3	(-36)	-9.6	(-66)	-18.6	(-128)
18	0.0387	(0.983)	-5.0	(-35)	-9.3	(-64)	-17.9	(-124)
19	0.0408	(1.036)	-4.8	(-33)	-9.0	(-62)	-17.3	(-120)
20	0.0429	(1.090)	-4.6	(-32)	-8.7	(-60)	-16.8	(-116)
21	0.0450	(1.143)	-4.4	(-30)	-8.4	(-58)	-16.2	(-112)
22	0.0471	(1.196)	-4.2	(-29)	-8.1	(-56)	-15.7	(-108)
23	0.0492	(1.249)	-4.0	(-27)	-7.8	(-54)	-15.0	(-103)
24	0.0513	(1.302)	-3.8	(-26)	-7.5	(-52)	-14.3	(-99)
25	0.0534	(1.356)	-3.6	(-25)	-7.2	(-49)	-13.8	(-95)
26	0.0555	(1.409)	-3.4	(-24)	-6.9	(-48)	-13.4	(-92)
27	0.0575	(1.462)	-3.3	(-23)	-6.6	(-46)	-12.9	(-89)
28	0.0596	(1.515)	-3.2	(-22)	-6.4	(-44)	-12.4	(-85)
29	0.0617	(1.568)	-3.0	(-21)	-5.9	(-41)	-11.5	(-80)
30	0.0638	(1.621)	-2.8	(-19)	-5.6	(-38)	-10.9	(-75)
31	0.0659	(1.674)	-2.6	(-18)	-5.3	(-37)	-10.5	(-72)
32	0.0680	(1.727)	-2.4	(-17)	-5.1	(-35)	-10.1	(-69)
33	0.0701	(1.781)	-2.4	(-17)	-4.9	(-34)	-9.8	(-68)
34	0.0722	(1.834)	-2.4	(-17)	-4.8	(-33)	-9.5	(-66)

STRESS RESOLVED ALONG GAGE AXES.

MODULUS OF ELASTICITY = 29.7 (X10⁶ PSI)

POISSON RATIO = 0.29

CARBON STEEL PIPE SECTION No. 1 Direction = HOOP
Specimen B5 RS5 Location

	DEPTH		STRESS 1		STRESS 2		STRESS 3	
	in.	(mm)	ksi	(MPa)	ksi	(MPa)	ksi	(MPa)
35	0.0743	(1.887)	-2.4	(-16)	-4.7	(-33)	-9.3	(-64)
36	0.0764	(1.940)	-2.4	(-16)	-4.5	(-31)	-8.9	(-62)
37	0.0785	(1.993)	-2.4	(-17)	-4.4	(-31)	-8.7	(-60)
38	0.0806	(2.046)	-2.6	(-18)	-4.5	(-31)	-8.7	(-60)
39	0.0826	(2.099)	-2.7	(-19)	-4.5	(-31)	-8.6	(-59)
40	0.0847	(2.152)	-2.8	(-19)	-4.5	(-31)	-8.4	(-58)
41	0.0868	(2.205)	-2.8	(-19)	-4.4	(-31)	-8.2	(-56)
42	0.0889	(2.259)	-2.9	(-20)	-4.5	(-31)	-8.0	(-55)
43	0.0910	(2.312)	-2.9	(-20)	-4.4	(-31)	-7.8	(-54)
44	0.0931	(2.365)	-3.0	(-21)	-4.5	(-31)	-7.7	(-53)
45	0.0952	(2.418)	-3.3	(-23)	-4.7	(-32)	-7.9	(-54)
46	0.0973	(2.471)	-3.5	(-24)	-4.8	(-33)	-8.0	(-55)
47	0.0994	(2.524)	-3.8	(-27)	-5.1	(-35)	-8.2	(-57)

PRINCIPAL STRESSES AND PRINCIPAL DIRECTION.

MODULUS OF ELASTICITY = 29.7 (X10⁶ PSI) POISSON RATIO = 0.29

CARBON STEEL PIPE SECTION No. 1 Direction = HOOP
Specimen B5 RS5 Location

	DEPTH		MAXIMUM STRESS		MINIMUM STRESS		PHI (Deg.)
	in.	(mm)	ksi	(MPa)	ksi	(MPa)	
1	0.0032	(0.080)	-65.7	(-453)	-83.8	(-578)	39.9
2	0.0053	(0.134)	-46.9	(-324)	-56.7	(-391)	32.6
3	0.0074	(0.187)	-32.5	(-224)	-41.3	(-285)	21.0
4	0.0094	(0.239)	-23.3	(-161)	-33.0	(-227)	15.0
5	0.0115	(0.293)	-17.8	(-123)	-28.7	(-198)	12.4
6	0.0136	(0.346)	-14.3	(-99)	-26.1	(-180)	9.9
7	0.0157	(0.399)	-11.8	(-81)	-24.2	(-167)	10.5
8	0.0178	(0.452)	-9.3	(-64)	-23.0	(-159)	10.5
9	0.0199	(0.505)	-8.6	(-59)	-23.2	(-160)	10.4
10	0.0220	(0.558)	-7.9	(-54)	-22.9	(-158)	10.3
11	0.0241	(0.612)	-7.0	(-48)	-22.2	(-153)	10.1
12	0.0262	(0.665)	-6.6	(-45)	-22.0	(-151)	9.9
13	0.0283	(0.718)	-6.2	(-43)	-21.6	(-149)	9.8
14	0.0304	(0.771)	-5.8	(-40)	-20.9	(-144)	9.7
15	0.0324	(0.824)	-5.4	(-37)	-20.2	(-139)	9.7
16	0.0345	(0.877)	-5.1	(-35)	-19.6	(-135)	9.6
17	0.0366	(0.930)	-4.9	(-34)	-19.0	(-131)	9.5
18	0.0387	(0.983)	-4.7	(-32)	-18.3	(-126)	9.3
19	0.0408	(1.036)	-4.4	(-31)	-17.7	(-122)	9.2
20	0.0429	(1.090)	-4.3	(-30)	-17.1	(-118)	9.0
21	0.0450	(1.143)	-4.1	(-28)	-16.5	(-114)	8.9
22	0.0471	(1.196)	-3.9	(-27)	-16.0	(-110)	8.7
23	0.0492	(1.249)	-3.7	(-26)	-15.2	(-105)	8.5
24	0.0513	(1.302)	-3.5	(-24)	-14.5	(-100)	8.2
25	0.0534	(1.356)	-3.4	(-23)	-14.0	(-97)	8.4
26	0.0555	(1.409)	-3.2	(-22)	-13.6	(-94)	8.3
27	0.0575	(1.462)	-3.1	(-21)	-13.1	(-90)	8.5
28	0.0596	(1.515)	-3.0	(-21)	-12.6	(-87)	8.6
29	0.0617	(1.568)	-2.8	(-19)	-11.7	(-81)	8.6
30	0.0638	(1.621)	-2.6	(-18)	-11.1	(-76)	8.6
31	0.0659	(1.674)	-2.5	(-17)	-10.6	(-73)	8.6
32	0.0680	(1.727)	-2.3	(-16)	-10.2	(-71)	8.5
33	0.0701	(1.781)	-2.2	(-15)	-10.0	(-69)	8.6
34	0.0722	(1.834)	-2.2	(-15)	-9.7	(-67)	8.9

PRINCIPAL STRESSES AND PRINCIPAL DIRECTION.

MODULUS OF ELASTICITY = 29.7 (X10⁶ PSI) POISSON RATIO = 0.29CARBON STEEL PIPE SECTION No. 1 Direction = HOOP
Specimen B5 RS5 Location

	DEPTH		MAXIMUM STRESS		MINIMUM STRESS		PHI
	in.	(mm)	ksi	(MPa)	ksi	(MPa)	(Deg.)
35	0.0743	(1.887)	-2.2	(-15)	-9.5	(-65)	8.7
36	0.0764	(1.940)	-2.2	(-15)	-9.1	(-63)	9.3
37	0.0785	(1.993)	-2.2	(-15)	-8.9	(-62)	10.0
38	0.0806	(2.046)	-2.3	(-16)	-8.9	(-62)	10.6
39	0.0826	(2.099)	-2.5	(-17)	-8.8	(-61)	10.6
40	0.0847	(2.152)	-2.6	(-18)	-8.6	(-59)	10.5
41	0.0868	(2.205)	-2.6	(-18)	-8.3	(-58)	10.5
42	0.0889	(2.259)	-2.7	(-19)	-8.2	(-57)	10.5
43	0.0910	(2.312)	-2.7	(-19)	-8.0	(-55)	10.4
44	0.0931	(2.365)	-2.9	(-20)	-7.9	(-55)	10.2
45	0.0952	(2.418)	-3.1	(-21)	-8.0	(-55)	10.6
46	0.0973	(2.471)	-3.3	(-23)	-8.2	(-56)	10.8
47	0.0994	(2.524)	-3.7	(-25)	-8.4	(-58)	11.5